

Dissertation

**NF-kappaB activation in infections
with *Helicobacter pylori*
or *Legionella pneumophila***

zur Erlangung des akademischen Grades doctor rerum naturalium (Dr. rer. nat.)
im Fach Biologie

eingereicht an der Mathematisch-Naturwissenschaftlichen Fakultät I
der Humboldt Universität zu Berlin

von Dipl.-Biol. Sina Bartfeld (geb. 06.01.1978 in Berlin)

Präsident der Humboldt Universität zu Berlin

Prof. Dr. Dr. h.c. Christoph Marksches

Dekan der Mathematisch-Naturwissenschaftlichen Fakultät I

Prof. Dr. Lutz-Helmut Schön

Gutachter: 1. Prof. Thomas F. Meyer

2. Prof. Wolfgang Uckert

3. Prof. Claus Scheidereit

Tag der mündlichen Prüfung: 30.6.2009

Table of content

Abbreviations	4
Abstract	6
Zusammenfassung	7
1 Introduction	8
1.1 The transcription factor family NF- κ B	9
1.2 The bacterium <i>Helicobacter pylori</i>	16
1.3 The intracellular bacterium <i>Legionella pneumophila</i>	21
1.4 RNAi-based screens	23
1.5 Aims of this thesis.....	24
2 Results and Discussion	25
2.1 Part I: Imaging NF- κ B activation using p65-GFP	25
2.1.1 A high throughput assay for cell lines expressing p65-GFP.....	25
2.1.2 Comparison of reporter cell lines and parental cell lines.....	27
2.1.3 Specific temporal control of p65-GFP translocations.....	28
2.1.4 Bacterial infection induces oscillations of p65-GFP.....	29
2.1.5 Discussion.....	32
2.2 Part II: RNAi-based screen identified regulators of NF- κ B signaling	35
2.2.1 Establishment of the RNAi-based screen.....	35
2.2.2 Performance of the screen	36
2.2.3 Quality control of the screen and identification of hits	37
2.2.4 Validation of identified genes.....	37
2.2.5 Time resolved analysis of NF- κ B regulators.....	40
2.2.6 Combinatorial effects of identified siRNAs.....	43
2.2.7 ALPK1 and CRKRS are important for NF- κ B activation	45
2.2.8 SKP2 is necessary for termination of NF- κ B activity	48
2.2.9 Discussion.....	51
2.3 Part III: Two tracks of NF- κ B activation induced by <i>L. pneumophila</i>	59
2.3.1 Biphasic p65 translocation during <i>L. pneumophila</i> infection	59
2.3.2 NF- κ B activation profiles of <i>L. pneumophila</i> wild-type strains....	60
2.3.3 Transient p65 translocation depends on intact flagella	60
2.3.4 Continuous p65 translocation depends on the Dot/Icm system.....	62
2.3.5 Involvement of single Dot/Icm secreted effectors	62
2.3.6 Bacterial replication and continuous p65 translocation	63
2.3.7 I κ B α is degraded during continuous activation	64
2.3.8 TLR5 and MyD88 are only important for early activation	65
2.3.9 Discussion.....	66
3 Conclusions and Outlook	70
4 Material and Methods	73
4.1 General suppliers	73

Table of content

4.2	DNA-constructs and molecular biology techniques	73
4.4	Lentiviral transduction and generation of monoclonal cell lines.....	75
4.5	Transient transfection of siRNA.....	76
4.6	Automated transient transfection of siRNA	76
4.7	Bacterial culture.....	77
4.8	Infections	78
4.9	Intracellular growth of <i>L. pneumophila</i>	78
4.10	Automated microscopy and software-based picture analysis	78
4.11	Live cell microscopy	80
4.12	Immunofluorescence after live cell microscopy.....	81
4.13	SDS-PAGE	81
4.14	Immunoblotting	81
4.15	Kinase assay	82
4.16	ELISA.....	83
4.17	qRT-PCR.....	83
5	Statistics	85
5.1	Statistical analysis of live cell microscopy	85
5.2	Statistical analysis of screen and hit validation	85
6	References.....	92
	Publications	104
	Selbstständigkeitserklärung.....	1045
	Acknowledgements.....	106

Abbreviations

AICD	activation induced cell death
ALPK1	alpha kinase 1
APS	ammonium peroxodisulfate
AURKB	aurora/IPL1-related kinase 2
BAFF	B cell-activating factor
Bcl-3	B cell lymphoma 3
βTrCP	β transducin repeat-containing protein
CagA	cytotoxin-associated gene A
CCNB1	G2/mitotic-specific cyclin B1
CCNB2	G2/mitotic-specific cyclin B2
CD40	cluster of Differentiation 40
CDC	cell division cycle
CDK	cyclin dependent kinase
Cezanne	cellular zinc finger anti NF-κB
c-FLIP	Fas-associated via death domain (FADD)-like interleukin-1-β-converting enzyme (FLICE/caspase 8)-inhibitory protein
CFP	cyan fluorescent protein
CFU	colony forming unit
CHED	cholinesterase-related cell division controller
c-IAP	inhibitor of apoptosis protein
Clk1	CDC-like kinase 1
c-Rel	v-rel reticuloendotheliosis viral oncogene homolog
CRKRS	CDC2-related kinase, arginine/serine rich
CYLD	cylindromatosis protein
DMEM	Dulbecco's modified eagle medium
DMSO	dimethyl sulfoxide
DNA	desoxyribonucleic acid
Dot	defective in organelle trafficking
DUB	de-ubiquitylation
DYRK1B	dual-specificity tyrosine-phosphorylation regulated kinase 1B
ECL	enhanced chemiluminescence
EGF	epidermal growth factor
EGFR	epidermal growth factor receptor
ELKS	protein rich in amino acids E, L, K and S
EMSA	electro mobility shift assay
EnhC	<i>Legionella</i> enhanced entry protein EnhC
ERK	extracellular signal-regulated kinase
FASTK	FAS-activated serine/threonine kinase
FCS	fetal calf serum
FGFR4	fibroblast growth factor receptor 4
FlaA	<i>Legionella</i> flagellin
FliA	<i>Legionella</i> flagellar biosynthesis sigma factor FliA
GAK	cyclin G-associated kinase
GAPDH	glyceraldehyde 3-phosphate dehydrogenase
GFP	green fluorescing protein
GRB2	growth factor receptor-bound protein 2
HRP	horse radish peroxidase
HSP	heat shock protein
Icm	intracellular multiplication
IκB	inhibitor of κB
IKK	IκB kinase
IL	interleukin
ILK1	integrin-linked protein kinase 1
IRAK	interleukin-1 receptor-associated kinase
kDa	kilodalton
LB	Luria Bertani
LCV	<i>Legionella</i> containing vacuole
LetA	<i>Legionella</i> transmission activator LetA
LPS	lipopolysaccharide
LT	lymphotoxin
LTK	leukocyte tyrosine kinase
LubX	<i>Legionella</i> U-box containing protein LubX
MALT	mucosa-associated lymphatic tissue
MAMP	microbe associated molecular pattern
MAPK	mitogen-activated protein kinase
MEF	mouse embryonic fibroblasts
MEKK	mitogen-activated protein/ERK kinase kinase
MHCK A	myosin heavy chain kinase a
MIP-2	macrophage inflammatory protein 2
MOI	multiplicity of infection
mRNA	messenger RNA
NOD	nucleotide binding and oligomerization domain
p100	NF-κB subunit p100
p105	NF-κB subunit p105
p50	NF-κB subunit p50
p52	NF-κB subunit p52
p65	NF-κB subunit p65
PAA	polyacrylamide
PAGE	polyacrylamide gel electrophoresis
PAI	pathogenicity island
PAK1	p21 protein (CDC42/Rac)-activated kinase 1
PCR	polymerase chain reaction
PG	peptidoglycan
PLK1	polo-like kinase 1
PRKACB	cAMP-dependent protein kinase, β-catalytic subunit
PRKCABP	PRKCA-binding protein
PRKD2	protein kinase C, D2 type
PRR	pattern recognition receptor
PSKH1	serine/threonine-protein kinase H1
PtsP	<i>Legionella</i> phosphoenolpyruvate protein phosphotransferase PtsP
PVDF	polyvinylidene fluoride
RelA	v-rel reticuloendotheliosis viral oncogene homolog A
RelB	v-rel reticuloendotheliosis viral oncogene homolog B
RING	really interesting new gene
RIP	receptor-interacting protein
RISC	RNA interference inducing silencing complex
RNA	ribonucleic acid
RNAi	RNA interference
SCF	Skp1, CDC53/Cullin1, F-box protein complex

Abbreviations

SdbA	<i>Legionella</i> substrate of the Dot/Icm system SdbA
SdhA	<i>Legionella</i> substrate of the Dot/Icm system SdhA
SdhB	<i>Legionella</i> substrate of the Dot/Icm system SdhB
SDS	sodium dodecyl sulphate
SHC1	sarcoma (SRC) homology 2 domain containing (SHC) transforming protein 1
shRNA	small hairpin RNA
SidC	<i>Legionella</i> substrate of the Dot/Icm system SidC
siRNA	small interfering RNA
SKP	S-phase kinase-associated protein
SOCS1	suppressor of cytokine signaling 1
SP3	specificity protein 3 transcription factor
STAT	signal transducers and activators of transcription
SUMO	small ubiquitin-like modifier
T4SS	type four secretion system
TAB	TAK1 binding protein
TAK1	transforming growth factor- β activated

	kinase 1
TANK	TRAF family member-associated NF- κ B activator
TBK1	TANK binding kinase 1
TCR	T cell receptor
TEMED	Tetramethylethylenediamine
TIR	toll/IL-1 receptor
TLR	toll-like receptor
TNF	tumor necrosis factor
TNFAIP3	TNF α -induced protein 3
TNF-R	TNF receptor
TNIK	TRAF2 and NCK interacting kinase
TRABID	TRAF-binding domain
TRADD	TNF receptor-associated death domain
TRAF	TNF receptor-associated factor
TRIAD3A	triad domain containing protein 3A
Ub^{Lys48}	lysine (Lys)-48-linked polyubiquitylation
Ub^{Lys63}	lysine (Lys)-63-linked polyubiquitylation
VacA	vacuolating toxin A
WB	western blotting
WEE1	wee1-like protein kinase

Abstract

Infection with pathogens such as the carcinogenic bacterium *Helicobacter pylori* or the intracellular bacterium *Legionella pneumophila* leads to activation of the transcription factor nuclear factor kappa B (NF- κ B). This contributes both to cytokine production, which triggers the immune response, and upregulation of anti-apoptotic genes. In infection with *H. pylori*, this dual function provides a mechanistic link between the chronic inflammation and cancer development. In infection with *L. pneumophila*, anti-apoptosis can be beneficial for the bacterium by ensuring host cell survival. Therefore, NF- κ B can set the course of disease and it is of central interest to understand mechanisms of NF- κ B activation. However, dynamics of NF- κ B activation and the signaling pathways leading to it are not well understood in these infections. Here, in order to investigate NF- κ B activation induced by *H. pylori* or *L. pneumophila*, a new technique was developed ideal for detailed single cell analysis of NF- κ B as well as high-throughput screening. Monoclonal cell lines were generated that stably express the NF- κ B subunit p65 fused to green fluorescent protein (GFP). Nuclear translocation of p65-GFP can be visualized by fluorescence microscopy and quantified by software-based picture analysis. Using this technology, inducer-specific temporal profiles of p65-GFP nuclear translocation could be observed including oscillations after *H. pylori* infection. To identify new factors important for NF- κ B activation, the new assay was used to conduct an RNAi-based screen. In the screen, infection with *H. pylori* was compared to induction with the cytokines TNF α and IL-1 β . In total, 24 key regulators for NF- κ B were identified. Network analysis highlighted the impact of a group of proteins known for their functions in the cell cycle. This included the cell cycle regulator SKP2 which was important for termination of NF- κ B activation. Two further factors, ALPK1 and CRKRS were necessary for *H. pylori*-induced p65 translocation. The identification of these factors broadens our understanding of NF- κ B signaling and could provide targets for future therapies. Finally, detailed observation of NF- κ B activation induced by *L. pneumophila* in single cells revealed a unique, biphasic NF- κ B activation. During the first hours, bacterial flagellin induced strong but transient activation. Then, p65 translocated continuously to the nucleus over hours without oscillation. Testing an array of bacterial mutants, a tight link between bacterial replication and continuous NF- κ B activation could be shown. Because this continuous nuclear localization is very unusual for a transcription factor of the NF- κ B family, this indicates that *L. pneumophila* could manipulate NF- κ B to ensure host cell survival.

Zusammenfassung

Bakterielle Infektionen, beispielsweise mit dem karzinogenen Bakterium *Helicobacter pylori* oder dem intrazellulärem Bakterium *Legionella pneumophila*, aktivieren den Transkriptionsfaktor Nuclear factor kappa B (NF- κ B). Dies trägt einerseits zur Zytokinproduktion bei, wodurch die Immunantwort aktiviert wird, andererseits zur Hochregulation von anti-apoptotischen Genen. In *H. pylori*-Infektionen stellt diese doppelte Funktion einen mechanistischen Link zwischen der chronischen Entzündung und der Krebsentstehung dar. Für *L. pneumophila* ist die Anti-Apoptose von Vorteil, da hierdurch das Überleben der Wirtszelle gesichert wird. NF- κ B kann daher den Ausgang von Infektionen entscheidend beeinflussen und es ist von zentralem Interesse, Mechanismen der NF- κ B-Aktivierung zu verstehen. Bisher sind jedoch sowohl die Dynamik der NF- κ B-Aktivierung, als auch die Signalwege, die zu der Aktivierung führen, nicht ausreichend untersucht. Um NF- κ B analysieren zu können, wurde hier eine neue Technik entwickelt, die sowohl Beobachtung von NF- κ B in einzelnen Zellen, als auch Anwendung im Hochdurchsatz erlaubt. Monoklonale Zelllinien wurden hergestellt, die ein Fusionsprotein der NF- κ B-Untereinheit p65 mit dem grün fluoreszierenden Protein (GFP) stabil exprimieren. Die Kerntranslokation von p65-GFP kann mit Fluoreszenz-Mikroskopie visualisiert und mit automatischer Bildanalyse quantifiziert werden. Mit dieser Methode konnten Stimulus-spezifische, zeitabhängige Profile der Kerntranslokation von p65-GFP gezeigt werden und zum ersten Mal eine durch ein Bakterium induzierte Oszillation von p65-GFP. In einem RNAi-basierten Hochdurchsatzscreen wurde diese Methode eingesetzt um neue Faktoren im NF- κ B-Signalweg zu identifizieren. Dabei wurde die Infektion mit *H. pylori* mit den Induktoren TNF α und IL-1 β verglichen. Insgesamt wurden 24 Regulatoren identifiziert. Bei einer Netzwerkanalyse trat eine Gruppe von Proteinen hervor, die durch ihre Funktion im Zellzyklus bekannt ist. Hierzu gehörte auch das Protein SKP2, das für die Termination der NF- κ B-Aktivierung wichtig war. Zwei weiteren Faktoren, ALPK1 und CRKRS waren notwendig für die *H. pylori*-induzierte NF- κ B-Aktivierung. Die Identifikation dieser Faktoren vertieft nicht nur unser Verständnis des NF- κ B-Signalweges, sondern bietet auch neue molekulare Ziele für mögliche zukünftige Therapien. Bei der detaillierten Analyse der *L. pneumophila*-induzierten NF- κ B-Aktivierung konnte ein einzigartiger, zwei-phasiger Ablauf gezeigt werden. Zunächst verursachte bakterielles Flagellin eine starke, aber kurze Aktivierung. Später war p65 dauerhaft über Stunden im Kern lokalisiert, was eng an die Replikation der Bakterien gekoppelt war. Da die kontinuierliche Kernlokalisation für Transkriptionsfaktoren der NF- κ B Familie sehr ungewöhnlich ist, könnte dies ein Hinweis für eine Manipulation durch das Bakterium sein, um das Überleben der Wirtszelle zu sichern.

1 Introduction

The tight interaction of pathogens such as bacteria, viruses and fungi and their hosts are marked by survival strategies on both sides. While pathogens have evolved to develop many strategies to manipulate their hosts, humans possess an effective defense system to counteract infections. Two immune systems facilitate the defense: The adaptive immune system adapts to the agent causing the infection and specifically targets this pathogen. The innate immune system uses general mechanisms common in infections to provide the initial and fast response. The latter is molecularly based on pattern recognition receptors (PRRs) of the host that recognize conserved microbe-associated molecular patterns (MAMPs). MAMPs encompass different structures such as lipids, glycans or nucleic acids, that are necessary for the bacteria but not present in host cells¹. The best known PRRs are the Toll-like receptors named after the Toll receptor in the fruit fly *Drosophila melanogaster* as well as the nucleotide-binding and oligomerization domain (NOD)-like receptors (NLRs)^{2,3}. To trigger an immune response, every TLR and NLR activates the transcription factor family nuclear factor (NF)- κ B⁴ which induces production of cytokines, chemokines and upregulation of costimulatory molecules important for immune cell activation⁵. In addition, NF- κ B regulates cell division and survival⁶.

Mediating such important responses, NF- κ B activation needs to be limited and uncontrolled NF- κ B signaling bears high damaging potential. Excess expression of NF- κ B-induced cytokines can be fatal (i.e. in septic shock⁷). NF- κ B regulated anti-apoptosis is important in tumorigenesis⁸ and permanent activation of the immune system drives chronic inflammatory diseases⁹. Especially in long-term infections such as the life-long colonization with the cancerogenic gastric pathogen *Helicobacter pylori*, a large part of the pathology can be attributed to the response of the host and NF- κ B is believed to play a central role in the development of such chronic diseases¹⁰. Accordingly, deregulation of NF- κ B is associated with chronic inflammatory diseases and many forms of cancer^{8,11}.

The NF- κ B system is a target of manipulation by pathogens. For example, intracellular pathogens that reside within a cell and are thus dependent on the life of this host cell, use the anti-apoptotic effect of NF- κ B to prevent host cell death. Therefore, NF- κ B plays two key roles in infection: First, it regulates the immune response to the pathogen and second, it controls survival of host cells. Because both functions determine disease outcome, it is

of central interest, to study NF- κ B activation in infections. This thesis analyses signaling leading to NF- κ B activation after the cancerogenic pathogen *H. pylori* and the intracellular pathogen *Legionella pneumophila*. Here, first, NF- κ B signaling will be introduced, then the two pathogens and finally the technique of RNA interference screening.

1.1 The transcription factor family NF- κ B

1.1.1 Function of NF- κ B

NF- κ B was discovered in B cells where it binds to the enhancer region of the κ light-chain gene of immunoglobulin after stimulation with the bacterial cell wall component lipopolysaccharide (LPS)¹². Soon after, NF- κ B was shown to be inducible in all cell types and to date, NF- κ B is known as transcriptional regulator of many genes. Two pathways of NF- κ B activation are known. One, called the classical pathway, is induced by pro-inflammatory cytokines such as cytokines tumor necrosis factor α (TNF α), interleukin (IL)-1 β as well as by engagement of TLRs. This is essential for rapid activation of the innate immune system in response to inflammatory stimuli. A second pathway, named the alternative or non-classical NF- κ B pathway depends on specific mediators and protein synthesis^{13,14} and regulates lymphoid organogenesis and adaptive immunity in a slow response to B cell-activating factor (BAFF), cluster of differentiation 40 (CD40)-ligand and lymphotoxin α (LT α)-LT β heterotrimers¹⁵. This thesis concentrates on the classical pathway.

Functions of NF- κ B are based on the effects of the target genes transcribed upon NF- κ B activation. When translocated into the nucleus, NF- κ B subunits bind to discrete sequence in regulatory regions of about 150 genes¹⁶, some of which promote inflammations such as the potent neutrophil attractor IL-8¹⁷ or the cytokines TNF α ^{18,19} and IL-1 β ²⁰. This has important functions in infection: Mice that lack the NF- κ B subunit p65 suffer from impaired leukocyte recruitment to sites of infection²¹. Other genes induced by NF- κ B promote proliferation including cyclin D1²² and again others have anti-apoptotic function such as cellular inducer of apoptosis (c-IAPs) or FADD (FAS associated death domain)-like IL-1 β -converting enzyme (FLICE) -inhibitory protein (c-FLIP)⁶ [www.nf-kb.org]. Therefore, activation of NF- κ B induces the immune response, proliferation and anti-apoptosis.

1.1.2 Components of NF- κ B signaling: subunits, inhibitors and kinases

The family of NF- κ B transcription factors comprises the five subunits p65 (RelA), RelB, c-Rel, p50/p105 (NF- κ B1) and p52/p100 (NF- κ B2). They can form any combination of ho-

mo- and heterodimers but with different functionality. The classical proteins p50 and p65 are ubiquitously expressed and form the dimer p65:p50 most prominently responsible for inflammation. RelB and p52 form the dimer of the alternative pathway and are therefore important for lymphoid organogenesis. Because p50 and p52 lack transcriptional activation domain but both bind DNA, homo- or heterodimers consisting only of these two proteins act as transcriptional inhibitors. The dimers p65:RelB, cRel:RelB and RelB:RelB are not able to bind DNA. All other dimers act as functional transcriptional activators²³.

Activation of NF- κ B was found not to require protein synthesis²⁴ but dissociation from an inhibitor termed inhibitor of κ B (I κ B)²⁵. Five inhibitors are known: I κ B α , I κ B β , I κ B ϵ , p105 and p100. The latter two are the precursor proteins of p50 and p52, respectively and their inhibitory C-terminal portions have been named alternatively I κ B γ and I κ B δ ²³.

Degradation of the inhibitor depends on the proteasome²⁶, which in turn depends on phosphorylation of the inhibitor²⁷. A complex was identified that could catalyze this phosphorylation and the major kinases in this complex were named inhibitor κ B kinase (IKK) 1 and 2 (later renamed IKK α and IKK β)²⁸⁻³⁰. IKK α was also identified in a two hybrid screen as a protein interacting with NF- κ B inducing kinase (NIK), a kinase named for its induction of NF- κ B when overexpressed³¹. A regulatory subunit of the IKK-complex was termed IKK γ ³² or NF- κ B essential modulator NEMO³³. The trimer of IKK α , IKK β and NEMO has a calculated molecular mass of 220 kDa but when the IKK complex is isolated from cells, it has a size of 700-900 kDa suggesting a possible oligomerization or additional compounds in the complex. The notion that IKKs can form dimers via their leucine zipper motifs and NEMO can form trimers or tetramers supports the hypothesis of a multimer-complex³⁴. ELKS, a protein named for the relative abundance of its constitutive amino acids: glutamic acid (E), leucine (L), lysine (K), and serine (S), has been proposed to be a regulatory component of the complex³⁵ but this is not finally established³⁶. Furthermore, additional components such as the heat shock protein (HSP) 90 and cell division cycle (CDC) 37 have been shown to be recruited to the complex in a transitory manner³⁷. Two additional IKK homologues have been identified: IKK ϵ (also named IKK-i) and TBK1 (TNFR-associated factor (TRAF) family member-associated NF- κ B activator (TANK) binding kinase 1, also known as NF- κ B activating kinase NAK). These kinases are expressed in few cell types and their exact function remains to be established³⁴.

1.1.3 Basic NF- κ B signaling principle and NF- κ B oscillation

In non stimulated cells, NF- κ B (most prominently p65:p50) resides sequestered by its inhibitor in the cytoplasm²⁵. Binding of I κ B α masks the nuclear localization sequence (NLS) of p65 but the remaining NLS of p50 plus an exposed nuclear export sequence (NES) of I κ B α leads to constant shuttling of the complex between the nucleus and the cytoplasm. Nevertheless, the complex is predominantly present in the cytoplasm³⁸.

Upon stimulation, the IKK complex phosphorylates I κ B proteins on two conserved serine residues (S32 and S36)^{39,40}. This leads to recognition of the complex by the beta transducin repeat-containing protein (β TrCP) F-box-protein, the component facilitating substrate specificity in the S-phase kinase-associated protein 1 (SKP1), CDC53/Cullin1, F-box protein (SCF) E3 ubiquitin-protein ligase complex called SCF ^{β TrCP}, which polyubiquitinylates the inhibitor^{41,42}. This leads to degradation of I κ B α by the proteasome, freeing the NF- κ B dimer to enter the nucleus and trigger transcription of target genes⁴³. Phosphorylation of p65 influences DNA-binding and transcription^{38,44}. One of its target genes is the inhibitor itself, which is rapidly synthesized, enters the nucleus and binds NF- κ B. Subsequently, the newly formed complex translocates into the cytoplasm^{45,46}.

As long as the external signal remains, the process of inhibitor degradation and re-synthesis will repeat itself leading to oscillations in translocations⁴⁷. Additional silencing mechanisms which will be discussed in more detail below lead to dampening of the oscillations and termination of the signal (Fig. 1).

1.1.4 Signaling to IKK

NF- κ B pathway can be activated by various stimuli such as cytokines TNF α and IL-1 β , TLR engagement by bacterial components like LPS, binding of ligand to T cell receptor (TCR) as well as chemical and physical stresses [www.nf-kb.org]. Signaling to the IKK complex is mediated through intracellular adaptor proteins (Fig. 1). Different inducers utilize similar adaptors, providing molecular modularity. Particularly the TNFR-associated factors (TRAFs) and receptor-interacting protein 1 (RIP1) are critical mediators. All TRAFs contain C-terminal coiled coil domains that facilitate interactions with other proteins and (with the exception of TRAF1) N-terminal zinc-binding motifs including a really interesting new gene (RING) finger³⁴. The latter can function as ubiquitin ligase, which has been shown for TRAF2 and TRAF6³⁶.

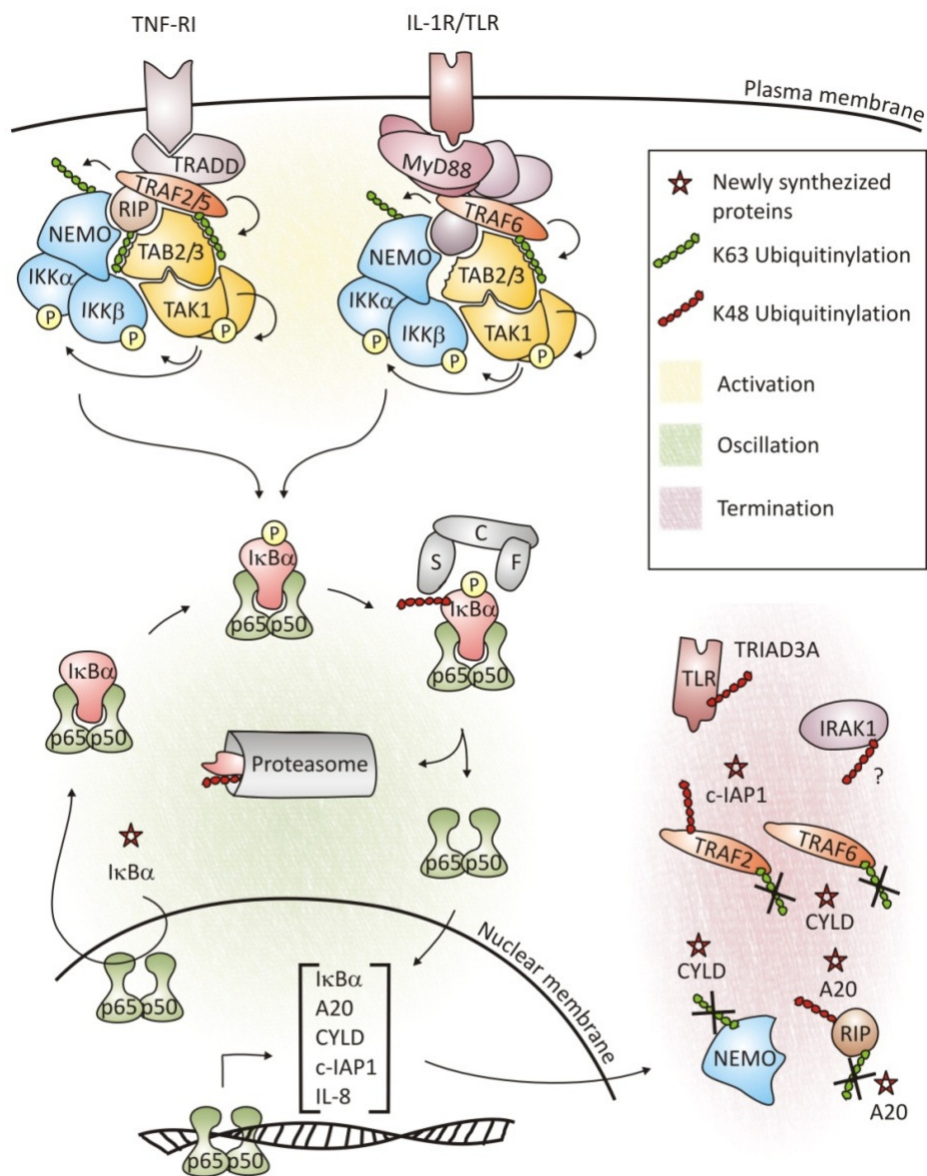


Fig. 1: Activation, oscillation and termination of NF- κ B signaling. Engagement of receptors (TNF-R1, IL-1R or TLRs) leads to recruitment of adaptor proteins specific for the respective receptor. TRAFs are also recruited to this complex and facilitate Lys63-linked ubiquitinylation of further mediators (RIP in the case of TNF signaling). This first complex recruits the IKK complex consisting of NEMO, IKK α and IKK β . NEMO is Ub^{Lys63}-modified which probably stabilizes the interaction. The third complex consisting of TAK1, TAB2 and TAB3 is thought to be recruited via ubiquitin binding sites of TABs. TAK1 undergoes autophosphorylation and subsequently phosphorylates IKKs. IKKs phosphorylate I κ B α which is then Ub^{Lys48}-modified by SCF^{TRC^P} E3 ligase and degraded by the proteasome. This frees the NF- κ B dimer (here p65:p50) to translocate into the nucleus and trigger transcription of target genes, some of which lead to negative-feedback. Re-synthesis of I κ B α leads to oscillation of NF- κ B dimers between the nucleus and the cytoplasm. In the termination phase, the de-ubiquitinylating enzymes CYLD and A20 remove activating Ub^{Lys63} chains and E3 ligases A20, c-IAP1 and TRIAD3A add Ub^{Lys48} chains to activators to mark them for degradation. IRAK1 is also degraded in the termination phase but ubiquitinylation is not yet demonstrated.

Much of the knowledge about NF- κ B signaling is gained from research on the pathway induced by TNF α receptor 1 (TNF-R1). Binding of the ligand to this receptor leads to recruitment of the adaptor molecule TNF receptor-associated death domain (TRADD) which in turn recruits TRAF2, TRAF5 and RIP1. TRAF2 facilitates Lys63-linked ubiquitylation of RIP1, which is thought to stabilize further interaction with downstream mediators but this function is not yet clearly established⁴⁸. Nevertheless, RIP1 binds to NEMO which is also Ub^{Lys63}-modified. These two complexes (Receptor/TRAFs/RIP1 and NEMO/IKK α /IKK β) now recruit the third complex consisting of transforming growth factor beta activated kinase 1 (TAK1), TAK1-binding protein 2 (TAB2) and TAB3. This recruitment is thought to be facilitated by ubiquitin-dependent interactions: TABs as well as NEMO have been shown to possess ubiquitin binding domains with binding preference for Ub^{Lys63} chains⁴⁹⁻⁵¹. Therefore, TABs or NEMO could bind ubiquitylated TRAFs, RIP or NEMO. Binding of the TAB2/TAB3/TAK1 complex to the other two complexes has two functions. First, TAK1 is activated, possibly via dimerization and trans-autophosphorylation⁵² and second, it brings TAK1 and the IKK complex in close proximity. IKK β is then activated by phosphorylation, probably by TAK1. In addition, mitogen-activated protein (MAP)/extracellular signal-regulated kinase (ERK) kinase kinase 3 (MEKK3 also known as MAP3K3) may play a role in activating IKK β but the underlying mechanism remains to be clarified³⁴.

Induction of NF- κ B by IL-1 receptor and TLRs is mechanistically similar to TNF α signaling but relies on different adaptor proteins. Both receptors signal through their intracellular Toll/IL-1 receptor (TIR) -homology domain. Binding of the ligand results in both cases in recruitment of the adaptor protein myeloid differentiation primary response gene 88 (MyD88) which also contains a TIR domain. This process involves other TIR-containing adaptor proteins depending on the receptor engaged. MyD88 dimerizes and recruits interleukin-1 receptor-associated kinase 1 (IRAK1) and IRAK4, which in turn are necessary for recruitment of TRAF6. TRAF6 oligomerizes and undergoes Lys63-linked trans-auto-ubiquitylation which probably leads to recruitment of the complex TAB2/TAB3/TAK1. Similar as in the case of TRAF2, the importance of E3-ligase activity of TRAF6 is not finally established^{34,36,48}. In spite of the remaining controversy about the importance of the E3-ligase activity of the TRAFs, the relevancy of Ub^{Lys63} is strengthened by the existence of several de-ubiquitylation (DUB) enzymes that are important for termination^{14,48}.

Pathways induced by TCR or DNA damage follow similar mechanisms with shared and additional adaptor molecules^{34,48,53}. However, as they are not part of this work they will not be discussed further.

In infections, the activation of PRRs, such as TLRs by MAMPs is well known. However, not all NF- κ B activation in infections can be attributed to PRR signaling and in some infections, such as in infections with *L. pneumophila* and *H. pylori*, the signaling leading to activation is enigmatic.

1.1.5 Termination of NF- κ B signaling

Termination of NF- κ B signaling still remains poorly understood. The first group of proteins silencing NF- κ B is comprised of the three I κ Bs: I κ B α in its direct feedback loop leads to nuclear export of NF- κ B subunits, but until the upstream signal is terminated, NF- κ B subunits will shuttle between nucleus and cytoplasm (Fig. 1). I κ B ϵ is also transcribed upon NF- κ B activation but re-synthesis is delayed in comparison to I κ B α . This kinetic effect leads to dampening of the oscillations^{54,55}. The third inhibitor, I κ B β , also undergoes slow degradation and re-synthesis like I κ B ϵ but its deletion has no dramatic effect on termination of NF- κ B signaling^{54,55}.

Ubiquitinylation plays a dual role in termination of NF- κ B: activating enzymes can be marked for degradation by Ub^{Lys48} modification or activating Ub^{Lys63} chains can be removed by DUB enzymes^{48,56} (Fig. 1). The first mechanism includes receptor degradation as well as degradation of downstream signal molecules. The E3 ubiquitin ligase triad domain containing protein 3A (TRIAD3A, named for the triad domain consisting of two RING domains and a double RING finger linked (DRIL) domain and also known as ring finger protein 216 (RFP216)) has been shown to ubiquitinylate TLR4 and TLR9 which leads to their degradation⁵⁷. Similarly, the signaling adaptors RIP1 and TRAF2 are marked for degradation by ubiquitinylation by E3 ligases A20 (also known as TNF α -induced protein 3 TNFAIP3)⁵⁸ and cellular inhibitor of apoptosis 1 (c-IAP1)⁵⁹, respectively. IRAK1 is also degraded following activation but the E3 ligase remains to be identified^{34,60}. Interestingly, both A20 as well as c-IAP1 are transcriptionally upregulated after induction of NF- κ B inducing a negative feedback loop⁴⁸. A20 plays a dualistic role as it serves not only as E3 ligase for Lys48-linked ubiquitinylation of RIP1, but its DUB domain removes activating Ub^{Lys63} chains from RIP1 prior to degradation⁵⁸. The second well known DUB enzyme is the protein of the cylin-

dromatosis gene CYLD. A defect in this gene is responsible for the turban tumor syndrome, a familial cancer. CYLD protein binds to TRAF2, TRAF6 and NEMO and removes activating Ub^{Lys63} chains⁶¹⁻⁶³. Two further DUB enzymes have been identified: cellular zinc finger anti NF- κ B (Cezanne) which also removes Ub^{Lys63} chains from RIP1⁶⁴ and TRAF-binding domain (TRABID) which was shown to interact with TRAF6⁶⁴.

In addition, promoter-bound p65 may be degraded by the proteasome⁶⁵. Suppressor of cytokine signaling 1 (SOCS1) might function as the E3-ligase for this reaction⁶⁶. It seems likely that more mechanisms exist to terminate NF- κ B signaling.

1.1.6 NF- κ B dynamics

One major remaining question in the field of NF- κ B research is how a system regulating such diverse functions can discriminate between different stimuli. Next to variations in post-translational modifications of NF- κ B subunits, combination of different NF- κ B subunits, selectivity toward certain binding sequences as well as combination with different co-activators, also the temporal control of NF- κ B signaling may account for the cell-type and stimulus-specificity²³. As stated above, the feedback loop of NF- κ B-I κ B α generates oscillations in nuclear translocations of NF- κ B^{47,54}. However, depending on the duration, the type and the concentration of the stimulus, different temporal profiles of the oscillations can be observed^{47,54,67,68}. Importantly, specific profiles can lead to activation of subsets of genes: Using short-term versus long-term activation of NF- κ B with TNF α , Hoffmann and coworkers could show that some genes (such as chemokine (C-X-C motif) ligand 10 (CXCL10)) are transcribed upon NF- κ B activation irrespective of the duration, while some genes (such as chemokine (C-C motif) ligand 5 (CCL5)) depend on long term NF- κ B activation⁵⁴. It is unclear, whether bacterial infections induce specific temporal profiles.

1.1.7 Monitoring NF- κ B dynamics

Although there are several assays to measure NF- κ B activation, studies investigating the dynamics of the transcriptional response are hampered by a lack of suitable methods. Commonly used tools for general NF- κ B analysis are reporter plasmids, in which an NF- κ B binding site drives the transcription of reporter genes like green fluorescent protein (GFP) or luciferase. Stable cell lines with these constructs are commercially available (i.e. from Invitrogen). However, these constructs as well as the cell lines are not suitable for real-time analysis of dynamics because they measure transcriptional responses accumulated

hours after activation. Furthermore, they do not discriminate between activities of single NF- κ B subunits but report the summarized transcriptional activity of NF- κ B dimers. Biochemical approaches like the electrophoretic mobility shift assay (EMSA) have been used successfully to detect oscillations in the temporal response of NF- κ B^{54,55,67,68}, but these strategies are time consuming and the protein extracts used for biochemical analysis average the potentially divergent responses of single cells.

Since activation of NF- κ B is marked by the translocation of NF- κ B subunits from the cytoplasm to the nucleus, many studies have followed the dynamics of NF- κ B activation using fluorescent protein fusions^{47,69-73}. It was Nelson and co-workers^{47,69} who first showed NF- κ B oscillations at a single-cell level, using live-cell microscopy of cells transiently transfected with NF- κ B proteins fused to fluorescent moieties; however, transient transfections entail important difficulties: inevitably, the amount of plasmid DNA varies from cell to cell, leading to variations in expression levels. Because the NF- κ B system is so tightly regulated, changes in expression levels can lead to changes in dynamics of signaling and therefore altered synchrony of the nuclear translocations⁷⁴. Therefore, asynchronous responses detected in previous studies using transiently transfected cells⁴⁷ may not reflect oscillations observed in untransfected cells⁷⁴. A system that integrates GFP technology with clonal cell lines where expression level variations due to different amounts of DNA are excluded, may be more insightful⁷⁴.

1.2 The bacterium *Helicobacter pylori*

Over a hundred years ago, the first bacteria were identified in patients with gastric cancer⁷⁵ but the contribution of bacteria to gastric pathologies was not widely recognized until Marshall and Warren identified *H. pylori* in biopsies of gastric cancers in 1984⁷⁶. *H. pylori* are gram-negative, highly successful bacteria, colonizing the stomachs of about fifty percent of all humans worldwide⁷⁷. Infection occurs mainly during childhood within families through close person-to-person contact, possibly fecal-orally or via vomitus⁷⁸. Once established, the bacterium resides in the gastric mucosa over decades. The chronic inflammation can develop into three types of pathologies: (i) asymptomatic mild gastritis (majority of the infected individuals), (ii) antral predominant gastritis leading to duodenal ulcers (10-15%) or (iii) corpus-predominant gastritis with increased risk of cancer (about 1%)⁷⁸. *H. pylori* is causally related to two forms of gastric cancer: mucosa associated lymphoid tissue (MALT) lymphoma (a non-Hodgkin B cell lymphoma) and the more common

gastric adenocarcinoma⁷⁹. The relationship is impressively demonstrated in MALT lymphoma, where, at an early stage, the lymphoma regresses upon antibiotic treatment that eradicates *H. pylori*⁸⁰. Consequently, *H. pylori* is recognized as a class I carcinogen by the World Health Organization (WHO)⁸¹. 60-90% of gastric cancers can be attributed to *H. pylori* infection⁸² and with 1.1 Mio estimated cases for 2010⁸³ as well as a poor prognosis of only 20% 5-year survival⁸⁴, *H. pylori* is a major cause of cancer-related deaths. On the other hand, *H. pylori* infection can have a protective effect for reflux disease and adenocarcinoma of the esophagus and it was proposed that the outcome of infection depends on host-pathogen interplay⁸⁵.

To survive in the stomach, *H. pylori* uses the enzyme urease to buffer the pH⁸⁶ and swims to the less acidic mucus layer⁸⁷ where it adheres to host cells via adhesins⁸⁸, a contact that is almost irreversible⁸⁹. *H. pylori* secretes the vacuolating toxin A (VacA) which induces formation of large cytoplasmic vacuoles and is thus considered highly damaging for the epithelium⁷⁸ (Fig. 2). At the epithelium, *H. pylori* strains that carry a 40 kilobase DNA fragment known as cytotoxin-associated gene pathogenicity island (*cagPAI*) can secrete at least one bacterial factor called CagA into the host cell cytoplasm via a type IV secretion system (T4SS)⁹⁰ (Fig. 2). Both CagA and T4SS are encoded by *cagPAI*. It is the *cagPAI*-positive strains that are associated with severe diseases⁹¹. Following injection into the host cell cytoplasm, CagA is phosphorylated by host cell kinases and interacts with various host cell proteins, leading to activation of various signaling cascades such as the mitogen activated protein kinase (MAPK) pathway and a change of host cell morphology as well as loss of epithelial cell-cell adhesion⁹².

On the host side, polymorphisms in human genes for IL-1 β , IL-1 β -receptor, TNF α , IL-10, IL-8, TLR4 and human leukocyte antigen (HLA) have been linked to *H. pylori* induced pathology⁹³⁻⁹⁶. Remarkably, all of these genes produce factors of the immune system, underlining the importance of the host's immune system in the development of severe diseases. This influence is thought to result from chronic inflammation: When neutrophils and monocytes are recruited to the site of infection, they release reactive oxygen intermediates which (together with the bacterial factors) damage the tissue. During the life-long course of inflammation, repeated damage and proliferation leads to a steady turnover of cells which increases the probability of genetic changes and thereby of malignancies⁹⁷. Therefore, the study of innate immune response is of crucial interest.

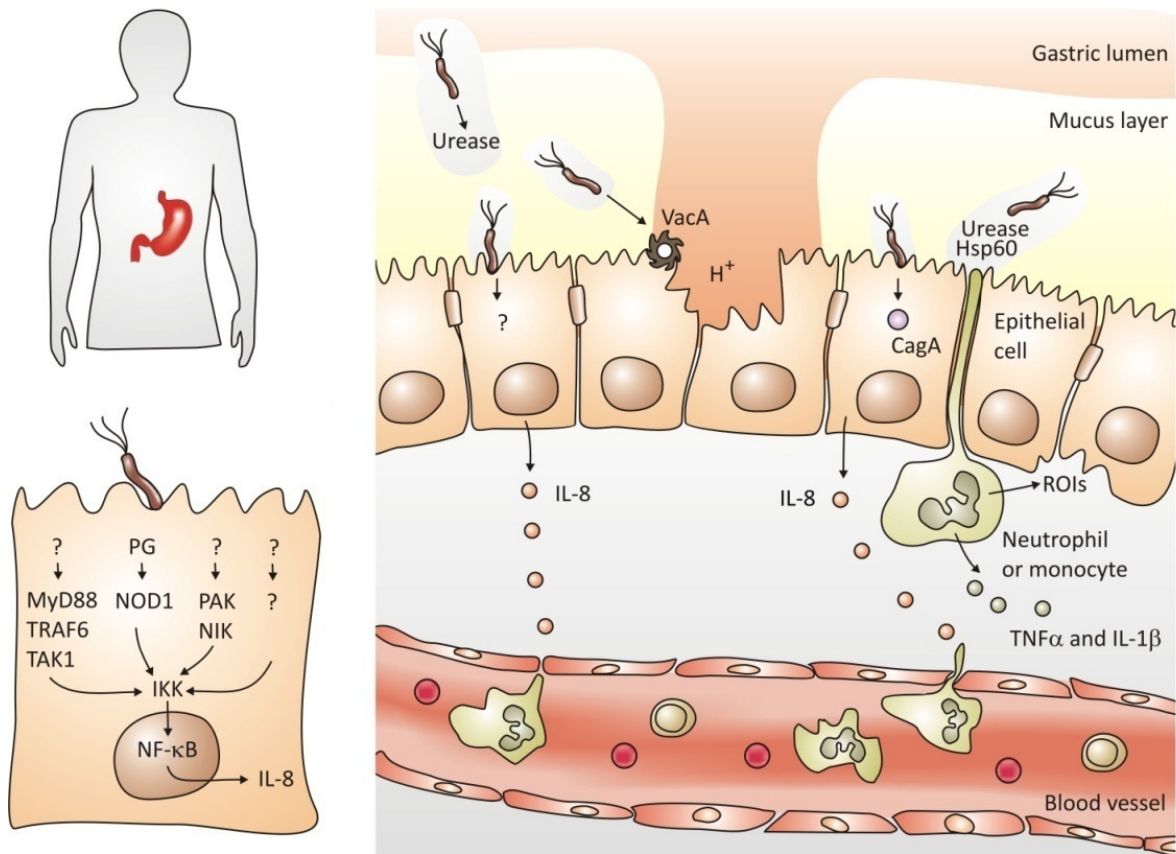


Fig. 2: Interaction between *H. pylori* and its host. Infecting the human gastric mucosa, *H. pylori* utilizes the enzyme urease to buffer pH and its flagella to reach the mucus layer. Secreted VacA induces vacuolization of the epithelial cells. Attaching to epithelial cells, *H. pylori* can translocate CagA via its T4SS into the host cell cytoplasm. Bacterial peptidoglycan and possibly other factors are also translocated into the host cell. This induces profound cellular changes as well as NF- κ B activity which lead to secretion of the neutrophil attractor IL-8. Neutrophils and monocytes extravagate from the blood vessel and cause tissue damage by releasing reactive oxygen intermediates (ROIs). Combined toxic activity of bacterial factors and ROIs lead to tissue damage enhanced by loss of the protective mucus layer. Neutrophils and monocytes also release further pro-inflammatory cytokines like TNF α and IL-1 β which stimulate parietal cells to decrease acid production, causing a raise of gastric pH and hypochlorhydria. This increases the risk of atrophic gastritis and subsequent development of gastric cancer. Lower left: In gastric epithelial cells, multiple pathways activate NF- κ B after infection with T4SS-positive *H. pylori*. Bacterial peptidoglycan activates NOD1. Other unknown factors are thought to activate MyD88, TRAF6 and TAK1 as well as PAK1 and NIK. Probably, additional so far unknown factors also activate NF- κ B (adapted from^{89,98}).

A potent regulator of the *H. pylori*-induced immune response is NF- κ B. NF- κ B-induced cytokines and chemokines have been shown to play an important role which can be divided into two distinct actions (Fig. 2). First, upon contact with *H. pylori*, the epithelium secretes IL-8⁹⁹ which recruits neutrophils and other immune cells to the site of infection. Second, the immune cells release TNF α and IL-1 β ⁹⁸. These cytokines reduce acid secretion by parietal cells causing a decrease in gastric acidity which in turn increases the risk of atrophic gastritis, a pre-malignant condition⁹⁸. In addition to these roles, the anti-

apoptotic function of NF- κ B is thought to enhance probability of survival of malignant cells that may have arisen in the process of cell proliferation^{10,100}.

The signaling pathways leading to NF- κ B activation seem to be very specific for the cell type and many different mediators have been proposed (Fig. 2). Generally, responses differ in mice and humans: IL-8 secretion in mice is independent of bacterial *cagPAI*^{101,102} while in humans it depends on *cagPAI*^{99,101}. Human macrophages and monocytes can also be activated by *cagPAI*-independent factors, such as *H. pylori* urease^{103,104} and HSP60¹⁰⁵. *H. pylori* LPS seems to play a minor role and only activates macrophages when applied in very high concentrations^{106,107}. Human gastric epithelial cells (primary cells and cell lines) exclusively react to *cagPAI* positive strains^{102,108-111}. To specify the *H. pylori* factors important for NF- κ B activation or IL-8 production in AGS cells, several groups analyzed isogenic mutants of *H. pylori* and showed that both, NF- κ B activation and IL-8 secretion, depend on *cagPAI* but not on CagA^{112,113}. Only during prolonged infections of 24-48 h, CagA influenced IL-8 secretion^{109,114}. Therefore, it is possible, that CagA could be necessary for a late-phase induction of IL-8.

To identify cellular receptors for NF- κ B activation by *H. pylori* in gastric epithelial cells, much interest has been focused on TLRs and NLRs¹⁰¹. TLR4 is not functionally expressed on gastric epithelial cells and can therefore not mediate NF- κ B activation in these cells^{101,115}. TLR9 does not recognize *H. pylori* DNA^{102,116}. Ectopically expressed TLR5 and TLR2 is able to induce NF- κ B activation in response to *H. pylori*¹¹⁷, however, endogenous TLR5 is not activated by *H. pylori* flagellin^{118,119} and HEK293 that do not express TLR2 can still be activated by *H. pylori*^{101,120,121}. Therefore, TLR2, TLR4, TLR5 and TLR9 do not play a major role in innate recognition of *H. pylori*. Recently, the intracellular PRR NOD1 has been implicated in sensing *H. pylori*¹²¹. NOD1 binds a specific motif of peptidoglycan (PG), a component of the gram-negative cell wall. It was proposed that bacterial PG could be transferred via the T4SS into the cell cytoplasm where it can trigger an NF- κ B response via NOD1. However, in *nod1* knockout mice, the secretion of macrophage inflammatory protein 2 (MIP-2), the murine homologue to IL-8, was only reduced, not abolished. Additionally, the authors were not able to show NOD1-dependent p65 nuclear translocation in gastric epithelial cells¹²¹ and other studies showed that RNAi targeting NOD1 had no impact on phosphorylation of I κ B α in AGS cells¹⁰². Thus it seems unlikely that NOD1 is exclu-

sively responsible for activation of NF- κ B and further work is needed to elucidate receptors leading to NF- κ B activation.

Several signaling pathways for NF- κ B activation by *H. pylori* have been proposed. Activation of both IKKs, IKK α and IKK β , has been shown repeatedly either by using dominant negative constructs or RNAi¹²²⁻¹²⁴. But upstream of IKKs, knowledge about the activating pathway remains fragmentary, especially because different groups have shown contradicting results. A number of studies suggested the involvement of NIK upstream of IKKs as expression of dominant negative NIK reduced NF- κ B promoter reporter activity in a range of gastric cell lines¹²³⁻¹²⁵. PAK1 was suggested to act upstream of NIK which was also shown with a dominant negative construct¹²⁴. However, NIK is thought to activate homodimers of IKK α in the alternative pathway and to be dispensable for the classical pathway³⁴. Although *H. pylori* has been implicated to be able to induce the alternative pathway in B cells¹²⁶, the transcriptional reporter construct used in the studies regarding NIK and PAK1 in epithelial cells is not specific for the alternative pathway but contains binding elements from the human immunodeficiency virus common for the classical p65:p50 dimer^{124,127}. Thus, involvement of NIK and PAK1 is not clearly established. Involvement of TRAF2 was also demonstrated using expression of dominant negative TRAF2¹²³. However, the same group showed in a later study that RNAi targeting TRAF2 had no effect on *H. pylori*-induced NF- κ B signaling¹⁰². Also the results regarding TAK1 were controversial. Expression of a dominant negative construct of TAK1 did not inhibit activity of a transcriptional NF- κ B reporter¹²⁵ while RNAi targeting the same gene inhibited *H. pylori*-induced phosphorylation of I κ B α and IL-8 secretion¹⁰². It seems that usage of dominant negative constructs can lead to different results as downregulation of endogenous gene products with RNAi. Although TLR2, TLR4, TLR5 and TLR9 are unlikely to play a role in NF- κ B activation in human epithelial cells, many of the mediators typical for TLR-signaling have been shown to be important in *H. pylori*-induced NF- κ B activation: RNAi targeting MyD88 and TRAF6 had an effect on phosphorylation of I κ B α and IL-8 secretion in AGS cells¹⁰². The same study showed no involvement of receptor-interacting serine-threonine kinase 2 (RIP2 also known as RICK) downstream of NOD1¹⁰².

In conclusion, knowledge about signaling pathways leading to NF- κ B activation after *H. pylori* infection remains both fragmentary and controversial. More detailed analysis is needed to elucidate the pathways leading to activation of this important pathway.

1.3 The intracellular bacterium *Legionella pneumophila*

Legionella pneumophila is an intracellular, gram-negative bacterium that causes severe pneumonia known as Legionnaires disease. It usually infects and resides within freshwater protozoa but when *Legionella* containing water droplets are inhaled, it can also infect human lungs¹²⁸. The intracellular lifestyle of *L. pneumophila* probably evolved to evade killing by predatory amoebae and to provide a niche to evade host immune response¹²⁹. However, to survive inside cells, *L. pneumophila* needs to prevent lysosomal degradation. To achieve this, the bacterium establishes an intracellular, membrane-bound compartment, called *Legionella* containing vacuole (LCV), which is resistant to fusion with lysosomes¹²⁹. During the replicative phase of its two-phased life cycle, *L. pneumophila* multiplies and recruits intracellular membranes from the endoplasmic reticulum for constant membrane supply for a growing LCV^{129,130}. After replication, *L. pneumophila* enters the transmissible, virulent phase which is marked by formation of a long flagellum¹³¹. Finally, it lyses the host cell, exits and finds the next host^{129,130}.

Essential for a successful infection, *L. pneumophila* employs a T4SS called Dot/Icm (defective in organelle trafficking/intracellular multiplication) to translocate effector proteins into the host cell. These effectors are pivotal for all steps of the infectious process, such as the establishment of the LCV, intracellular replication and release from the host cell¹³². Several studies have identified an array of Dot/Icm-translocated substrates which have been assigned different functions such as the recruitment of cellular organelles like mitochondria and membranes from the endoplasmic reticulum. However, the functions of many of the effectors remain unknown^{129,133,134}.

In humans, *L. pneumophila* can infect alveolar macrophages¹³⁵, but it is likely that infection spreads to lung epithelial cells, which in turn secrete cytokines, thereby promoting the disease^{136,137} (Fig. 3). *In vitro* it has been shown that *Legionella* infects human epithelial cells¹³⁸⁻¹⁴¹, leading to the secretion of cytokines and chemokines such as IL-8 in an NF- κ B-dependent manner^{137,142,143}.

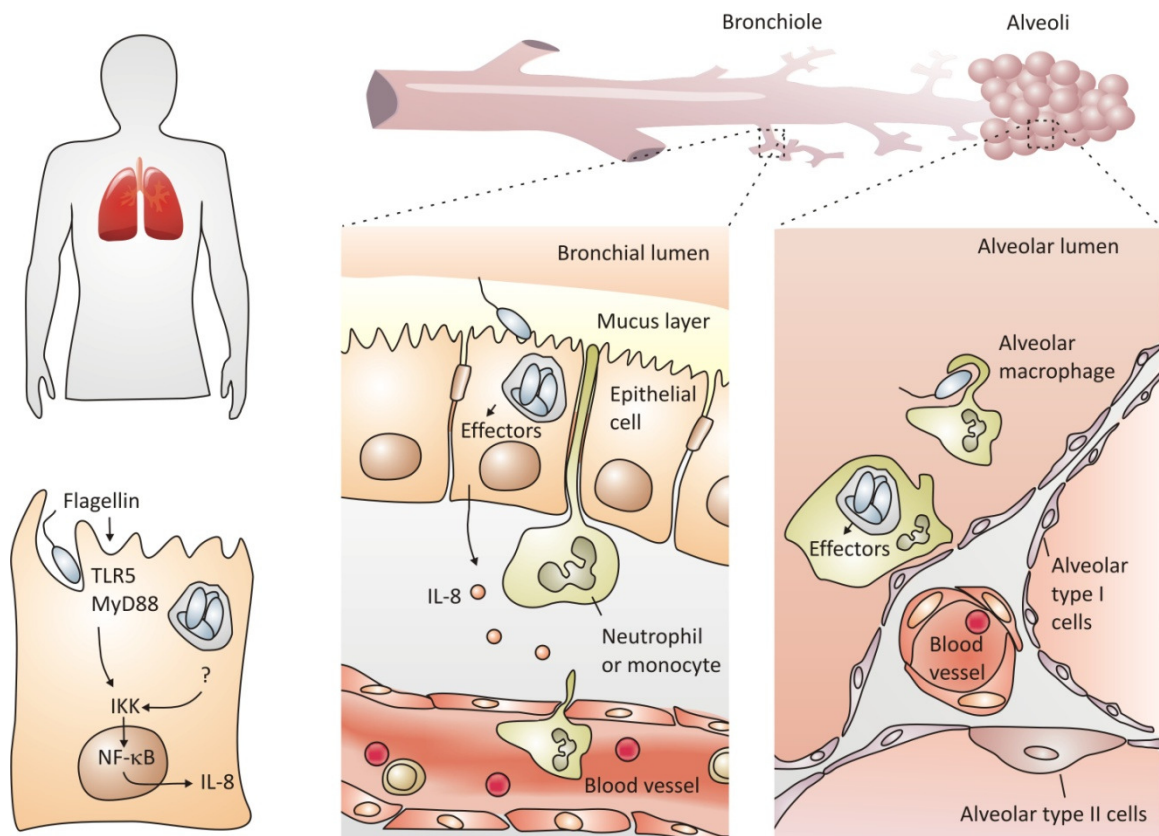


Fig. 3: Interaction between *L. pneumophila* and its host. The airway epithelium serves as first barrier against the pathogen and epithelial cells line the bronchioles as well as the alveoli. In alveoli, epithelium is referred to as type I and type II cells. *In vivo*, *L. pneumophila* is known to infect alveolar macrophages, but infection of the epithelium is also likely as the bacterium has been shown to infect epithelial cells *in vitro*. This leads to secretion of cytokines like IL-8 via NF- κ B which is thought to play an important role in the promotion of inflammation. In epithelial cells as well as in macrophages, *Legionella* secretes several effectors into the host cell cytoplasm via its T4SS which leads to the formation of the *Legionella* containing vacuole where the bacteria replicate. Lower left: In epithelial cells, bacterial flagellin is recognized by TLR5 which activates NF- κ B via MyD88. In addition, other factors, possibly secreted by the T4SS of the bacteria, can also activate NF- κ B.

The ability of *Legionella* to replicate successfully in human cells relies upon evasion and/or manipulation of host cell defenses and survival of the host cell it resides in. A critical factor regulating relevant cellular processes like proliferation, apoptosis, innate immunity and inflammation responses is the NF- κ B family of transcription factors. NF- κ B activation by *Legionella* has been demonstrated in macrophages and also in epithelial cells, which in turn secrete cytokines and chemokines^{137,142,143}. In this respect, NF- κ B activation as part of the host defense mechanism is beneficial for the host by triggering an innate immune response. On the other hand, it is also known that NF- κ B activation has anti-apoptotic effects, which is thought to be beneficial for intracellular pathogens that depend on host cell survival. Indeed, that was demonstrated for several pathogens including *Legionella*¹⁴⁴, *Rickettsia rickettsii*¹⁴⁵, *Toxoplasma gondii*^{146,147} and *Theileria parva*¹⁴⁸.

Two bacterial factors, flagellin and the Dot/Icm system, have been implicated in NF- κ B activation during *L. pneumophila* infection (Fig. 3). The structural component of the bacterial flagellum, flagellin, induces IL-8 secretion via NF- κ B in epithelial cells^{137,143}. Consistently, flagellin of *Legionella* is recognized by TLR5¹⁴⁹, and NF- κ B signaling depends on the TLR adaptor protein MyD88¹⁵⁰. The Dot/Icm system has also been shown as necessary for NF- κ B activation and subsequent upregulation of anti-apoptotic genes in infections of human macrophages^{144,150}. Losick and Isberg demonstrated an influence of the multiplicity of infection (MOI) on NF- κ B activation¹⁵⁰: Low dose infections (MOI 1) led to Dot/Icm-dependent and MyD88-independent NF- κ B activation, whereas at an MOI 10 or higher signaling occurred via MyD88 and in a Dot/Icm-independent manner. The reason for this observation is not known.

1.4 RNAi-based screens

RNA interference (RNAi) is a mechanism that post-transcriptionally inhibits specific genes. The key to this process are double-stranded small interfering RNAs (siRNAs) that have complementary nucleotide sequence to the targeted mRNA sequence. One of the strands of the siRNA guides the RNA interference inducing silencing complex (RISC) to bind and then cleave complementary mRNA. Thus, the expression of this gene is inhibited¹⁵¹.

Since the discovery of RNAi in *Caenorhabditis elegans* ten years ago¹⁵² and the subsequent demonstration, that RNAi is also effective in mammals¹⁵³, RNAi became a powerful tool to unravel gene functions. It also opened new possibilities of straightforward loss-of-function screens to identify novel components of any pathway. Due to the history of RNAi discoveries and the simplicity of RNAi delivery in *D. melanogaster* as well as in *C. elegans*, most screens have been conducted in these model organisms but recently, the number of screens conducted in the human system is growing. For example, recent screens in human cell lines have identified factors important for entry or propagation of pathogens such as human immunodeficiency virus (HIV)¹⁵⁴⁻¹⁵⁶, *Salmonella typhimurium*¹⁵⁷ and west nile virus¹⁵⁸. Up to date, no screen has exploited the possibilities to understand a host cell signaling response after infection.

1.5 Aims of this thesis

Despite its crucial importance of NF- κ B signaling in infections with *H. pylori* or *L. pneumophila*, the induction of NF- κ B by these pathogens and the dynamics of the activations are not well understood. In *H. pylori* infection, many signaling mediators have been proposed but the picture remains fragmentary. Therefore, it is hypothesized here, that other, so far unknown factors regulate NF- κ B activation induced by *H. pylori*. An aim of this thesis is, to identify these new factors with an RNAi-based screen. In *L. pneumophila* infection, two pathways are involved in NF- κ B activation and it has been implicated, that the decision, which of the pathways is activated, depends on the multiplicity of infection. However, the underlying mechanism is unclear. Here, analysis of dynamics and signaling are used to clarify NF- κ B activation induced by *L. pneumophila*.

To study signaling and dynamics, first, a suitable technique needed to be developed. This method should be amenable for high throughput screening as well as detailed analysis on single-cell level. For this purpose, monoclonal, lentivirally transduced cell lines were generated stably expressing p65-GFP. Nuclear translocation of p65-GFP can be observed in fluorescence microscopy and quantified by software-based picture analysis. Using this new technique, temporal control of p65-GFP translocation specific for the inducer could be shown, including oscillations after *H. pylori* infection.

This new method could then be utilized for an RNAi-based screen. To identify factors which might specifically act in infection, three inducers were compared: *H. pylori*, TNF α and IL-1 β . Knowing the responses induced by each stimulus, different time points in the dynamic process of p65-GFP nuclear translocation were observed to identify not only factors important for activation, but also for termination of NF- κ B signaling. The primary hits were then validated with additional siRNAs. The importance of single factors was further demonstrated by assessing the impact on upstream factors (IKK activity) and target genes (IL-8 secretion), functionality of bacterial T4SS, and induction of MAPK pathways.

In *L. pneumophila* infection, time-resolved monitoring of p65-GFP dynamics showed two subsequent activations of NF- κ B. Utilizing different mutant strains and RNAi, important bacterial and host cell factors could be identified.

2 Results and Discussion

2.1 Part I: Imaging NF- κ B activation using p65-GFP

2.1.1 A high throughput assay for cell lines expressing p65-GFP

To analyze p65 nuclear translocation within a large number of cells, an automated high-throughput assay based on nuclear translocation of p65-GFP was developed. First, a lentiviral vector was constructed that carries the genetic information of the NF- κ B subunit p65 fused to GFP. With this vector, four cell lines were transduced: the human alveolar epithelial cell line A549, human gastric epithelial cell line AGS, human cervical epithelial cell line HeLa and mouse fibroblasts cell line L929. From the lentivirally transduced cells, monoclonal cell lines (A549 SIB01, AGS SIB02, HeLa SIB04 and L929 SIB01) were selected. The expression ratio compared to endogenously expressed p65 was quantified with western blot analysis and is 1fold in A549 SIB01, 7fold in AGS SIB02, 5fold in HeLa SIB01 and 7fold in L929 SIB01 (Fig. 4a). In non stimulated cells, p65-GFP is mainly localized in the cytoplasm and upon stimulation with TNF α 10 ng/ml, p65-GFP translocates into the nucleus (Fig. 4b). In contrast to the three other cell lines, HeLa SIB04 displayed high heterogeneity and was therefore excluded from further analysis.

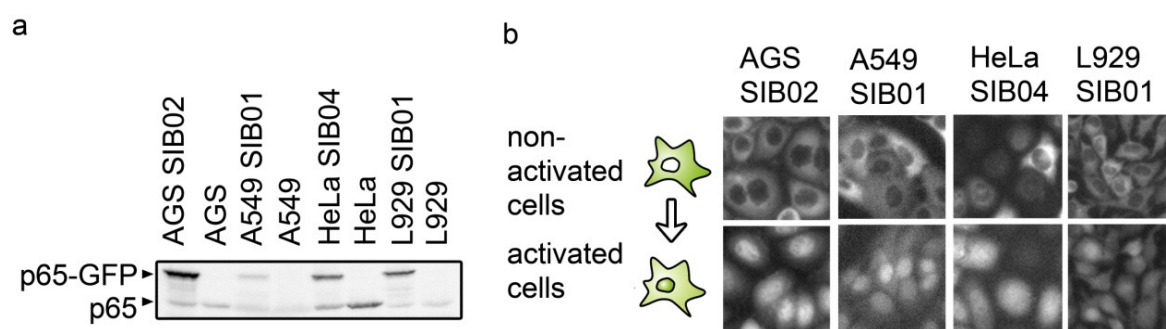


Fig. 4: Expression and nuclear translocation of p65-GFP in monoclonal cell lines. a) Western blot analysis of cell lines expressing p65-GFP and their parental cell lines shows overexpression of p65-GFP. This experiment is representative of at least five independent experiments. b) Nuclear translocation of p65-GFP can be visualized by fluorescence microscopy. Cell lines A549 SIB01, AGS SIB02, HeLa SIB04 and L929 SIB01 were seeded in 96-well-plates and either non activated or activated with TNF α 10 ng/ml. Cells were fixed after optimal activation time and pictures were taken with an automated microscope (Olympus Scan^R System). Shown are representative cell samples as depicted in the analysis software.

For the high throughput assay, automated microscopy was coupled to software-based picture analysis of p65-GFP. For this, cells were seeded into 96-well-plates, stimulated for 30 min with TNF α 10 ng/ml, fixed and nuclei stained with Hoechst. Images of cells were

acquired using automated microscopy. Cell nuclei were detected and the surrounding cytoplasmic area set using image analysis software (Fig. 5a).

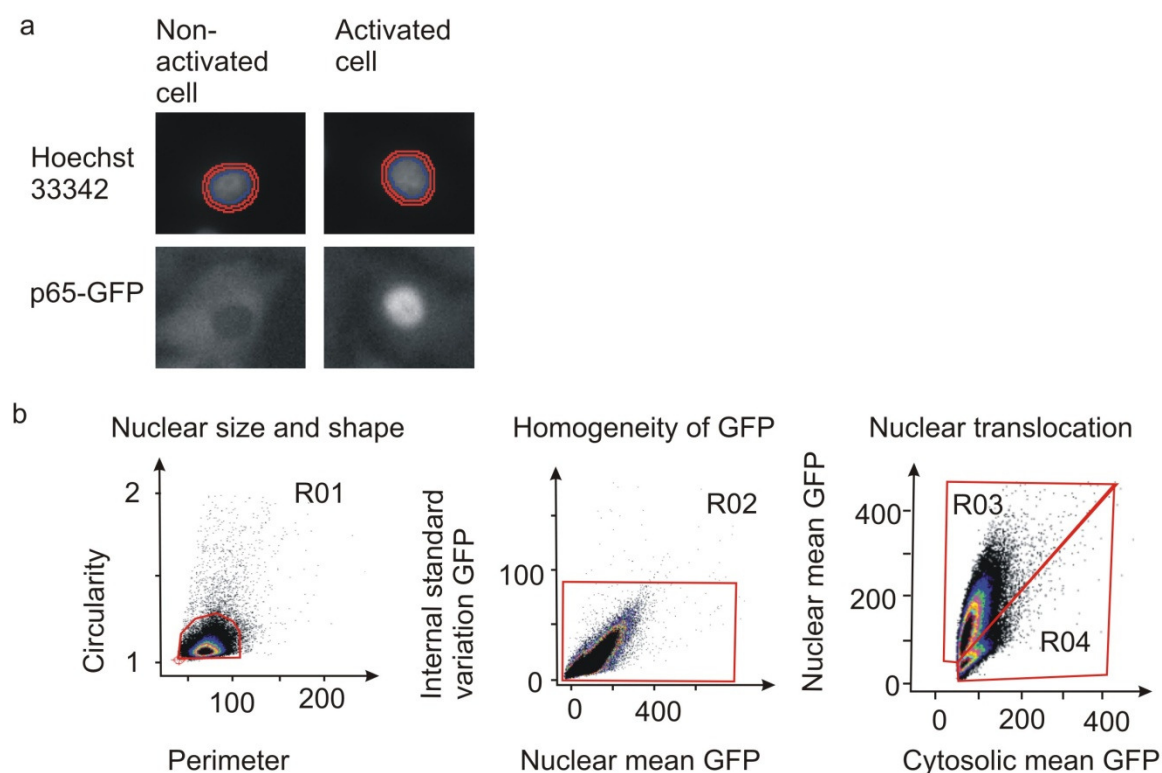


Fig. 5: Quantification of nuclear translocation of p65-GFP using automated microscopy and software-based picture analysis. a) Subcellular areas defined for the translocation assay in the Scan[^]R software. As an example, A549 SIB01 cells are shown. Blue: Defined nuclear area, Red: Defined cytosolic area. Cells were fixed and stained with Hoechst 33342. Depicted are one activated and one non-activated cell. b) Translocation assay for A549 SIB01 using Scan[^]R Analysis. Cells were seeded on 96-well-plates and partially activated with TNF α 10 ng/ml in order to have mixed populations of activated and non-activated cells. Cells were fixed, stained with Hoechst 33342 and analyzed by automated microscopy. Dot plots as depicted in analysis software are shown. Cells are gated for circularity and size (Region R01), intensity of GFP and standard variation of GFP intensity (Region R02) and the ratio of nuclear to cytoplasmic GFP intensity (Region R3 or R4). Cells are taken into account when they are in gates R01 and R02. They are defined “active” when they are also in gate R03 or “non-active” when they are also in gate R04. For graphs, the percentage of activated cells per well is calculated by the equation: Percentage of active cells = active cells / sum of active and non-active cells x 100.

To provide quantitative analysis of the nuclear translocation of p65, cells were then depicted on dot plots and gated according to three definitions: (i) to gate for nuclear size, circularity and perimeter of Hoechst-stained objects was used. (ii) To gate for homogeneity of GFP signal, standard deviation of GFP signal was used. (iii) To gate for cells with nuclear p65-GFP, a ratio of intensity of nuclear and cytoplasmic GFP was used (Fig. 5b). Cells with nuclear GFP were defined as active (Fig. 5b). Individual assays for each of the three

cell lines were optimized (see Methods for details). After the assay was finally set, all experiments were analyzed by the same assay.

2.1.2 Comparison of reporter cell lines and parental cell lines

It has been noted before that analysis of cells ectopically expressing proteins coupled to fluorescence moieties can alter the dynamics of the respective signaling module⁷⁴. Therefore, the parental, non-transduced cell lines were compared with the p65-GFP expressing cell lines. They show very similar patterns of I κ B α degradation over a period of 90 minutes after stimulation with TNF α 10 ng/ml or 0.5 ng/ml (Fig. 6). Only L929 showed slightly prolonged I κ B α degradation. The degradation of I κ B α in the parental and the p65-GFP expressing cell lines corresponds to the percentages of activated cells calculated using the automated p65 translocation assay.

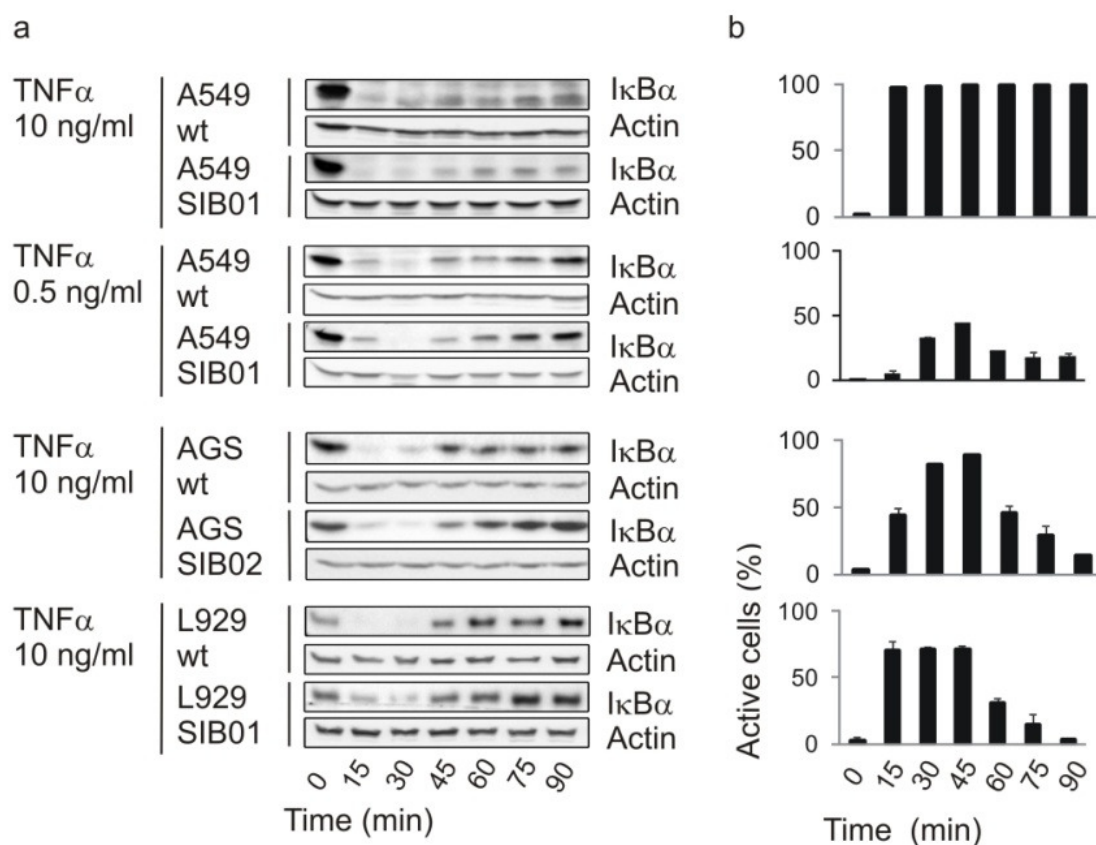


Fig. 6: a) Reporter cell lines respond to NF- κ B stimuli similarly as the parental lines. Cells were infected with the indicated inducer for the indicated time and the degradation of I κ B α and actin control analyzed by western blot. b) The automated readout gives results corresponding to western blot results. The reporter cell lines were activated with the indicated inducer for the indicated time, fixed, stained with Hoechst 33342 and analyzed by automated microscopy as shown in Fig. 5. Error bars = SD of experiment performed in triplicates. Results are representative of three independent experiments.

2.1.3 Specific temporal control of p65-GFP translocations

Using these cell lines, it became apparent very quickly that there is not a uniform response to TNF α , but that each of the three cell lines has a distinctive pattern of NF- κ B activation. To further characterize this specificity, the response of the three cell lines to different inducers was analyzed: the cytokines TNF α and IL-1 β , the bacterial cell wall component LPS and the bacterium *H. pylori* (Fig. 7). Cells were seeded in 96-well-plates, activated by the respective inducer, fixed after the indicated time and p65 translocation was quantified by automated microscopy and software-based picture analysis.

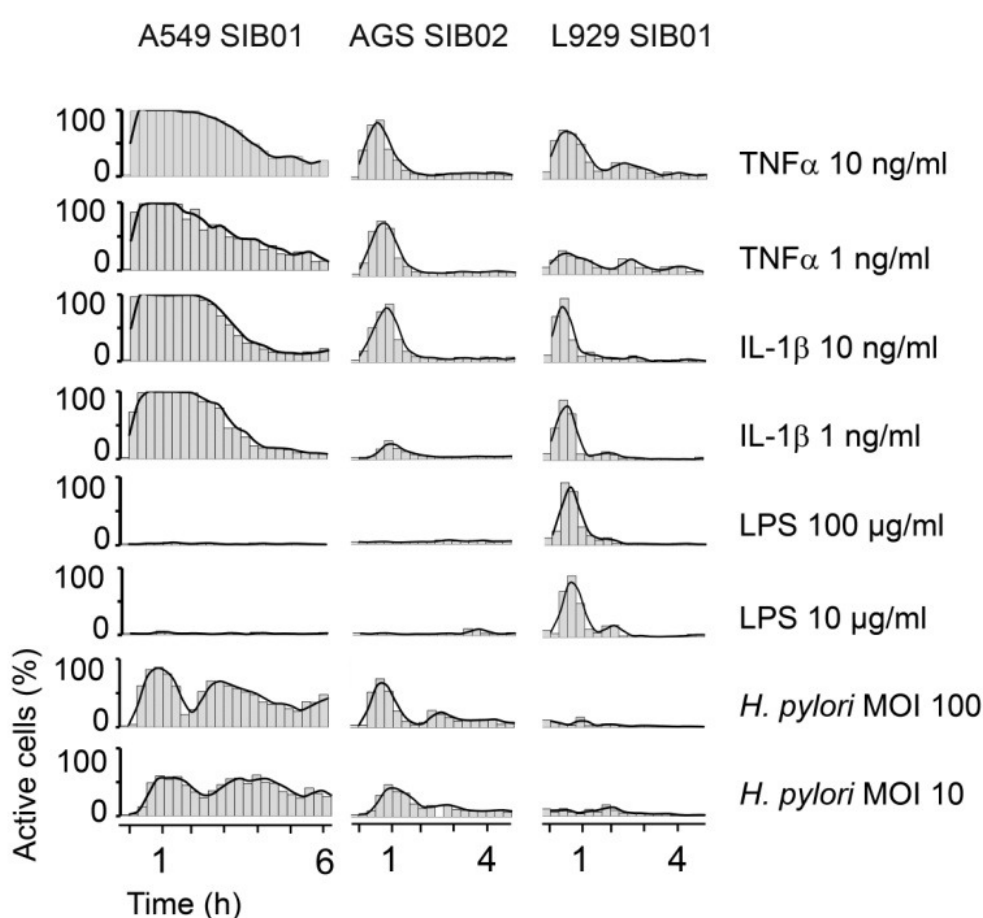


Fig. 7: Inducer specific activation profiles of cell lines A549 SIB01, AGS SIB02 and L929 SIB01. The cell lines were activated with the indicated inducer for 0 to 6 h: A549 SIB01 cells were activated for 0-345 min, AGS SIB02 cells and L929 SIB01 cells for 0-270 min, each in steps of 15 min. Cells were fixed, stained with Hoechst 33342 and analyzed by automated microscopy as described in Fig. 5. Mean percentages from duplicate experiments are shown as bars (grey) and the calculated moving average of 2 is depicted as a line (black). Results are representative of at least 3 independent experiments. Standard deviations are not shown for graphical reasons. One data point is missing in AGS *H. pylori* MOI 10 due to technical issues.

The resulting profiles were highly specific for cell lines and inducers (Fig. 7). The main characteristics were: 1) Human epithelial cell lines did not respond to LPS and mouse fibrob-

lasts did not respond to *H. pylori*, pointing to general stimulus specificity, probably due to functional receptors and/or signaling pathways present on the respective cells. 2) Temporal profiles were stimulus specific. A549 show damped oscillations after infection with *H. pylori*, but stable translocation after stimulation with TNF α or IL-1 β . Stable translocations in A549 in response to TNF α were verified using live-cell imaging (data not shown). 3) The amplitude, but not the temporal profile was variable to the dose of the inducer. 4) Thresholds were cell-line-specific. Low-dose challenge of AGS with IL-1 β produced small amplitudes of response, while the same doses yielded a full response in A549 and L929 cell lines. 5) The duration of the response varied between cell lines. A549 generally showed much longer responses, implying more amplification of the signal or less dampening mechanisms in this cell line. 6) The background level of p65 translocation which can be seen at time 0 (no stimulus) is very low in all cell lines.

2.1.4 Bacterial infection induces oscillations of p65-GFP

Damped oscillations of p65 translocation have been observed in response to *H. pylori* using the automated microscopy assay (Fig. 7); however, as this was the first time oscillations of NF- κ B activation have been demonstrated using a bacterial infection model, observations were verified using live-cell imaging. For this, AGS SIB02 cells were infected with *H. pylori* stained with a live dye (Syto 61) at an MOI of 5. Attachment of a single bacterium to one cell led to translocation of p65-GFP (Fig. 8a).

To analyze the properties of these oscillations, average GFP intensities of nine cells from one experiment were compared. Individual cells were activated at different time points, each roughly 20 min after the attachment of one or more bacteria (Fig. 8b). Mathematical alignment of the different oscillations for the first peak revealed remarkable features: While the first peak seems highly synchronous in all cells, the second peak and its interval are variable (Fig. 8c). Analysis of additional 33 cells under various experimental conditions (MOI and time), showed that while the majority of cells exhibited the expected damped oscillations (high first peak followed by smaller second peak), the opposite was also possible (lower first peak followed by higher second peak) (data not shown). Peak intervals measured in 18 cells ranged from 40 to 140 min, with the most frequent intervals between 80-100 min (Fig. 8d).

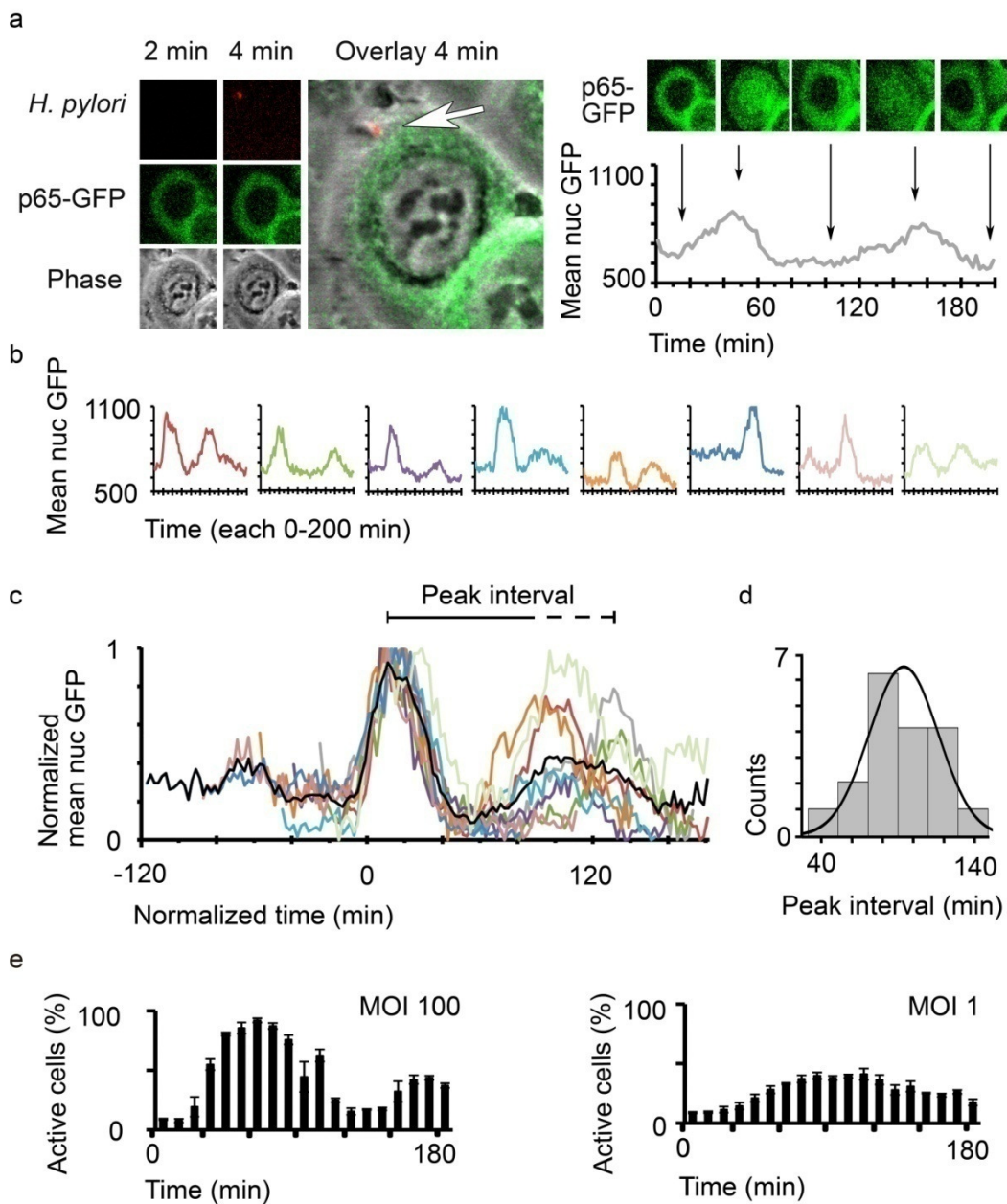


Fig. 8: *H. pylori* induces damped oscillations of p65 nuclear translocations. a) p65-GFP expressing AGS SIB02 were infected with *H. pylori* stained with Syto 61 and analyzed by confocal live cell microscopy. The upper panel shows a single bacterium attaching to a cell shortly after beginning of acquisition (arrow indicates position of bacterium). Graph shows average intensity of GFP in a representative nuclear region of this cell measured with Metamorph software. b) Graph shows average intensities of GFP in other cells from the same experiment (to which one or more bacteria attached at different time points) c) Alignment of normalized average intensities of GFP within representative nuclear regions of the nine single cells shown in (a) and (b). Mean GFP intensity of the nine cells is shown as a black line. d) Peak interval of oscillating cells ranges from 40-140 min and distribution follows a Gaussian curve. Cells were treated as in (a) and 18 oscillating cells from four separate experiments were analyzed. e) At high MOIs, oscillations are synchronous on population level. AGS SIB02 cells were infected with *H. pylori* at the indicated MOI, fixed, then analyzed by automated microscopy and the percentage of active cells per well calculated as described in Fig. 5. Error bars = SD of experiment performed in triplicates. Results are representative of three independent experiments. Mathematical peak alignment and identification of peak interval was performed in collaboration with Johannes Schuchhardt, Microdiscovery, Berlin, Germany.

Taken together, these observations demonstrate cell-to-cell variability in *H. pylori*-induced p65 nuclear translocation oscillations. Importantly, similar oscillation profiles were obtained within single cells and at population level (Fig. 8e). However, for oscillations visible at population level, high MOIs of 10-100 were necessary. Only under these conditions can bacteria reach the majority of cells at the same time and induce synchronous activation. Using a low MOI, oscillations at a population level are masked by variations in the time required by individual bacteria to reach cells. This experiment demonstrates the ability of this system to unify population and single cell analysis (Fig. 8d).

2.1.5 Discussion

Here, a simple and cost effective method amenable to high-throughput applications for NF- κ B analysis is described. It combines the use of p65-GFP expressing monoclonal cell lines with automated microscopy and analysis to provide synchronous real-time analysis of NF- κ B activation dynamics at a single-cell and population level.

There are many different oscillatory systems, most of them regulated by positive and negative feedback loops¹⁵⁹ and expression of fluorescent fusion proteins have been a useful tool to study dynamics of these and also non oscillatory signaling systems^{47,160-164}. Available methods to analyze NF- κ B activation dynamics at a single-cell level have relied on transient expressions, but these bear some difficulties, as expression of the respective oscillator might influence the fine-tuning of the regulator system. For NF- κ B, it has specifically been noted that ectopic expression of p65 can influence NF- κ B oscillations⁷⁴. Also, discrepancies have been observed in oscillation synchrony between population and single-cell analysis with transient transfected cells, which have been attributed to varying expression levels within single cells⁷⁴.

The major advantage of the model presented here overcomes these limitations via the use of monoclonal cell lines: all cells have the same expression level and oscillations within single cells and populations are synchronous. Second, comparison with parental cell lines showed that there is little influence of ectopic expression as I κ B α -degradation occurs in p65-GFP expressing cell lines highly similarly as in their parental cell lines. A third advantage is that unlike other cell lines that need selection pressure (i.e. G418) to keep the transgen, the cell lines presented here are lentivirally transduced, thus the p65-GFP carried by the virus has been integrated into the cellular genome and no selection pressure is needed. Fourth, an important advantage is that no additional material is needed, avoiding unnecessary addition of experimental variables and also making this system highly cost effective. Lastly, the method presented here provides high sensitivity as background activity levels are very low.

The new cell lines were used here to compare the specificity and temporal nature of NF- κ B activation dynamics within three different cell lines: two human epithelial cell lines, of lung and gastric origin, respectively, and one mouse fibroblast cell line. Signature NF- κ B response profiles were found for every inducer and cell line. Translocation of p65-GFP was

found to oscillate or present stable activation; the amplitude of the activation varied with the dose of the inducer. Both observations are consistent with previous findings^{67,68,165}.

Oscillations of p65 have been shown using the cytokine TNF α ^{47,54,55,68,69,166} and the topoisomerase II inhibitor etoposide⁴⁷, but it remained an open question whether oscillations occur in infections. Data presented here show, for the first time, oscillations after infection with the bacterium *H. pylori*. With live-cell imaging, it could be shown here that the smallest possible live unit, a single bacterium, is capable of inducing translocation of p65-GFP. Most importantly these data showed synchronization between activation responses at the single cell and population level. As with other inducers of NF- κ B such as TNF⁴⁷, *H. pylori* infection elicited a moderate cell- to-cell variability in p65 oscillations. Future experiments will clarify whether the observed variations of peak intervals in single cell oscillations are due to the strength of induction and/or repeated infection by individual bacteria, as likely found during bacterial infection *in vivo*. Also, oscillations after infections with *Neisseria gonorrhoeae* were observed on the single cell level but because oscillations were asynchronous they could not be detected on population level (data not shown).

Stimulus specific temporal control of NF- κ B activation has also been observed in mouse embryonic fibroblasts (MEFs) using EMSAs: when stimulated with TNF α they displayed oscillatory behavior, when stimulated with LPS they displayed stable behavior. The stable activation could be designated to a positive feedback that leads through secretion of TNF α to an overlap of two signaling pathways both oscillatory when isolated, but leading to stable activation when overlapping^{67,68}. Here, it is not addressed whether or not a similar mechanism lies beneath the observation here, but it should be pointed out that both TNF α and IL-1 β lead to single translocations in A549 with the stimulus remaining in the medium, thus it seems unlikely that a potential feedback loop would involve these two cytokines. It might also be possible, that there is an intracellular trigger that decides between oscillations or stable activations.

But why do cells have different p65 translocations? Why not a single way? One possible answer lies in the biological diverse functions of NF- κ B signaling. This system needs to differentiate between a wide range of stimuli and provide the appropriate transcriptional response – temporal signatures provide a way to encode for different inducers. The work of Hoffmann and coworkers has demonstrated this elegantly⁵⁴: Short peaks of NF- κ B acti-

vation induced transcription of one set of genes while oscillations induced transcription of a different set. It remains an interesting question for future research to analyze the importance of temporal control for physiological functions.

Based on experimental data, a mathematical model of temporal regulation of NF- κ B signaling has been developed⁵⁴. Data generated using the clonal cell presented here, could be used to refine and broaden this and similar models by providing further experimental details of population and single-cell level oscillations within different cell types.

Next to the new cell lines presented here, the p65-GFP carrying lentivirus itself provides interesting new features for further research. Not only can it be used to generate any other cell line desired, but, as lentiviruses can also infect non-dividing cells, it can even be used to transduce difficult to reach primary cells. Remarkably, this system also enables the user to influence the expression level of p65-GFP by varying the copy number of viruses per cell, i.e. using higher virus titers would lead to high numbers of integrated copies per genome and thus to higher expression levels.

Owing to the crucial roles that NF- κ B plays in inflammation, immunity and cancer, both the pharmaceutical industry as well as research groups are actively pursuing the discovery of new compounds that modulate NF- κ B¹⁶⁷. The cell lines and the microscopic assay presented here could be of great benefit to these efforts; for instance, in combination with high-throughput analysis in compound or RNAi-based screens. Also, the assay is highly cost effective because no additional materials are required and promising newly identified factors can be further analyzed on a single-cell basis using the same system. Furthermore, this assay has the unique quality that a delay of activation or a sustained nuclear translocation can also be observed; enabling for the first time to implement analysis of dynamics in screens which can identify factors that delay or prolong translocation, thereby opening new doors for therapeutic discovery and understanding of disease.

2.2 Part II: RNAi-based screen identified regulators of NF- κ B signaling

To identify new factors important in NF- κ B signaling, an RNAi-based screen was performed using the p65-GFP translocation assay described in the first part of this thesis. To enable distinction of genes generally acting on NF- κ B signaling from genes selectively acting in NF- κ B signaling induced by *H. pylori*, the infection was compared to induction with the cytokines TNF α or IL-1 β . Furthermore, using different time points of activation, not only factors important for activation, but also for termination of the signal were identified. The main goals of this part were: The establishment of RNAi-based screening procedures, identification of controls, performance of the high-throughput screen, statistical analysis, verification of identified genes, and further analysis of single, newly identified factors.

2.2.1 Establishment of the RNAi-based screen

For high-throughput performance, a semi-automated platform was established. AGS SIB02 cells were seeded manually in 96-well-plates and automatically transfected the next day. After a minimum of 60 h allowing high probability of efficient reduction of target protein, cells were manually activated by one of three stimuli: infection with *H. pylori* MOI 100, addition of TNF α 1 ng/ml or addition of IL-1 β 10 ng/ml. Induction was stopped by fixation and nuclei were stained with Hoechst. 96-well-plates were subjected to automated microscopy and p65 translocation was quantified as described above (Fig. 9).

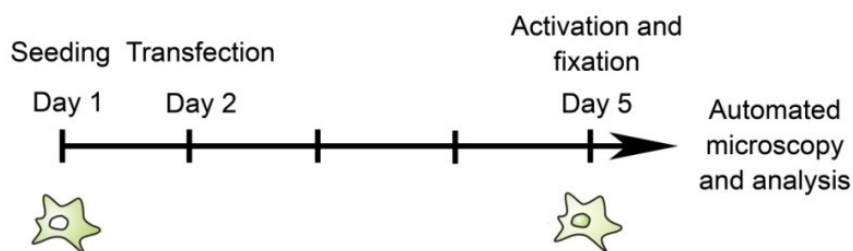


Fig. 9: Workflow of RNAi-based screen for factors involved in translocation of p65. AGS SIB02 cells are seeded in 96-well-plates on day 1, automatically transfected with siRNAs on day 2. After a minimal transfection time of 60 h cells are manually activated with *H. pylori*, TNF α or IL-1 β on day 5. Cells are fixed, stained with Hoechst 33342 and analyzed by automated microscopy as described in Fig. 5

In a screen, controls are needed to establish suitable screening procedures, to verify performance of the experiments during the screen and as references for data analysis. To identify control siRNAs for the screen, several known components of NF- κ B signaling were tested (Fig. 10). Used siRNAs have been validated previously within the department and each siRNAs has been shown to reduce target mRNA levels by at least 70%.

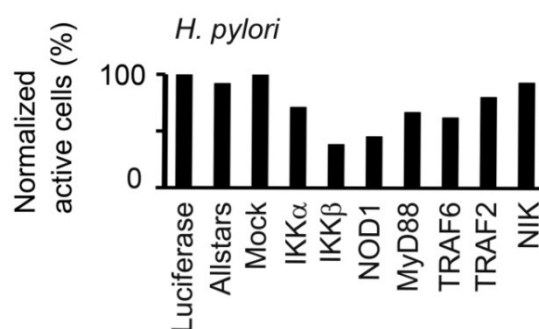


Fig. 10: Identification of siRNA controls for *H. pylori*. AGS SIB02 cells were transfected with the indicated siRNAs, activated with *H. pylori* MOI 100 for 45 min, fixed and analyzed by automated microscopy. Bars represent results from experiment performed in single wells. Results are representative of three independent experiments.

In *H. pylori* infection, siRNAs targeting NIK and TRAF2 had no effect, siRNAs targeting MyD88, TRAF6 and IKK α had a moderate effect and siRNAs targeting NOD1 and IKK β showed profound inhibitory effect on p65-GFP translocation (Fig. 10). Because siRNAs targeting IKK β led to the strongest inhibition, they were used as control. For TNF α , siRNA against the receptor TNF-R1 completely abolished TNF α -induced p65 translocation and was used as control for this inducer. Similarly, MyD88 was used for IL-1 β (Fig. 11).

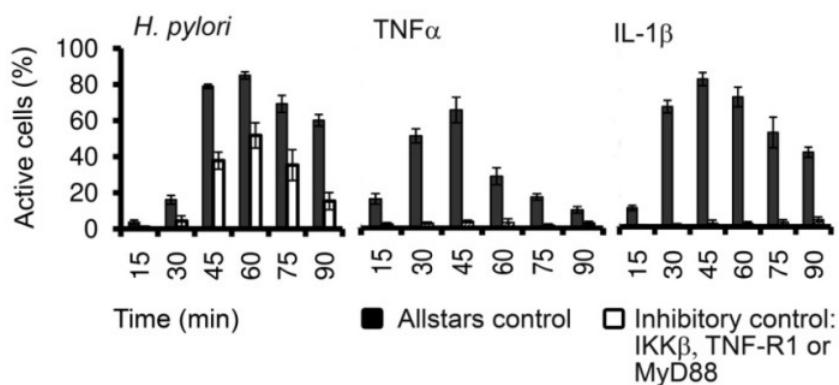


Fig. 11: Control siRNAs against known activators of NF- κ B reduce translocation of p65-GFP. AGS SIB02 cells were infected with *H. pylori* MOI 100, activated with TNF α 1 ng/ml or IL-1 β 10 ng/ml for the indicated time, fixed, analyzed by automated microscopy and image processing and percentages of activated cells per well were calculated. Inhibitory siRNA: IKK β for *H. pylori*, TNF-R1 for TNF α , MyD88 for IL-1 β . Results are shown as bars representing experiment performed in triplicates with standard deviation. Results are representative of at least three independent experiments.

2.2.2 Performance of the screen

The screen was conducted using a library of siRNAs targeting 646 kinases and associated proteins, with two siRNAs per gene. Because siRNAs were not validated, the library contains an unknown number of non-functional siRNAs. To reduce sample size, two siRNAs

for each gene were pooled. Each pool of two siRNAs was tested for its influence on p65 translocation in at least three independent experiments. Two time points were tested: First, one time point at the top of the curve to screen for factors involved in activation of p65 translocation (this was 45 min for *H. pylori* and IL-1 β , 30 min for TNF α). Second, one time point was selected at the pit of the curve to screen for factors involved in termination of p65 translocation (90 min for *H. pylori* and IL-1 β , 75 min for TNF α).

2.2.3 Quality control of the screen and identification of hits

In depth description of statistical analysis is provided in the Statistic part of this thesis. In summary, robustness of the assay met the standard criteria for high throughput screens; quality control showed a normal distribution of results on a plate with a minor position effect (left-right shift). To compare results of different plates, raw data was normalized (either using plate-median or, in comparison, z-score) and significance was assessed with Welch's t-test. In total, 160 primary hits were identified combining statistical significance (p-value ≤ 0.05) and the strength of the effect on p65 translocation. For each inducer, approximately 5% top candidates were taken into account for further analysis: the best 52-56 genes were selected for inhibition of p65-GFP translocation and the best 13-18 genes for promotion of p65-GFP translocation. Primary hits include genes common for two or three inducers as well as targets specific for one of the inducers.

An important result was the identification of known members of the NF- κ B pathway: The primary hit list included IKK α , IKK β , TAB1, TAB2 and IRAK1, highlighting the quality of the screen. Interestingly, IKK α was only identified for *H. pylori* and IKK β was only identified for *H. pylori* and TNF α . This indicates a functional redundancy of the kinases which will be addressed more specifically below.

2.2.4 Validation of identified genes

Several reports demonstrated that an observed phenotype was not caused by the down-regulation of the target gene¹⁶⁸⁻¹⁷⁰ but by two off-target effects: the interferon response which is unspecifically induced by siRNAs^{171,172} and the sequence-specific miRNA effect. miRNAs are naturally occurring RNAs that regulate gene expression similarly as externally delivered siRNAs¹⁷³. Because for miRNA-mediated silencing, only seven bases are crucial^{174,175}, externally delivered siRNAs are bound to encompass the risk of silencing multiple mRNAs via this pathway. To date, it is not possible to eliminate these sequence-

specific off-target effects by siRNA design^{176,177}. Therefore, sequence specificity needs to be demonstrated with at least two siRNAs targeting the same gene using different sequences^{176,177}. To verify the identified genes in p65 translocation, here, additional four siRNAs were tested. Of the 160 primary hits, 24 were confirmed with at least two siRNAs each with a z-score of ≤ -1 or ≥ 1 (table 1). To visualize possible connections of these genes, a map was assembled with the program “String” (Search Tool for the Retrieval of Interacting Genes/Proteins)¹⁷⁸ (Fig. 12).

Tab. 1: Genes identified by RNAi-based screen. Factors are necessary for activation or termination of p65 translocation. Names of genes that were confirmed in the hit validation with at least two siRNAs with z-scores of ≤ -1 or ≥ 1 are listed alphabetically. To give indication of the strength of the effect, the sum of z-scores of all four siRNAs during hit validation in all conditions is listed (H1 = *H. pylori* 45 min; H2 = *H. pylori* 90 min; T1 = TNF α 30 min; T2 = TNF α 75 min; I1 = IL-1 β 45 min; I2 = IL-1 β 90 min). Negative z-scores indicate inhibition and positive z-scores indicate promotion of p65-translocation. For comparison with data from the primary screen, bold colored font marks the condition in which the hit validation confirmed the effect in the primary screen (red for inhibition, blue for promotion of p65-translocation). For example, IKK β was selected for inhibition of *H. pylori*- and TNF α -induced activation, therefore only these z-scores are marked blue. However, during the hit validation, of which the z-scores are listed here, the inhibitory effect was also visible in IL-1 β induction.

Abbreviation	Name	H1	H2	T1	T2	I1	I2
ALPK1	A kinase 1 (= Lymphocyte α kinase (LAK))	-8,1	2,4	-1,3	1,0	0,7	1,3
AURKB	Aurora/IPL1-related kinase 2	0,6	0,5	-2,8	-3,9	-1,1	-1,6
CDC2	Cell division control protein 2	-0,9	1,7	-6,3	-5,2	-0,5	2,0
CDC2L2	Cell division cycle 2-like protein kinase 2 (= CDK11)	-1,8	4,3	-1,5	-1,4	0,0	2,2
CRKRS	CDC2-related kinase, arginine/serine rich	-4,0	-0,8	-0,1	1,0	-0,8	-0,6
DYRK1B	Dual-specificity tyrosine-phosphorylation regulated kinase 1B	1,1	1,8	-0,4	-0,8	-1,7	-0,4
EGFR	Epidermal growth factor receptor	2,1	3,6	-1,8	0,3	-0,2	0,9
FASTK	Fas-activated serine/threonine kinase	-0,5	-0,3	1,5	1,4	2,2	0,1
GAK	Cyclin G-associated kinase	-0,7	1,6	1,4	2,7	0,8	1,8
IKK α	Inhibitor of nuclear factor κ B kinase α subunit	-4,2	-6,1	-2,0	-3,6	-0,8	-1,0
IKK β	Inhibitor of nuclear factor κ B kinase β subunit	-8,5	-5,8	-3,5	-2,3	-5,7	-2,4
ILK	Integrin-linked protein kinase 1	-0,6	4,3	7,9	4,0	2,4	3,0
IRAK1	Interleukin-1 receptor-associated kinase 1	-2,2	-1,8	-0,2	0,0	-8,1	-9,9
LTK	Leukocyte tyrosine kinase	1,5	5,3	-2,4	1,9	0,4	4,8
MAPK11	Mitogen-activated protein kinase 11	-0,3	1,6	-0,3	0,1	-4,8	-2,5
NME2	Nucleoside diphosphate kinase B	0,7	0,7	-0,7	-0,3	-1,9	-1,3
PLK1	Polo-like kinase 1	-4,0	2,6	-1,0	2,9	-1,1	4,4
PRKACB	cAMP-dependent protein kinase, β -catalytic subunit	3,0	4,4	2,8	3,2	2,8	2,9
PRKCABP	PRKCA-binding protein	-0,5	3,5	-2,2	0,3	-3,0	0,5
PRKD2	Protein kinase C D2 type	-1,2	1,5	0,5	0,7	-3,9	-1,8
PSKH1	Serine/threonine-protein kinase H1	-1,0	0,5	0,2	0,0	-2,3	-0,5
SKP2	S-phase kinase-associated protein 2	0,9	2,0	-0,5	2,3	4,2	5,8
TNIK	TRAF2 and NCK interacting kinase	-1,5	-2,2	-0,6	-0,3	-2,5	0,3
WEE1	Wee1-like protein kinase	0,3	-2,1	-3,4	-2,7	-2,0	0,3

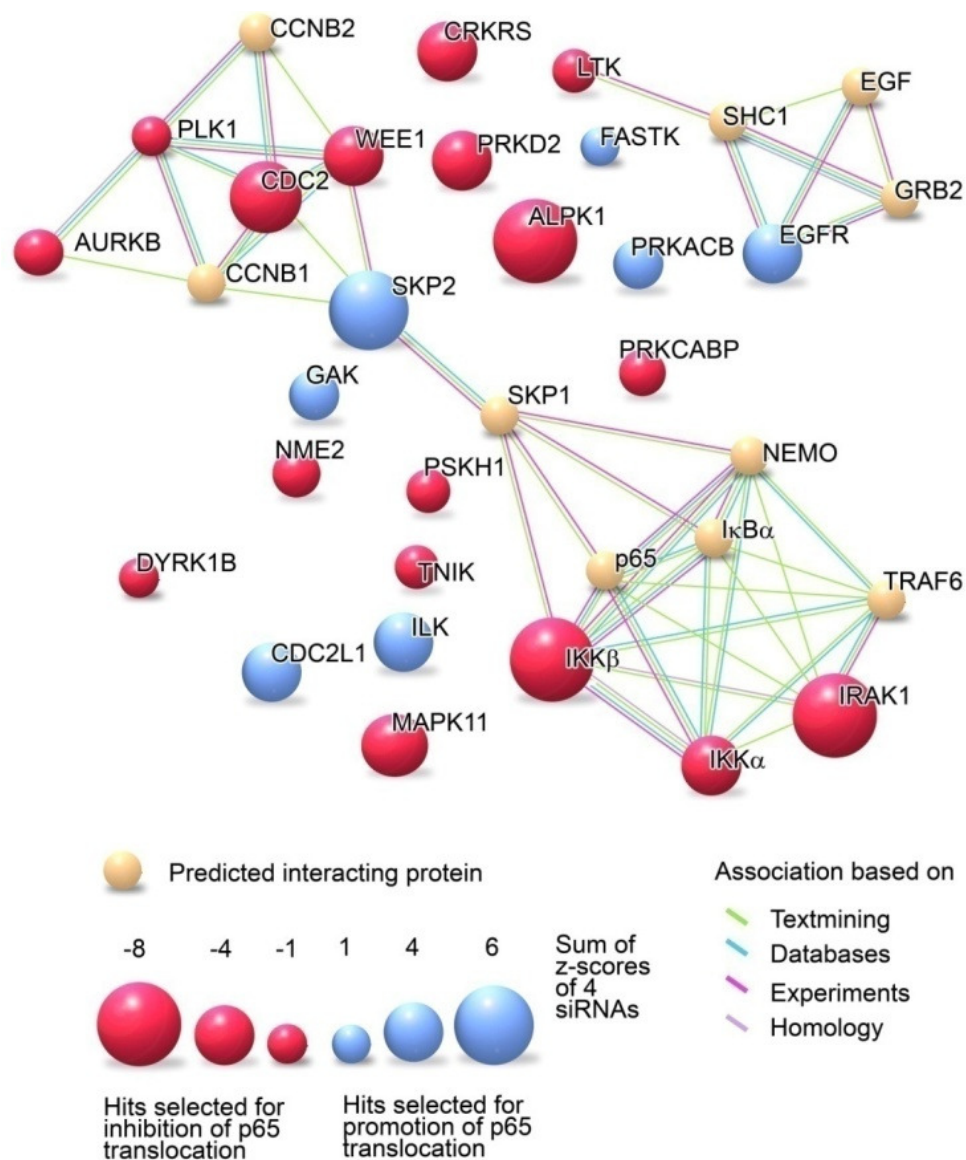


Fig. 12: Map of genes identified by the screen to be important in activation or termination of p65 translocation. Genes that were confirmed with at least two siRNAs with a z-score of ≤ -1 or ≥ 1 are depicted in a network with predicted interaction partners assembled by the program “String” (<http://string.embl.de>). Information about the strength of the effect was added manually (color code and size of nodes). Networks are: NF- κ B pathway (lower right), cell cycle (upper left) and EGF pathway (upper right). For each gene, the sum of z-score is depicted for the condition in which hit validation data confirmed screen data. Please refer to table 1 for abbreviations and to identify which gene affects which inducer.

String is a database of known and predicted protein-protein interactions which are derived from different sources (text mining of literature, homology searches, high-throughput experiments etc.). The resulting map was modified so that color and size would indicate the strength of the effects. In this map, three pathway connections are highlighted: first, the NF- κ B pathway, connected via the F-box protein SKP2 to the second network which encompasses cell cycle proteins: CDC2, WEE1, PLK1, AURKB. Third, the

software showed a link of LTK and EGFR within EGF-network. All other genes were unconnected (Fig. 12). Genes identified by the screen are listed in table 1 and predicted interaction partners are listed in table 2.

Tab. 2: Putative interaction partners of genes identified in the screen predicted by the program “String” <http://string.embl.de>. Associations can be based on text mining, databases, experiments or homologies.

Abbreviation	Name
CCNB1	G2/mitotic-specific cyclin B1
CCNB2	G2/mitotic-specific cyclin B2
EGF	Epidermal growth factor
GRB2	Growth factor receptor-bound protein 2
IκBα	Inhibitor of NF- κ B α
NEMO	NF- κ B essential modulator (=IKK γ)
p65	NF- κ B subunit p65 (= RelA)
SHC1	SHC transforming protein 1
SKP1	S-phase kinase-associated protein 1

2.2.5 Time resolved analysis of NF- κ B regulators

The effect of the identified siRNAs was evaluated in an expanded time course. First, genes known in NF- κ B signaling were tested. In this experiment, two further questions were addressed that arose from the screen: (i) putative false negatives (such as IRAK4, TAK1 and TAB2) were re-tested. Because the library contained an unknown number of non-functional siRNAs, these genes could have been false negatives and siRNAs for these genes were included in the experiment. (ii) Results from the screen suggested redundant functions of IKK α and IKK β . To analyze this effect, siRNAs for IKK α and IKK β were combined in this experiment. Results were assembled as time courses normalized to Allstars siRNA control and show several interesting characteristics (Fig. 13): 1) if a siRNA induces reduction of p65 translocation it does so during the entire experiment. Other possibilities, i.e. a delay of activation were not observed with the tested genes. 2) Combination of siRNAs for IKK α and IKK β greatly increases the effect of the single siRNAs. This combination nearly abolished p65 translocation with all three inducers. 3) siRNAs targeting TAK1 showed strong effects after *H. pylori* infection. Therefore, TAK1 can be accounted as false negative in the screen, indicating that siRNAs used in the screen did not effectively reduce protein levels. 4) siRNAs against the associated proteins TAB1 and TAB2 did not show strong effects. Thus, the effect of TAB1 siRNA in the screen was not confirmed. 5) siRNAs targeting IRAK1 confirmed the screen results and were effective in IL-1 β induction, whe-

reas siRNAs against IRAK4 did not have an effect. 6) siRNAs targeting MAP3K3 (also known as MEKK3) had a weak effect on p65 translocation using all three inducers.

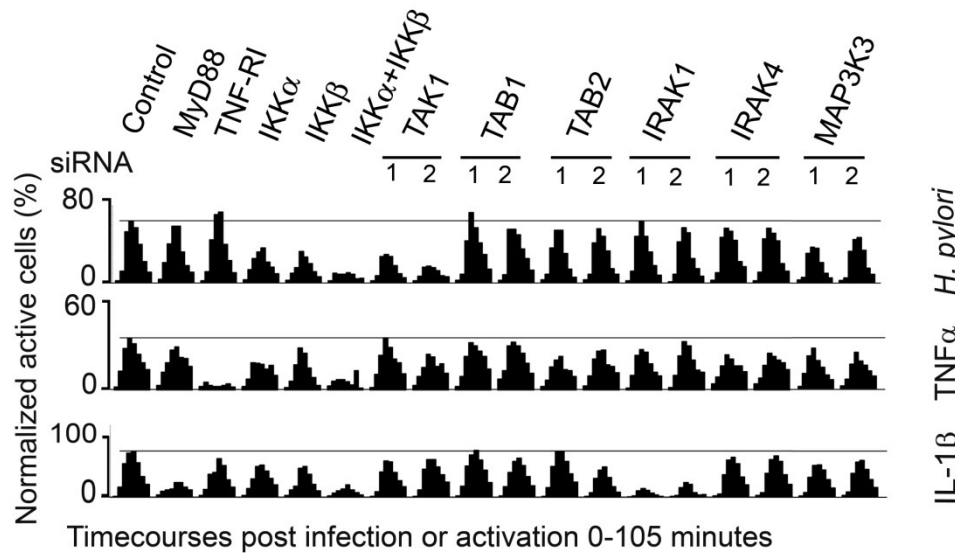


Fig. 13: Specific effects of siRNAs targeting known members of NF- κ B on different inducers over time. Three days post siRNA transfection, cells were activated with one of the three inducers *H. pylori*, TNF α or IL-1 β . Cells were fixed without activation (0 min) or after 15, 30, 45, 60, 75, 90 and 105 min, stained and analyzed by automated microscopy as described in Fig. 5. Results are presented as mean of normalized data of at least four independent experiments. The control is Allstars siRNA. For better comparison, a line indicates the peak of the curve of the control.

Next, the genes newly identified in the screen were analyzed (Fig. 14). Of the 24 genes confirmed in the validation, nine were taken into account for this experiment: ALPK1, CRKRS, TNIK, Wee1, and CDC2 for inhibition, SKP2, ILK, CDC2L1 for promotion of p65 translocation. In addition, two genes were added because they showed strong effects, although they did not meet the requirement of at least two siRNAs with a z-score of ≤ -1 or ≥ 1 . These genes were fibroblast growth factor receptor 4 (FGFR4) and cyclin dependent kinase 2 (CDK2). For each gene, two siRNAs were tested over a time course of 0-105 min and results were normalized to Allstars control (Fig. 14). RNAi targeting ALPK1 and CRKRS strongly reduced p65 translocation over the entire tested period of time (Fig. 14a). Both genes showed selective importance for *H. pylori*. Only one siRNA against ALPK1 had a slight effect on TNF α . Of the genes selected for more than one inducer, both siRNAs against FGFR4 showed a clear effect on all three inducers. Influence of TNIK was only weakly visible in *H. pylori*-infected cells. Of the two genes selected for their effect on TNF α -induced p65 translocation, CDC2 and WEE1, RNAi targeting CDC2 showed a reduction of p65 translocation over the entire time course and RNAi targeting WEE1 delayed

activation. Regarding genes that were important in termination of p65 translocation, SKP2 had the strongest effect (Fig. 14b). Most pronounced in IL-1 β induction, the effect was also visible in TNF α induction and to a lesser extent in infection with *H. pylori*. Further, siRNAs targeting ILK1 profoundly prolonged TNF α -induced p65 translocation. siRNAs against CDK2 did not confirm the upregulation observed in the screen and siRNAs against CDC2L1 showed adverse effects depending on siRNA and inducer with a prolonging effect in infection with *H. pylori* and induction with IL-1 β , but with a rather inhibitory effect of one siRNA in induction with TNF α (Fig. 14b).

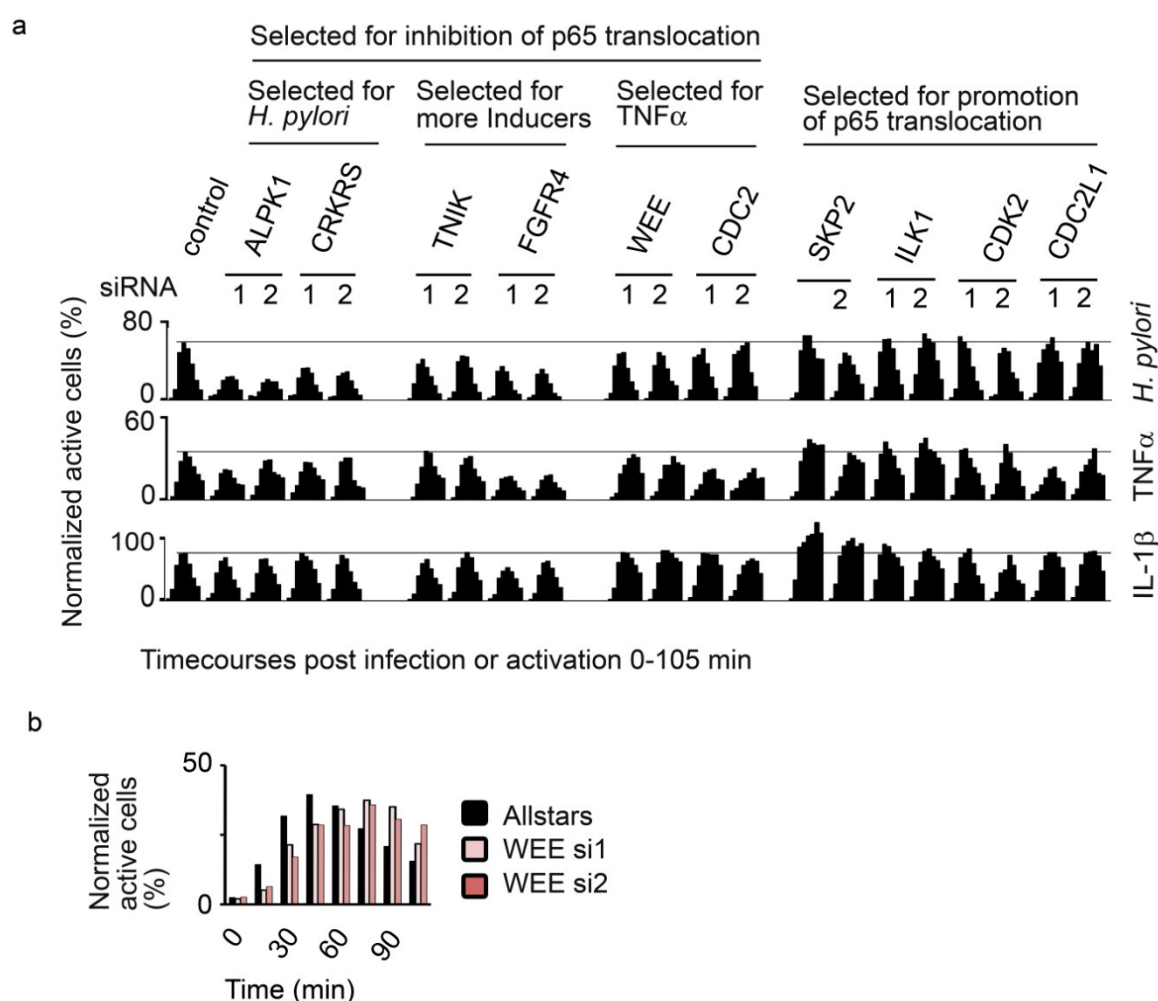


Fig. 14: a) Specific effects of siRNAs targeting newly identified genes important for NF- κ B signaling. b) Down-regulation of WEE1 induces delay of p65 translocation after induction with TNF α (enlarged view of data presented in a). Three days post siRNA transfection, cells were activated with one of the three inducers *H. pylori*, TNF α or IL-1 β . Cells were fixed without activation (0 min) or after 15, 30, 45, 60, 75, 90 and 105 min, stained and analyzed by automated microscopy as described in Fig. 5. Results are presented as mean of normalized data of at least four independent experiments. The control is Allstars siRNA. For better comparison, a line indicates the peak of the curve of the control.

2.2.6 Combinatorial effects of identified siRNAs

The clear combinatorial effects of siRNAs against IKK α and IKK β led to the question whether possible effects of other combinations might reveal insights into parallel functions. To investigate this, siRNAs targeting different genes were combined and tested for influence on p65 translocation. For clearer display, results are shown in two figures: figure 15 shows an excerpt of the data, and figure 16 shows full results. Analog to an additional effect of IKK α and IKK β , also combination of siRNAs targeting CRKRS and ALPK1 had an additional effect and nearly abolished p65 translocation in *H. pylori* infection (Fig. 15). Similar but weaker effects were observed combining siRNAs targeting IKK α and TAK1 in TNF α induction and combining siRNAs targeting IRAK1 and IRAK4 IL-1 β induction (Fig. 15).

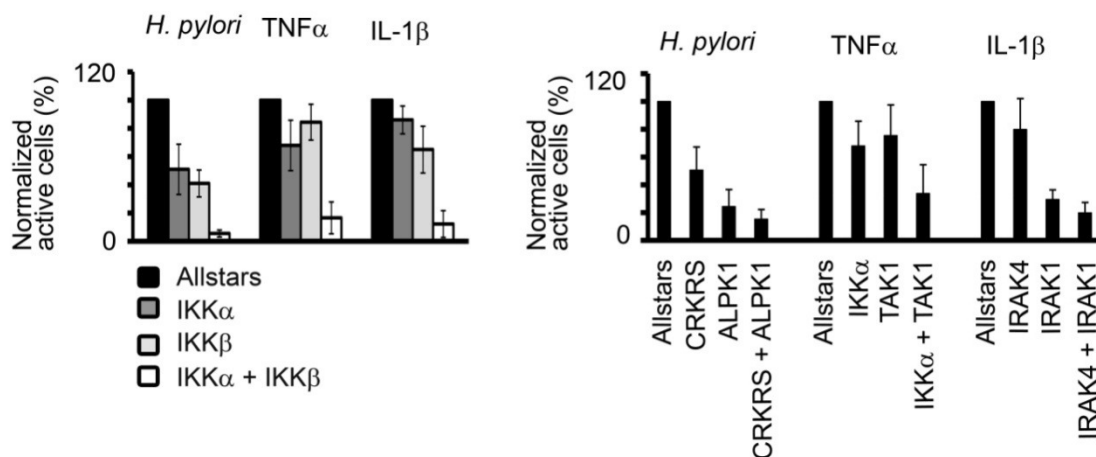


Fig. 15: Combination of siRNAs lead to enhanced inhibition of p65 translocation. AGS SIB02 cells were transfected using a combination of siRNAs targeting the indicated genes. Cells were activated by *H. pylori* MOI 100 45 min, TNF α 1 ng/ml 30 min, or IL-1 β 10 ng/ml 45 min, fixed, analyzed by automated microscopy and image processing and percentages of activated cells per well were calculated. Results of individual experiments were normalized to Allstars control and the mean of four independent experiments is shown. Error bars = standard deviation of four experiments. This figure shows an excerpt of the data underlying Fig. 16.

Further effects are visible in figure 16: (i) Only the combination of IKK α and IKK β in TNF α or IL-1 β induction had a so called “synthetic” effect, meaning an effect where only the combination, not the single siRNAs, reveal a phenotype¹⁷⁹. Synthetic effects are seen in genes that buffer each other’s function¹⁸⁰. (ii) Many genes showed “additive effects” where combination of both siRNAs led to an addition of the phenotypes of single down-regulations¹⁷⁹. Here, combinations of ALPK1 and CRKRS *H. pylori* infection or IRAK1 and IRAK4 in IL-1 β induction are examples. In most cases observed here, the phenotype of the combined downregulation equaled less than the sum of the single effects.

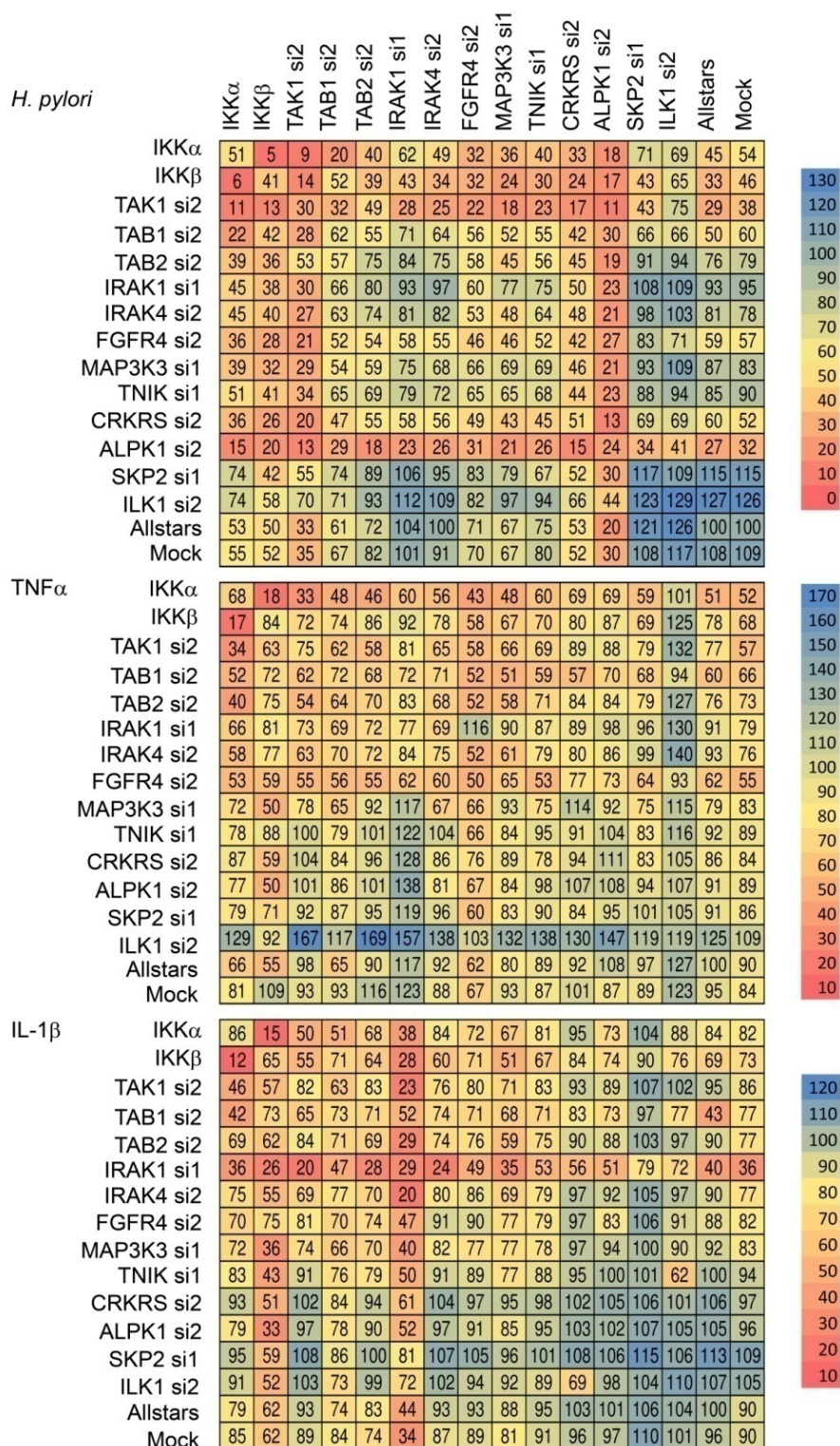


Fig. 16: Combination of siRNAs leads to enhanced inhibition of p65 translocation. AGS SIB02 cells were transfected using a combination of siRNAs targeting the indicated genes. Cells were activated by *H. pylori* MOI 100 45 min, TNF α 1 ng/ml 30 min, or IL-1 β 10 ng/ml 45 min, fixed, analyzed by automated microscopy and image processing and percentages of activated cells per well were calculated. Results of individual experiments were normalized to Allstars control and a mean normalized percent activated cells of four independent experiments is shown. si1 = siRNA 1, si2 = siRNA 2.

2.2.7 ALPK1 and CRKRS are important for NF- κ B activation

Three highly interesting proteins emerged from the screen: ALPK1 and CRKRS with specific impact on *H. pylori* induced NF- κ B activation and SKP2 which exerted strong effects on the termination of p65 translocation. Therefore, these genes were analyzed further. To exclude a possible influence of the expression of p65-GFP, the parental cellline of AGS SIB02, AGS, was used for these experiments.

Background information about ALPK1 and CRKRS is very limited. ALPK1 is one of six known alpha kinase which has been shown to function in apical protein transport by phosphorylating myosin 1a¹⁸¹. CRKRS belongs to the family of cyclin related kinases and was implicated in alternative splicing¹⁸². Because both genes have not yet been connected to the NF- κ B pathway, the next experiments targeted verification of their influence. First, to ensure functionality of the siRNAs used for detailed analysis, efficiency of mRNA reduction was analyzed by RT PCR (Fig. 17).

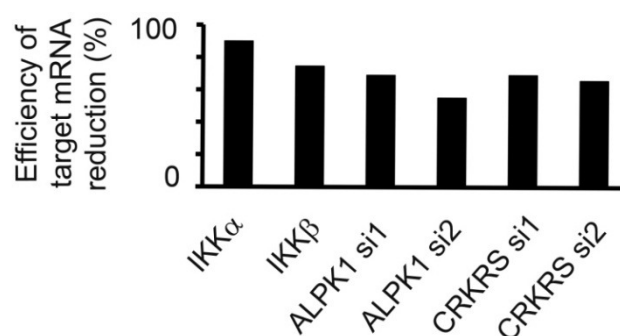


Fig. 17: Evaluation with RT-PCR shows that the used siRNAs reduce target gene mRNA level by 60-95%. After transfection and three days of incubation, cells were lysed, mRNA levels measured with RT-PCR, normalized to glyceraldehyde 3-phosphate dehydrogenase (GAPDH) housekeeping gene and referenced to target mRNA levels measured in Allstars siRNA treated controls. si1= siRNA 1, si2 = siRNA 2.

To assess the effect on expression of NF- κ B target genes, secretion of the cytokine IL-8 was measured with an enzyme-linked immunosorbent assay (ELISA). Results showed a clear reduction of about 50% of IL-8 secretion after downregulation of ALPK1 or CRKRS in comparison to an Allstars siRNA control (Fig. 18). A second control combining siRNAs targeting IKK α and IKK β abolished IL-8 secretion (Fig. 18). Thus, ALPK1 and CRKRS are important for IL-8 secretion after *H. pylori* infection.

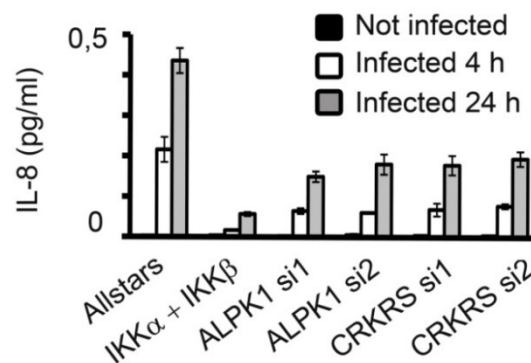


Fig. 18: Downregulation of ALPK1 or CRKRS inhibits secretion of IL-8 after infection with *H. pylori*. AGS were transfected with the indicated siRNAs and after three days infected with *H. pylori* MOI 100. Supernatant was collected after the indicated time and IL-8 was measured by ELISA. Bars represent means of triplicates. Error bars = SD of triplicates. si1= siRNA 1, si2 = siRNA 2. ELISAs were performed in collaboration with Bianca Bauer, MPI for Infection Biology, Berlin, Germany.

To analyze, whether ALPK1 and CRKRS act upstream or downstream of the IKK complex, kinase activity was measured in a kinase assay. Analogous to the results of the IL-8 measurement, both siRNAs targeting ALPK1 as well as both siRNAs targeting CRKRS strongly reduced kinase activity (Fig. 19).

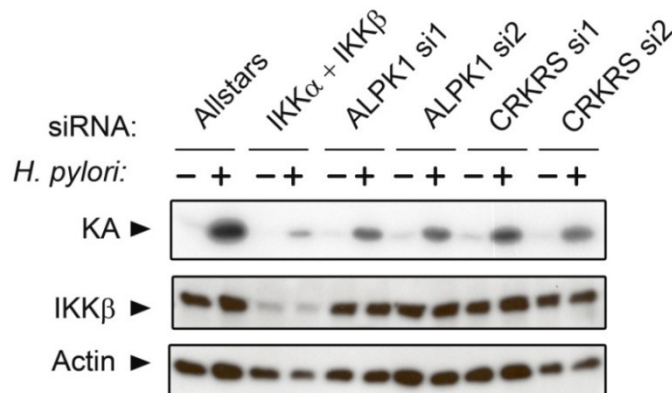


Fig. 19: Downregulation of ALPK1 or CRKRS inhibits IKK kinase activity after infection with *H. pylori*. AGS were transfected with the indicated siRNAs and after three days infected with *H. pylori* MOI 100. Cells were lysed after 30 min and IKK-complexes were precipitated with antibodies against NEMO. The combined kinase activity of IKK α and IKK β was measured with kinase assay (KA). For this purpose, precipitates were incubated with a synthetic peptide harboring the phosphorylation site of I κ B α in the presence of [32P]- γ ATP. Probes were subjected to SDS page and phosphorylated substrate detected with autoradiography. As controls, samples were collected for western blot analysis and probed for IKK β and actin. Results are representative of three independent experiments. si1= siRNA 1, si2 = siRNA 2. Kinase assay was performed in collaboration with Michael Hinz, Max Delbrück Center, Berlin, Germany.

To control equal protein contents, cell lysates were subjected to western blotting and probed for IKK β or actin. Western blots also showed a clear reduction of IKK β protein le-

vels after IKK β siRNA treatment whereas IKK β protein levels were unaffected by other siRNAs (Fig. 19). These results indicate that ALPK1 and CRKRS act upstream of IKK.

Because NF- κ B signaling depends on the adherence of bacteria to the cells and a functional T4SS, a reduction of NF- κ B signaling could possibly be due to less bacteria adhering to the cells or to impaired T4SS function. To specifically address this question, translocation of bacterial CagA was assessed by western blot analysis with phosphor-tyrosine-specific antibodies. Results indicated that translocation of CagA was not reduced after downregulation of ALPK1 or CRKRS (Fig. 20). Subsequent analysis of western blots with anti-CagA antibodies detecting intra- and extracellular CagA showed similar amounts of CagA in all samples, indicating that similar amounts of bacteria adhered to the cells (Fig. 20). Therefore, downregulation of ALPK1 and CRKRS does not inhibit binding of bacteria to the cells and translocation of CagA.

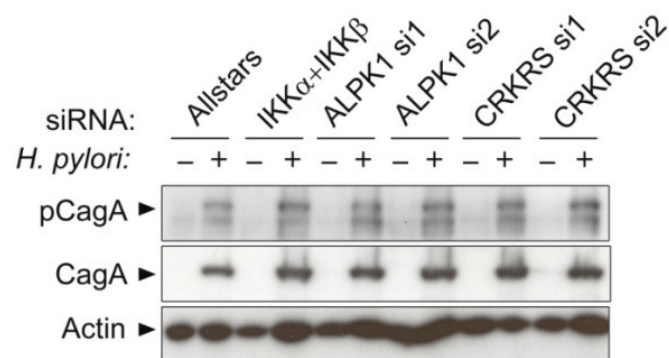


Fig. 20: Downregulation of ALPK1 or CRKRS does not inhibit phosphorylation of CagA after infection with *H. pylori*. AGS were transfected with the indicated siRNA, split after 24 h and after a minimum of 60 h post transfection infected with *H. pylori* MOI 100 for 4 h. Cells were lysed and subjected to western blot analysis and probed with antibodies detecting phosphor-tyrosine (and phosphorylated CagA), CagA, or actin. Results are representative of at least three independent experiments. si1= siRNA 1, si2 = siRNA 2.

Because the data showed the impact of ALPK1 and CRKRS on NF- κ B signaling on three different levels, IKK activity, p65 translocation and expression of the NF- κ B target gene IL-8, the question arose, whether other signaling pathways induced by *H. pylori* would be affected as well. To test this hypothesis, two pathways known to be induced by *H. pylori* were tested: activation of MAP kinases ERK and p38. Western blot analysis showed that both, phosphorylation of ERK1/ERK2 and p38 were not affected by downregulation of ALPK1 or CRKRS (Fig. 21).

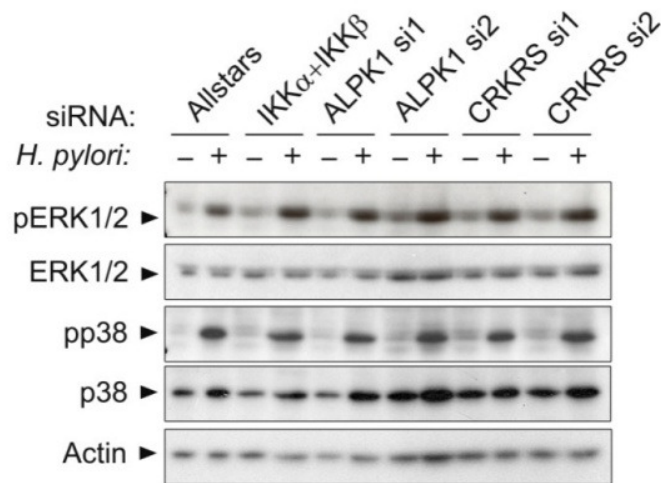


Fig. 21: Downregulation of ALPK1 or CRKRS does not inhibit *H. pylori*-induced activation of ERK and p38. AGS were transfected with the indicated siRNA, split after 24 h and after a minimum of 60 h post transfection infected with *H. pylori* MOI 100 for 30 min. Cells were lysed and subjected to western blot analysis using the indicated antibodies. Results are representative of at least three independent experiments. si1= siRNA 1, si2 = siRNA 2.

For experiments shown in Fig. 17-21, a single batch of cells was transfected and split on the following day in separate wells for the individual experiments. Therefore, IL-8 secretion, kinase activity, ERK- and p38-phosphorylation, CagA-phosphorylation and knock-down efficiency have all been measured in cells of the same transfection and results shown in Fig. 17-21 are directly comparable.

In conclusion, the results indicate that ALPK1 and CRKRS are important for NF- κ B activation after *H. pylori* infection and act upstream of IKKs but both genes have no impact on ERK and p38 signaling induced by *H. pylori* and do not inhibit function of bacterial T4SS.

2.2.8 SKP2 is necessary for termination of NF- κ B activity

SKP2 was identified in the screen as a gene important for termination of p65 translocation and its effect was visible most prominently in time courses where RNAi targeting SKP2 lead to prolonged translocation of p65-GFP. In addition, network analysis displayed SKP2 in the center of two networks of which many factors were identified in the screen: the cell cycle and NF- κ B pathway. SKP2 connects these pathways mainly in two ways: first, *skp2* is known to be a target gene of NF- κ B¹⁸³. Second, SKP2 is part of the SCF complex¹⁸⁴. Interestingly, also other F-box proteins such as β TrCP can be part of the SCF complex, providing molecular modularity. And while SCF^{SKP2} is most importantly known for its function in the

cell cycle ubiquitylating cell cycle regulators, SCF ^{β TrCP} ubiquitylates I κ Bs and plays a central role in NF- κ B signaling¹⁸⁴. Therefore, SKP2 might be an important link between cell cycle and NF- κ B pathway but so far, no direct influence has been shown for SKP2 on NF- κ B signaling.

Previous experiments showed that upon downregulation of SKP2, the percentage of activated cells does not decrease within the analyzed time. To evaluate whether termination was delayed or completely blocked, a longer time course experiment was performed. Because the effect was most prominently visible with IL-1 β , all following experiments were conducted with this inducer. After downregulation of SKP2, AGS SIB02 cells were stimulated with IL-1 β up to 3.5 h and p65 translocation was quantified by automated microscopy. Results indicated that downregulation of SKP2 led to a delay of termination: while in the controls, after 1.5 h, almost no cells with nuclear p65-GFP were detected, in the probes with SKP2 downregulation this was the case only after 3 h (Fig. 22). This prolongation of p65 translocation could also be observed on single cells using live cell microscopy. Again, in control cells, p65-GFP was visible in the nucleus for about 1.5 h while in cells transfected with SKP2 siRNA, p65-GFP remained in the nucleus for up to 3 h (Cindy Rechner, MPI for Infection Biology, Berlin, Germany, unpublished data).

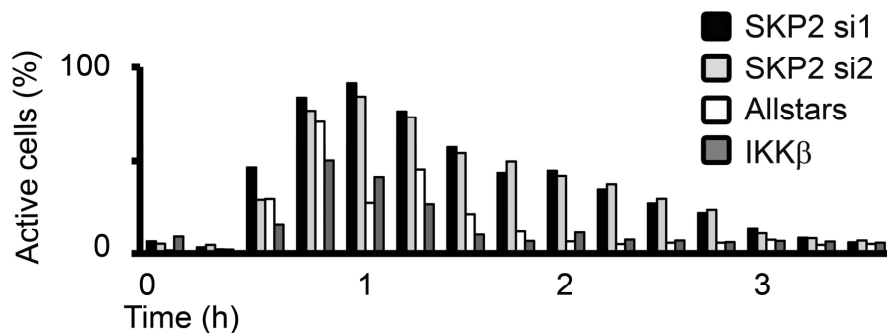


Fig. 22: SKP2 is necessary for termination of p65 translocation. AGS SIB02 cells were transfected with the indicated siRNAs and after three days stimulated with IL-1 β 10 ng/ml. Cells were fixed after the indicated time and p65 translocation was quantified by automated microscopy. Results are representative of three independent experiments. si1= siRNA 1, si2 = siRNA 2.

To evaluate whether SKP2 affected NF- κ B signaling upstream of p65 translocation, degradation of I κ B α after RNAi-mediated downregulation of SKP2 and subsequent induction with IL-1 β was analyzed by western blot. Unexpectedly, results showed that levels of I κ B α were generally slightly lower in cells treated with SKP2 siRNA compared to cells treated with control Allstars siRNA even without stimulus (Fig. 23 time point 0). Upon stimulation,

I κ B α was degraded in both cases but in SKP2 knockdown, the degradation is slightly prolonged (Fig. 23). The latter effect was subtle and not visible in all experiments.

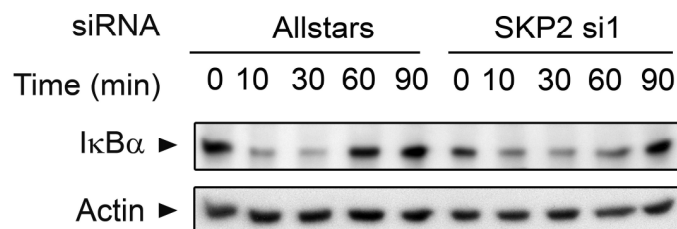


Fig. 23: SKP2 influences degradation of I κ B α . AGS SIB02 cells were transfected with the indicated siRNAs and after three days stimulated with IL-1 β 10 ng/ml for the indicated time. Cells were lysed, subjected to western blot and levels of I κ B α and actin control detected with antibodies. Results are representative of at least three independent experiments. si1= siRNA 1.

To evaluate IKK kinase activity, a kinase assay was performed after downregulation of SKP2 and subsequent induction with IL-1 β . To exclude a possible effect of p65-GFP, the parental cell line of AGS SIB02, AGS, was used. Results showed a prolonged activity of IKK α and IKK β after downregulation of SKP2 (Fig. 24).

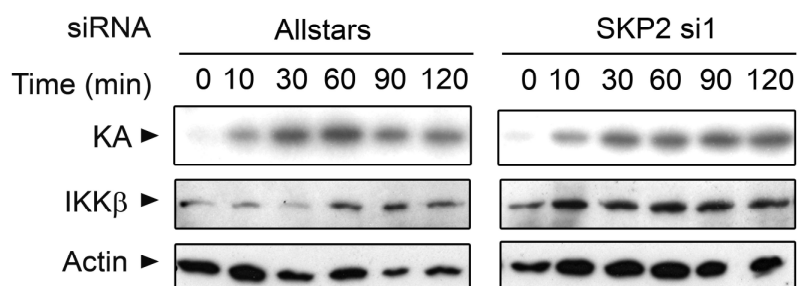


Fig. 24: Downregulation of SKP2 prolongs activity of IKK kinases. AGS were transfected with indicated siRNAs and stimulated with IL-1 β 10 ng/ml after three days. Cells were lysed after the indicated time and the IKK complex was immunoprecipitated using antibodies targeting NEMO. Kinase activity was measured by kinase assay (KA). As controls, lysates were analyzed by western blot for IKK β and actin. Results are representative of three independent experiments. si1= siRNA 1. Kinase assay was performed in collaboration with Michael Hinz, Max Delbrück Center Berlin, Germany.

In summary, SKP2 is important for termination of NF- κ B signaling. When SKP2 is downregulated, IKK activity, I κ B α and translocation of p65 are prolonged. Interestingly, even without stimulation, levels of I κ B α were slightly influenced by SKP2 downregulation, indicating that SKP2 might also play a role not only in the termination of signaling but also in general stabilization of I κ B α .

2.2.9 Discussion

Here, an RNAi-based screen is presented that identified 24 factors important in NF- κ B signaling after *H. pylori* infection or stimulation with TNF α or IL-1 β . Within this, the screen identified a connection between the cell cycle and NF- κ B. The relevance of the new NF- κ B regulators was demonstrated by further analysis of three selected genes: ALPK1, CRKRS and SKP2, the first two important for NF- κ B activation after *H. pylori* infection and the latter important for termination of the activation.

Important limitations of RNAi-based screens are false positives and false negatives^{176,177}. Here, to eliminate false positives, primary hits were validated with four siRNAs and 24 hits were confirmed with at least two siRNAs. In addition, three of these factors were also confirmed in other assays. Therefore, it can be concluded that the screen identified true key regulators. Although the number of false positives is within the range of other screens^{185,186}, two effects might have increased the number of false positives in this screen: (i) pooling of two siRNAs as used here in the primary screen can increase off-target effects [<http://www.ambion.com/techlib/tn/121/11.html>] and (ii) the NF- κ B pathway might be prone to off-target effects, because it is influenced by broad signaling networks, i.e. the cell cycle as the results in this work implicate. Therefore, off-target effects affecting connected networks could also alter NF- κ B activation. Regarding false negatives, here, two types have been observed. First, genes such as TAK1 that could in principle be detected by RNAi but the used siRNAs have failed to score in the primary screen. This was due to an unknown number of non-functional siRNAs in the library. The second type of false negatives observed did not meet threshold criteria although the gene might be involved. An example is FGFR4 which did not meet the criteria of the hit validation but the effect could be shown clearly in time course experiments. This type of false negatives may be caused by dose-dependency or redundant functions. As RNAi only reduces protein levels and seldom eliminates the protein completely, the remaining protein might be sufficient to display a phenotype that is not strong enough to meet the threshold set. In addition, complementing actions of other proteins can further reduce the phenotype.

Combinatorial downregulation of genes mediated by siRNAs can be a powerful tool to identify redundant proteins^{187,188}. Redundancy of proteins has evolved to buffer gene function and in humans, genetic buffering is achieved by the presence of two alleles of each gene, by duplicated genes with conserved functions, and by genes that have differ-

ent functions but still influence the same phenotype¹⁸⁰. Here, single knockdown of IKK α or IKK β did not induce a phenotype in TNF α or IL-1 β -induced signaling, whereas double knockdown abolished p65 translocation, indicating that IKK α and IKK β buffer each other's function. Apart from this, conclusions about functions and positions in a pathway that can be drawn from combinatorial effects are rather limited. Combinatorial downregulation of both, factors acting in parallel (such as IKK α and IKK β) as well as factors acting subsequently (such as IKK α and TAK1) can have additive effects. Therefore, other observed effects, for example the additive effect of ALPK1 and CRKRS cannot determine whether these two proteins act in parallel or subsequently. Future research is needed to clarify why some genes in the same pathway display buffering interactions, but not others, how much weakening of a process can be buffered, and how many buffering principles underlie such a complex network as NF- κ B signaling¹⁸⁰.

Here, evidence is presented that links the cell cycle to NF- κ B activation. A map of genes identified in this screen highlighted a network of cell cycle regulators consisting of WEE1, CDC2, AURKB, PLK1 and SKP2. Downregulation of the first four genes inhibited or delayed translocation of p65-GFP while downregulation of SKP2 promoted it (Fig 25a). It is possible that WEE1, CDC2, AURKB and PLK1 exclusively act in TNF α signaling but this should be confirmed using other assays. Although several reports demonstrated the impact of NF- κ B on proliferation¹⁸⁹ and cell cycle regulators such as Cyclin D1^{22,190} or SKP2^{183,191}, only few studies have addressed the question whether there is an influence *vice versa*. While G0 phase arrest was shown not to influence NF- κ B¹⁹², S phase arrest elevates NF- κ B activity¹⁹³, but p100 processing is inhibited during S-phase¹⁸³. To my knowledge, a clear study, analyzing NF- κ B responses to various stimuli in the different cell cycle phases has not been conducted.

The cell cycle-regulating functions of the five genes identified here are known. CDC2 is alternatively named CDK1 and is the key kinase that promotes entry into mitosis. WEE1 is the kinase that phosphorylates CDC2. Activation of CDC2 depends on dephosphorylation by the phosphatase CDC25C. PLK1 in turn is important in activating CDC25C and may downregulate WEE1. In addition, PLK1 cooperates with CDC2 to initiate formation of the anaphase promoting complex/cyclosome (APC/C). Also, PLK1 and AURKB have been implicated in control of cytokinesis¹⁹⁴. SKP2 is a part of the SCF complex and can activate CDC2 by ubiquitinylation of its inhibitor p27 that is subsequently degraded¹⁸⁴ (Fig. 25b).

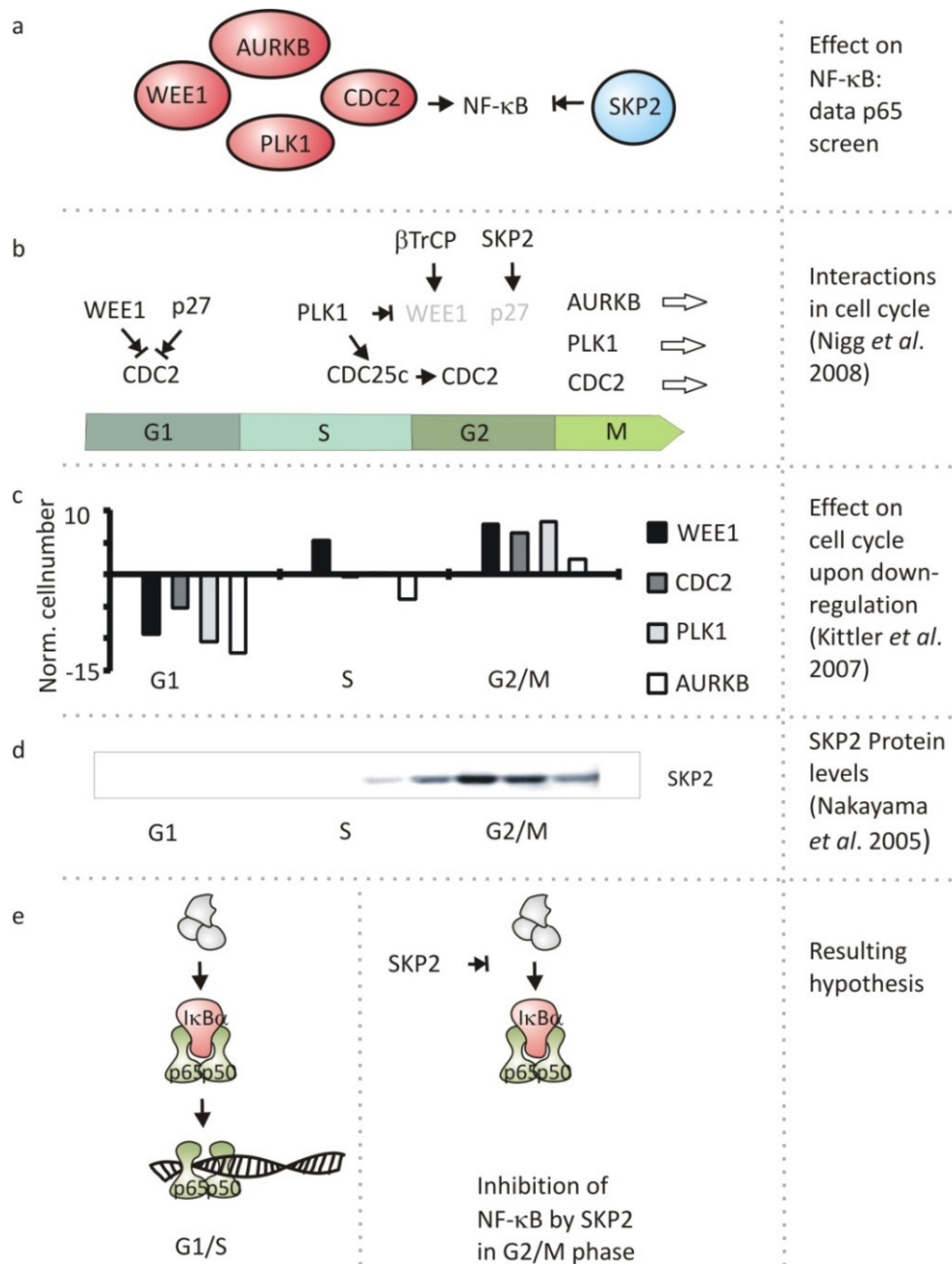


Fig. 25: Influence of cell cycle regulators on NF- κ B: a model for G2/M arrest-induced NF- κ B inhibition. a) Data presented in this work showed WEE1, CDC2, AURKB and PLK1 are important for activation of NF- κ B and SKP2 is important for termination of NF- κ B signaling. b) The four factors important for activation act in closely related positions in the cell cycle and are important for G2/M transition and mitosis¹⁹⁴. Please see discussion for details. c) RNAi-mediated downregulation of the four factors led to G2/M arrest in a published RNAi based screen in HeLa cells¹⁹⁵. HeLa cells were transfected with esiRNAs (endonuclease-prepared siRNAs), fixed, and stained with propidium iodide and DNA content was measured using automated picture analysis. Cell numbers and percentages of cells with G1, S, G2/M phase was quantified, normalized to negative controls and the mean of two independent experiments is shown here. d) Expression of SKP2 during the cell cycle (adapted from¹⁹⁶). Freshly isolated mouse lymphocytes in G0 phase were stimulated with phorbol ester and calcium ionophore for the indicated times. Cell lysates were subjected to western blot analysis with antibodies to SKP2. SKP2 is not expressed in G0 and G1 phase but is abundant during S and G2 phase. e) Model for G2/M arrest-induced NF- κ B inhibition. While NF- κ B is activated normally in G1 and S phase, NF- κ B activation is inhibited or delayed by elevated protein levels of SKP2 in G2/M phase.

To better understand possible phenotypes that are associated with RNAi-mediated knock-down of the four genes important for NF- κ B activation, the information available from a published RNAi-based screen analyzing the cell cycle in HeLa cells¹⁹⁵ was assessed. In this screen, knockdown of SKP2 did not have an effect, while all four genes important for NF- κ B activation led to highly increased percentages of cells in the G2/M phase, indicating G2 arrest or cell division defect (Fig. 25c). Out of 13 closely related genes (CDKs, PLKs, AURKs) only AURKA (=STK6) showed a similar but weaker phenotype¹⁹⁵. Downregulation of AURKA also had a highly reproducible inhibitory effect on p65 translocation in the primary screen, but this effect was below the threshold for primary hits. It seems unlikely to be a coincidence that the exact same genes out of a pool of related genes have an effect on NF- κ B activation as well as on the cell cycle. It might be possible that a G2 arrest generally leads to inhibition or delay of NF- κ B activation. Interestingly, SKP2 (which was identified here as important for NF- κ B termination) is highly upregulated in G2 phase¹⁹⁶. Therefore, as a working hypothesis for future experiments, it is possible that the inhibitory effects of CDC2, WEE1, PLK1 or AURKB knockdown could be due to G2 arrest, upregulation of SKP2 and eventually NF- κ B inhibition by SKP2 (Fig. 25).

The mechanism, by which SKP2 functions as negative regulator of NF- κ B so far, can only be subject to speculation. Here, downregulation of SKP2 had two effects: (i) NF- κ B activation was prolonged, which affected IKK activity, I κ B α degradation and translocation of p65-GFP on population level as well as on single cell level. (ii) Levels of I κ B α were generally slightly reduced. This suggests two inhibitory actions of SKP2: a negative feedback upstream of the IKK complex and a general one downstream of it. The first seems to be a delayed response after activation and implies a negative feedback whereas the second might be rather general and independent of activation. Previous studies have shown that RelB regulates *skp2* during the cell cycle and p65 also binds the promoter^{183,191}, suggesting a possible negative feedback. SKP2 can be part of the SCF complex, in which different F-box proteins confer substrate specificity. F-box proteins are named for an F-box motif first identified in Cyclin F¹⁹⁷. Currently, 69 F-box proteins have been identified in humans but only six have proposed substrates, two of which are SKP2 and β TrCP¹⁸⁴. While SCF ^{β TrCP} is well known to ubiquitinylate I κ Bs and is therefore an important part of NF- κ B signaling, SCF^{SKP2} degrades p27¹⁸⁴. In *skp2*^{-/-} mice, p27 accumulates which leads to impaired growth of these mice¹⁹⁸. Double knockout of *skp2* and *p27* abolishes this phenotype, indicating

that p27 is the most important target of SKP2^{199,200}. Based on this, two working hypotheses are feasible. (i) Similarly as A20 or c-IAP1^{58,59}, SCF^{SKP2} could ubiquitinate an activator of NF- κ B upstream of the IKK complex which is subsequently degraded. (ii) SKP2 could be a competitor for β TrCP in the SCF complex. Given the assumption that the “stable” components of the SCF complex (SKP1, Cul1 and RING protein) remain on the same protein level while protein levels of one F-box protein dramatically increase, this F-box protein could replace others. In a knockdown situation, a lack of SKP2 could lead to increased numbers of SCF-complexes containing β TrCP. This unbalanced situation could even confer increased I κ B α degradation without stimulus. Nevertheless, a competitor hypothesis would not explain the prolonged IKK activity. Future work has to investigate whether SKP2 acts via one or both mechanisms: activator degradation as well as competition – or possibly a third, so far not predicted process (Fig. 26).

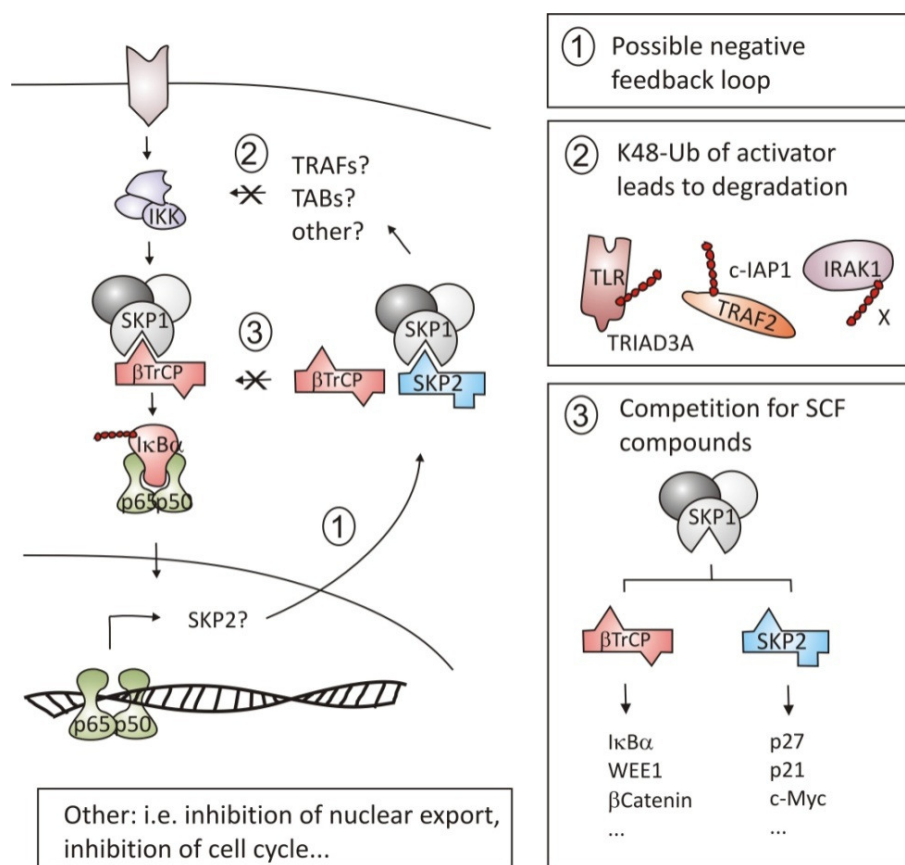


Fig. 26: Model of NF- κ B inhibition by SKP2. Activation of NF- κ B could possibly induce *skp2* gene transcription, leading to upregulated SKP2 protein levels to induce negative feedback. SKP2 may act on two levels: ubiquitinylation of an activator upstream of IKK could lead to degradation of the activator which would terminate IKK activity. Ubiquitinylation and degradation is for example known from TLRs, TRAF2 and IRAK1. In addition, competition with β TrCP for SCF complex could lead to reduced levels of SCF ^{β TrCP} available for degradation of I κ B α . Other mechanisms are also possible.

The connection between SKP2, the cell cycle and NF- κ B probably plays a role in cells where NF- κ B signaling induced in resting cells leads to a different response than in cycling cells. An example for this could be T cells: resting T cells are activated by TCR engagement; while repeated encounter with TCR ligand can induce cell death (activation induced cell death AICD). AICD plays a major role in downregulating an immune response. Interestingly, previous studies showed an influence of NF- κ B signaling in AICD²⁰¹, including a correlating loss of nuclear p65 with induction of AICD²⁰². If future experiments would verify the connection via the cell cycle, it would deepen our understanding of an important immunological function. Furthermore, because both, SKP2 as well as NF- κ B play a role in cancer development and have been implicated as targets for cancer therapy^{59,184} it might be important for therapeutic approaches to further analyze this relationship.

Here, ALPK1 and CRKRS have been shown to be necessary for *H. pylori*-induced p65-translocation, IKK activity and IL-8 secretion. Both factors specifically act in NF- κ B signaling and do not play a role in adhesion of bacteria, function of T4SS and ERK or p38 signaling. Both acted exclusively on p65 translocation induced after *H. pylori* infection but not after TNF α or IL-1 β stimulation. However, recent and preliminary experiments using a transcriptional reporter assay indicate that both genes might also have an impact on TNF α and IL-1 β -induced NF- κ B activation (Cindy Rechner, unpublished data). Functions of both factors, ALPK1 and CRKRS are not well understood. ALPK1 is a member of an atypical kinase family called alphakinases. Up to date, six alphakinases are known²⁰³. In contrast to the tyrosine- and serin/threonine-kinases, together known as conventional kinases, which recognize phosphorylation sites within loops, turns or irregular structures²⁰⁴, alphakinases recognize phosphorylation sites within alphahelices²⁰⁵. A recent publication showed that ALPK1-mediated phosphorylation of myosin 1a is necessary for apical delivery of raft-carrying vesicles¹⁸¹. Therefore, a feasible hypothesis would be that ALPK1 is important in apical transport of a receptor or receptor-interacting proteins important in recognizing *H. pylori*. If ALPK1 would be involved in general transport to the membrane, also other signaling, such as TNF α - or IL-1 β -induced NF- κ B activation could be affected. It is also known that further but so far unidentified substrates of ALPK1 exist¹⁸¹. Therefore, it is also possible that ALPK1 phosphorylates other mediators of NF- κ B signaling.

CRKRS was first identified as a member of the cyclin related kinases²⁰⁶, a family of kinases that in their kinase domain share a high sequence homology with CDC2 but do not de-

pend on cyclins. Within the family of CRKs, CRKRS shares the highest homology with cholinesterase-related cell division controller (CHED, alternatively named CDC2-like5)²⁰⁶. CHED has been suggested to be involved in hematopoiesis²⁰⁷ and a related protein, CHED-like kinase, is involved in insect immunity²⁰⁸. CRKRS was shown to be localized in the nucleus in speckled structures that colocalize in part with spliceosome components, specifically the phosphorylated form of the major subunit of RNA polymerase II²⁰⁶. Therefore, it was suggested, that CRKRS might be involved in regulation of RNAse polymerase II activity²⁰⁶. A second study has implicated CRKRS in alternative splicing¹⁸². Taken together, a connection to the NF- κ B pathway does not seem obvious but it can be envisioned that the function of NF- κ B mediators may depend on alternative splicing. However, new and so far unidentified functions of CRKRS could also cause the phenotype observed here.

Although the main focus of this work has been the identification of novel factors such as SKP2, ALPK1 and CRKRS, signaling components previously known in *H. pylori*-induced NF- κ B signaling have also been tested. The key role of IKK α and IKK β , both well known from literature^{102,123,124} was not only confirmed but it was also shown, that a combination of siRNAs targeting IKK α and IKK β abolished *H. pylori*-induced NF- κ B activation. Therefore, the IKK complex is indispensable for the activation. Involvement of TAK1 in *H. pylori*-induced NF- κ B activation has been questioned, because only RNAi targeting TAK1¹⁰², but not expression of a dominant negative construct¹²⁵ inhibited NF- κ B signaling. The data provided in this work clearly confirms the involvement of TAK1 after *H. pylori* infection: two independent siRNAs led to strong reduction of p65 translocation. Furthermore, the role of TRAF6, MyD88 and NOD1^{102,121} was confirmed, whereas involvement of TRAF2 and NIK, which has been shown using dominant negative constructs^{120,123-125}, was not confirmed. This supports the previous finding that RNAi targeting TRAF2 also showed no involvement of TRAF2 in *H. pylori* induced NF- κ B activation¹⁰². Because the siRNAs used in this experiment were only validated in previous experiments [Nikolaus Machuy, unpublished] but not in the specific experiments, it is possible that the remaining protein levels were sufficient to prevent expression of a phenotype and based on the data presented here, involvement of TRAF2, NIK and TAB2 cannot be excluded. However, this study has focused on identification of new regulators and has therefore not elucidated effects of previously published factors in detail.

In summary, it seems probable, that *H. pylori* triggers multiple pathways. While peptidoglycan may stimulate NOD1¹²¹, in parallel, a so far not tested TLR could be activated to induce MyD88/TRAF6/TAK1 dependent signaling. In addition, further so far unknown pathways are likely to play a role. ALPK1 and CRKRS could either act directly or indirectly by influencing other mediators on NF- κ B signaling. The bottleneck leading to p65 translocation is activation of IKK α and IKK β (Fig. 27).

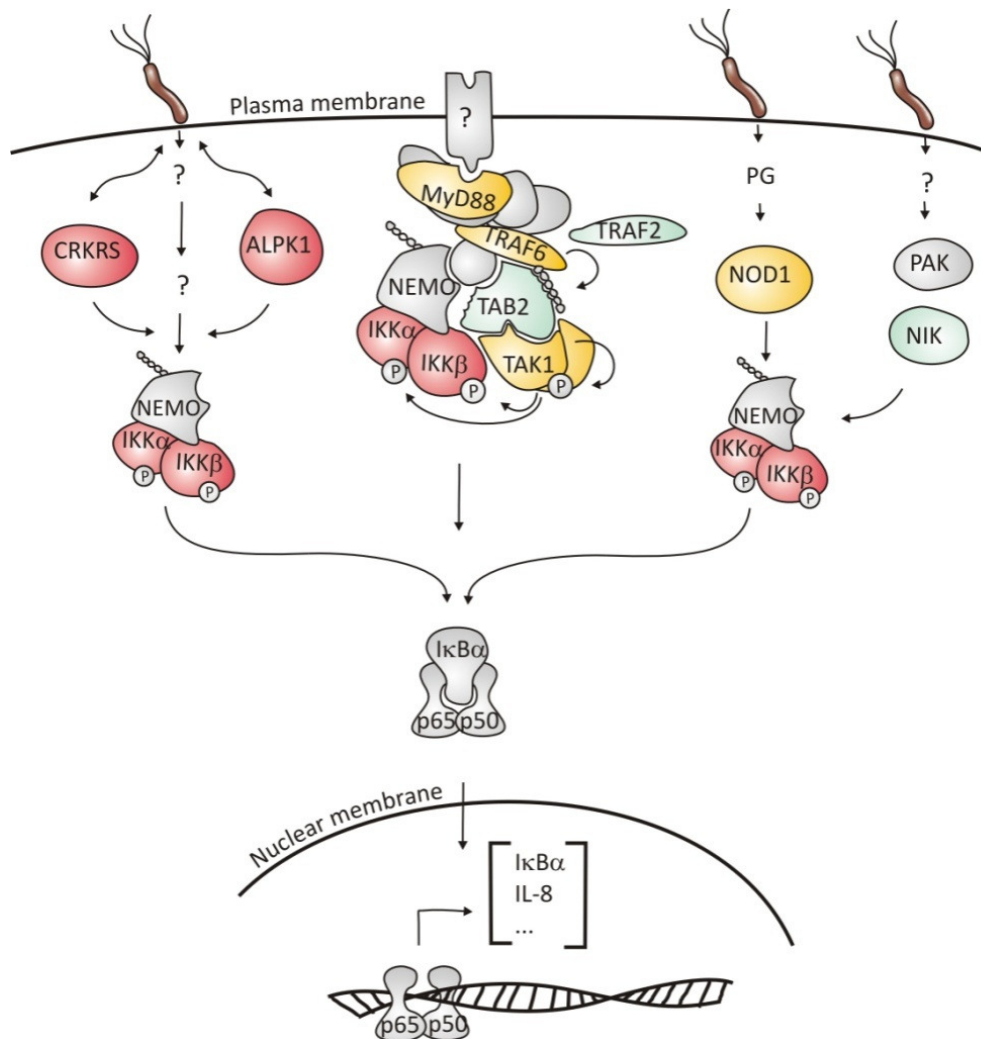


Fig. 27: Multiple pathways may lead to NF- κ B activation after *H. pylori* infection in human epithelial cells. Screening a library of 646 kinases, in this work, four genes were identified to be important in NF- κ B activation: IKK α , IKK β , CRKRS, and ALPK1 (red). In addition, other known regulators were tested and either confirmed (MyD88, TRAF6, TAK1, and NOD1 (orange)) or not confirmed (NIK, TRAF2, and TAB2 (blue)). Because downregulation of a single gene did not lead to more than approximately 50% reduction, it seems probable, that multiple pathways act in parallel. The mechanisms of ALPK1 and CRKRS interaction with the NF- κ B pathway have not yet been identified. It is possible that they act as new mediators in the NF- κ B pathway or that they influence other (known) mediators or receptors.

2.3 Part III: Two tracks of NF- κ B activation induced by *L. pneumophila*

2.3.1 Biphasic p65 translocation during *L. pneumophila* infection

To investigate NF- κ B activation induced by *L. pneumophila* A549 SIB01 cells were infected with *L. pneumophila* at an MOI of 100 and translocation of p65-GFP was monitored by live cell microscopy. Upon bacterial entry, a short and transient translocation of p65 to the nucleus could be detected. This was later followed by a continuous p65-translocation to the nucleus (Fig. 28).

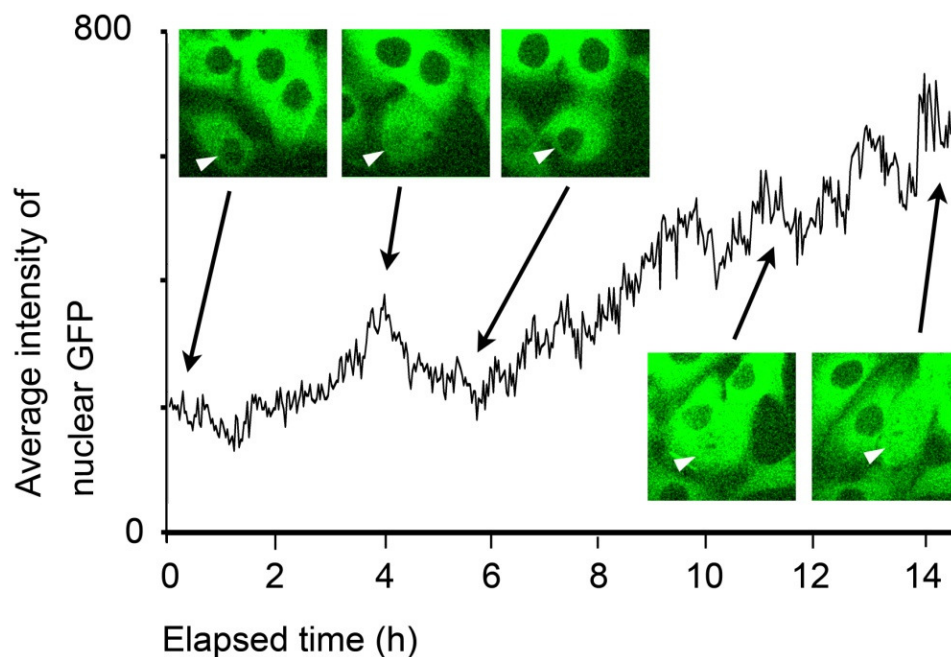


Fig. 28: Biphasic nuclear translocation of p65-GFP after infection with *L. pneumophila*. A549 SIB01 cells stably expressing p65-GFP were infected with *L. pneumophila* strain Philadelphia-1 (MOI 100) without centrifugation and monitored with live cell confocal microscopy. White arrow indicates the nucleus. Intensity of GFP was measured by Metamorph software in a representative nuclear region.

The continuous nuclear localization of the p65-GFP could be seen until the cells rounded up and detached from the matrix, about 30 hours after infection. Phase contrast during live cell microscopy revealed that the activated cells contained a vacuole in the cytoplasm that increased in size over time. After fixation and staining with anti-*Legionella* antibodies, confocal microscopy confirmed that this vacuole contained *L. pneumophila* (Fig. 29). Continued live cell microscopy showed motile bacteria leaving a cell after two days of infection which had included 30 h of continued nuclear localization of p65-GFP (data not shown).

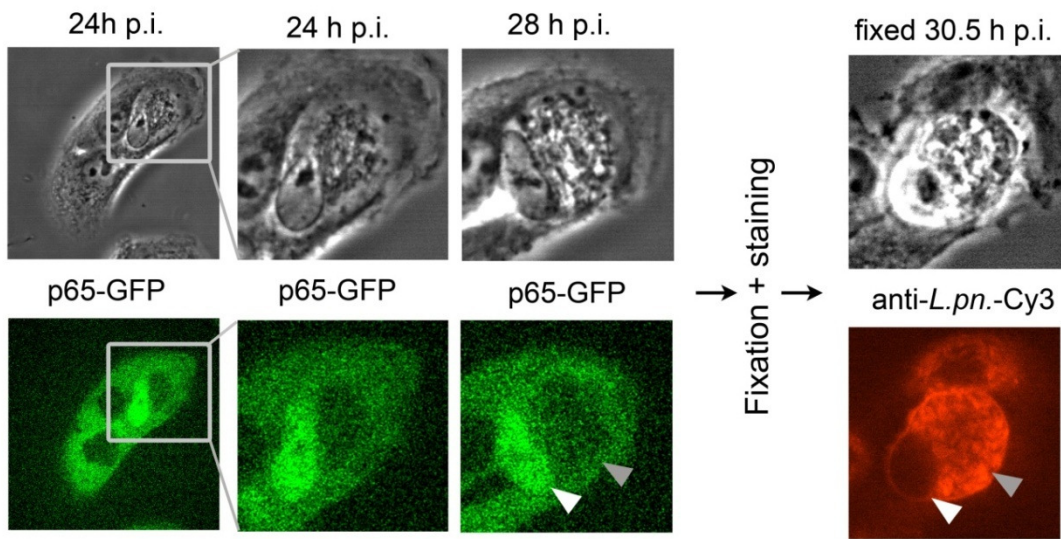


Fig. 29: *L. pneumophila* replicates in cells with permanent nuclear localization of p65-GFP. A549 SIB01 cells were infected with *L. pneumophila* strain Philadelphia-1 (MOI 100). After 24 h of infection, nuclear localization of p65-GFP was observed with confocal live cell microscopy over 6.5 h. One cell was permanently activated while neighboring cells were not. Subsequently, cells were fixed, stained with anti-*Legionella* antibodies and analyzed by confocal microscopy. a) Overview b) Zoom-in. White arrows indicate the nucleus; grey arrows indicate the *Legionella* containing vacuole. p.i. = post infection.

2.3.2 NF- κ B activation profiles of *L. pneumophila* wild-type strains

To analyze possible strain specific differences of *L. pneumophila* wild type strains, a variety of strains were tested for their ability to induce p65 translocation in A549 SIB01 cells. Both activation phases of NF- κ B were observed in all four wild type strains tested (JR32, Philadelphia-1, Paris, Corby), but the second activation was shortened in the Corby strain. The strongest effect on long-term NF- κ B activation was observed in the Paris strain (Fig. 30a).

2.3.3 Transient p65 translocation depends on intact flagella

To identify bacterial factors involved in short and long term activation events, respectively, several *Legionella* mutant strains were tested for their capacity to activate NF- κ B. Because flagellin has previously been shown to activate NF- κ B^{137,143}, several mutants deficient in flagellin were tested. Corby Δ *flaA* is defective in flagellin production (*flaA* encodes flagellin), Paris Δ *fliA* does not produce the sigma factor 28 (FlhA), which directly controls FlaA synthesis and some other genes¹³¹. Paris Δ *letA* does not produce the response regulator LetA, which is part of the two-component system LetS/LetA. This system is needed to counteract the carbon storage regulator CsrA, a pivotal regulator of the replicative phase of the *Legionella* life cycle. Accordingly, LetS/LetA is indispensable for entry into the transmissible, virulent phase, the phase in which *L. pneumophila* becomes motile. There-

fore, *letA/letS* mutants are non-motile, and lack flagellin²⁰⁹. All three mutants did not induce the first activation (Fig. 30b). Therefore, flagellin only causes the first, transient activation.

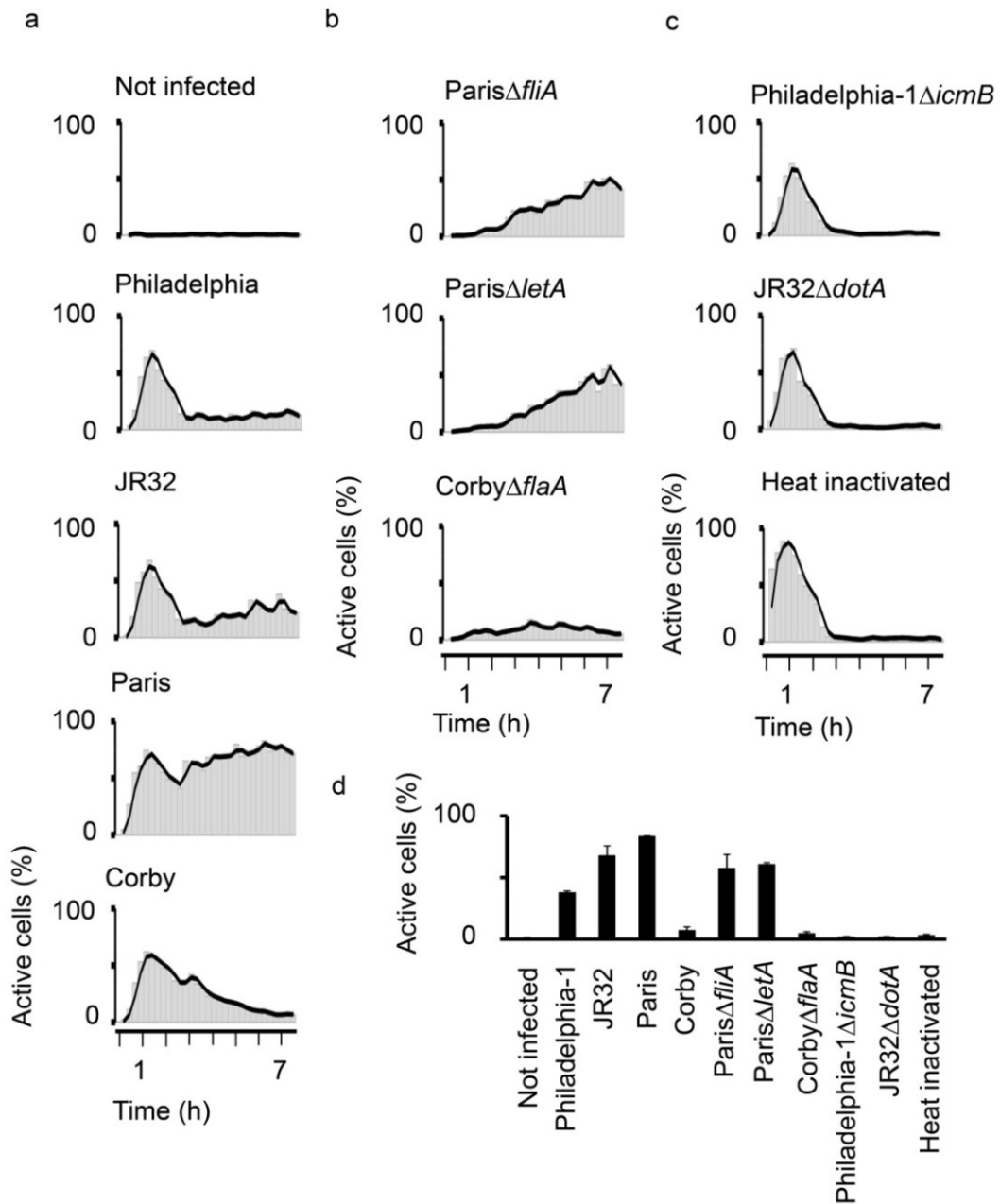


Fig. 30: Transient NF- κ B activation by *L. pneumophila* depends on flagellin, continuous NF- κ B activation on Dot/Icm system. A549 SIB01 cells were infected with wild type strains (a), mutant strains lacking flagellin (b) or mutant strains lacking the Dot/Icm system (c). Cells were infected with the indicated strains (MOI 100) without centrifugation (a, b, c) or with centrifugation (d). Cells were fixed after the indicated time, stained with Hoechst 33342 and analyzed by automated microscopy as in Fig. 5. Results are presented as bars of duplicates (grey) and moving average of 2 (black line) (a, b, c) or as bars of duplicates with standard deviation (d). The heat inactivated strain is Philadelphia-1 MOI 100.

2.3.4 Continuous p65 translocation depends on the Dot/Icm system.

Because previous work has implied the bacterial Dot/Icm system in NF- κ B activation^{144,150}, mutants deficient in this system were tested next: JR32 Δ *dotA* and Philadelphia-1 Δ *icmB/dotO*. Both mutants failed to induce continuous activation of NF- κ B (Fig. 30c), indicating that either one or several effectors released by the Dot/Icm secretion system were necessary for this long-term effect. Furthermore, heat killed bacteria also induced the first transient activation but not a continuous activation. Notably, bacteria were not removed from the cells in this experiment. Therefore, the first, transient activation was terminated in spite of a remaining stimulus, while the second activation is not.

To enhance the strain- and mutation-specific differences in the late activation, the contact between bacteria and cells was promoted by centrifugation, thereby increasing probability of successful infection and the rate of activated cells. Results confirmed that the late activation does not depend on flagellin, but on the Dot/Icm system of bacteria (Fig. 30d).

2.3.5 Involvement of single Dot/Icm secreted effectors

To investigate whether specific effectors secreted by the Dot/Icm system were involved in continuous activation, mutants of single effectors were tested (Fig. 31).

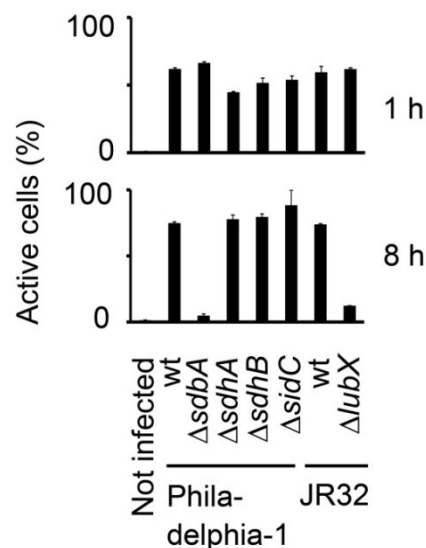


Fig. 31: SdbA and LubX are important for permanent p65 translocation. A549 SIB01 cells were infected with the indicated strains at an MOI of 100 either without centrifugation for 1 h to analyze the first activation (upper panel) or with centrifugation for 8 h to analyze the permanent p65 translocation (lower panel). Cells were fixed and p65 translocation was analyzed by automated microscopy. Error bars = SD of duplicates. Results are representative of at least three independent experiments.

Since NF- κ B signaling is well known to be strongly dependent on ubiquitin signaling, it was hypothesized here that *Legionella* U-box protein LubX, which has been shown to act as ubiquitin ligase (E3) and to mediate polyubiquitinylation of the host cell protein CDC-like kinase 1 (Clk1)¹³³, could interfere with NF- κ B signaling. To compare with other Dot/Icm effectors, mutants lacking *sdbA*, *sdhA*, *sdhB* or *sidC* were chosen. These genes have been reported to have roles in protection from host cell death (*sdhA*)²¹⁰, ER-recruitment (*sidC*)^{211,212}, and replication within macrophages (*sdbA*)²¹³. Of the tested mutants defective in *sdbA*, *sdhA*, *sdhB*, *sidC* or *lubX*, only mutants defective in *sdbA* and *lubX* showed no continuous activation albeit a normal flagellin-dependent transient activation (Fig. 31).

2.3.6 Bacterial replication and continuous p65 translocation are tightly linked

Results from above experiments indicated a possible link between long-term p65 translocation and intracellular replication. Hence, the replication efficiency of *L. pneumophila* mutants, Δ *sdbA*, Δ *lubX* and Δ *sdhA* in was evaluated A549 cells: In contrast to the wild type strains, but similar to the Δ *dotA* mutants known to be deficient in growth, both Δ *sdbA* and Δ *lubX* did not replicate. Δ *sdhA* replicated, but less well than the wild type (Fig. 32 for *lubX* and Cecilia Engels, MPI for Infection Biology, Berlin, Germany, unpublished data for *sdbA* and *sdhA*). Thus, so far, all genes identified as important for long-term p65 translocation, were also found to be important for intracellular growth in A549.

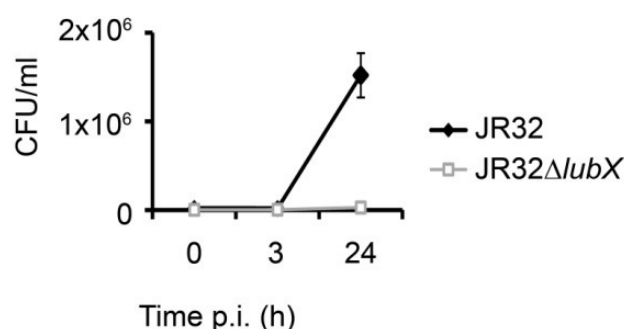


Fig. 32: LubX is important for intracellular growth in A549 cells. Cells were infected with the indicated strains at an MOI of 100 with centrifugation. After 1.5 h, extracellular bacteria were removed by washing, remaining extracellular bacteria were killed by gentamicin, and multiplication of *Legionella* was assessed by CFU counting. Error bars = SD of triplicates. Results are representative of three independent experiments.

To further test the hypothesis that continuous NF- κ B activation is linked to intracellular growth, additional mutants with known growth defects were tested (Fig. 33).

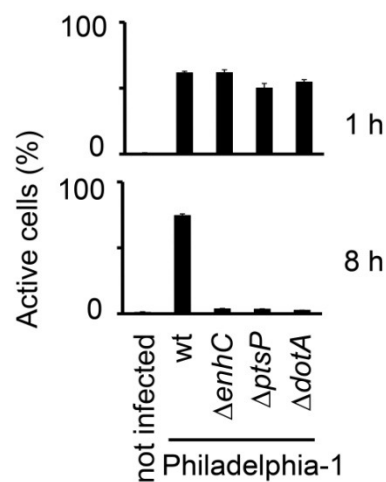


Fig. 33: Bacteria with known growth-defects do not induce permanent p65 translocation. A549 SIB01 cells were infected with the indicated strains (MOI 100) either without centrifugation for 1 h to analyze the first activation (upper panel) or with centrifugation for 8 h to analyze the permanent p65 translocation (lower panel). Cells were fixed and p65 translocation was analyzed by automated microscopy. Error bars = SD of duplicates.

The mutant $\Delta enhC$ was originally identified as being defective for uptake into host cells²¹⁴, and recently described as defective in efficient intracellular growth in TNF α -stimulated macrophages²¹⁵. Mutants deficient in the gene *ptsP*, which encodes a phosphoenolpyruvate-protein phosphotransferase, a component of the phosphoenolpyruvate-dependent nitrogen-metabolic phosphotransferase system, have been shown to be growth deficient in A549 cells, and in both lung and spleen of guinea pigs²¹⁶. Here, the $\Delta enhC$ and $\Delta ptsP$ mutants induced a normal first, transient p65 translocation, consistent with the fact that they possess a functional flagellum, but no second long-term activation.

2.3.7 $\kappa B\alpha$ is degraded during continuous activation

To exclude a possible effect of p65-GFP expression on the continuous nature of the NF- κ B activation, degradation of $\kappa B\alpha$ was observed in the parental cell line. For comparison, both cell lines were infected in parallel over 8 hours, p65 translocation was quantified in A549 SIB01 and $\kappa B\alpha$ degradation was analyzed by western blot in A549. $\kappa B\alpha$ degradation in A549 corresponded well to long-term p65 translocation (Fig. 34). Therefore, permanent NF- κ B activation by *L. pneumophila* is not specific to the p65-overexpressing cell line and involves $\kappa B\alpha$ degradation. To further exclude a possible effect specific to the A549 cell line, results were confirmed in a second cell line, AGS SIB02 (data not shown).

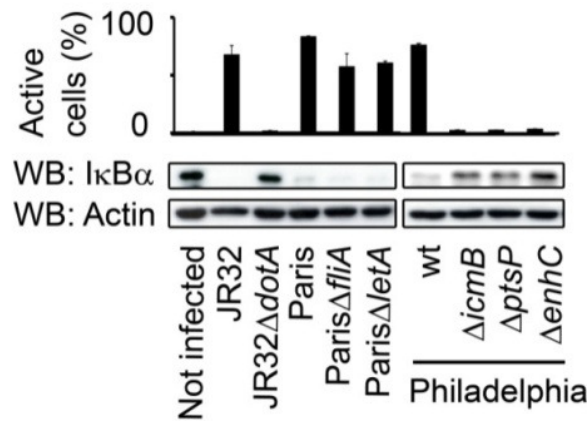


Fig. 34: Degradation of I κ B α after infection with *L. pneumophila*. The p65 indicator cell line A549 SIB01 (for the analysis of p65 translocation) or the parental cell line A549 (for monitoring I κ B α degradation) were simultaneously infected with the indicated strains at MOI 100 with centrifugation. After 8 h of infection, A549 SIB01 cells were fixed and analyzed by automated microscopy. Results are shown as graph (upper panel). A549 were lysed and subjected to western blot analysis. Error bars = SD of duplicates. Results are representative of at least three independent experiments.

2.3.8 TLR5 and MyD88 are only important for early activation

To identify possible host cell signaling mediators, involvement of different factors was analyzed by RNAi. As expected, the first, transient activation was partly dependent on TLR5 and strongly dependent on MyD88, but not on NOD1. None of the tested siRNAs showed an influence on long-term p65 translocation (Fig. 35).

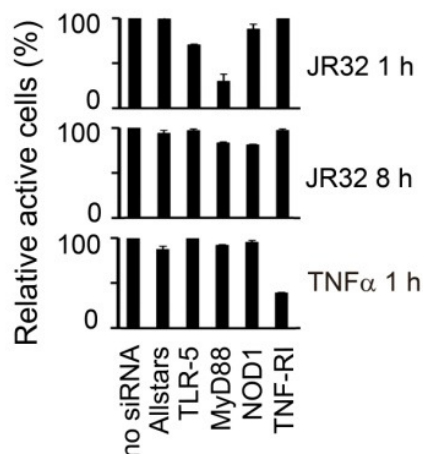


Fig. 35: Early, transient p65 translocation depends on MyD88 and TLR5. A549 SIB01 cells were transfected with the indicated siRNAs and after three days infected with JR32 MOI 100 without centrifugation for 1 h (upper panel), with JR32 MOI 100 with centrifugation for 8 h (middle panel) or as control activated with TNF α 10 ng/ml for 1 h (lower panel). Cells were fixed and p65 translocation analyzed by automated microscopy. Error bars = SD of duplicates. Results are representative of at least four independent experiments.

2.3.9 Discussion

Here it is shown that infection with *L. pneumophila* induces a biphasic activation of NF- κ B: early in infection, bacterial flagellin induces transient NF- κ B activation via TLR5 signaling and at later time points, an unknown factor that depends on bacterial replication and a functional Dot/Icm system induces continuous nuclear localization of p65. This time-resolved activation provides new insights into the two apparently opposing effects of NF- κ B activation upon *Legionella* infection, one beneficial for the host (the activation of the innate immune response), and one beneficial for the pathogen (anti-apoptosis).

The importance of flagellin, TLR5 and MyD88 in *L. pneumophila* infection is well known. Alveolar macrophages isolated from wild type mice secrete TNF α in response to purified *L. pneumophila* flagellin while those of TLR5^{-/-} knockout mice do not²¹⁷. Early IL-8 secretion in *L. pneumophila*-infected A549 cells depends on bacterial flagellin^{137,143}. This study corroborates these findings by demonstrating the early nuclear translocation of p65 is dependent on bacterial flagellin and the host cell proteins TLR5 and MyD88. TLR signaling is a central part of the innate immune system²¹⁸. TLRs recognize a variety of conserved MAMPs, such as flagellin, and subsequently trigger a signaling cascade culminating in activation of NF- κ B, which induces the production of cytokines, chemokines and upregulation of co-stimulatory molecules important for immune cell activation⁴. Accordingly, it has been demonstrated that TLR5-mediated recognition of *L. pneumophila* flagellin has an important function in host defense. Human genetic studies have found that a common stop codon polymorphism in TLR5 alters susceptibility to Legionnaires' disease¹⁴⁹. TLR5^{-/-} knockout mice showed an impaired immune response to *L. pneumophila* during the first four hours of infection²¹⁷ and mice deficient in the TLR adaptor protein MyD88 were highly susceptible to infection with *L. pneumophila*²¹⁹. Therefore, it can be concluded that the first wave of NF- κ B activation upon *L. pneumophila* infection is a normal and necessary part of the host's defense.

In contrast to the first, transient activation, the second NF- κ B activation demonstrated here lasted for many hours and even days. This permanent nuclear translocation of p65 is highly unusual, but in agreement with previous work reporting a sustained and Dot/Icm-dependent activation of NF- κ B in response to *Legionella* infection in macrophages^{144,150}. Both previous studies reported a strong nuclear association of the NF- κ B subunit p65 in macrophages for up to 12 or 14 h post infection, however, the dynamics of NF- κ B nuclear

translocation remained enigmatic due to the use of fixed and immune-stained cells at a few selected time points after infection. Therefore, it was expected initially that p65 would oscillate between the nucleus and the cytoplasm, a well described phenotype that is a direct consequence of the NF- κ B-I κ B α negative feedback loop^{47,54} and has been demonstrated in response to *H. pylori* in the first part of this thesis. However, surprisingly, live-cell experiments here could show here that NF- κ B activation induced by *L. pneumophila* involves permanent nuclear translocation of p65 without oscillations.

Usually, NF- κ B activation is tightly controlled and soon terminated. This is also visible in signaling induced by *L. pneumophila* flagellin: despite excess flagellin in the medium (i.e. after heat killing of bacteria), TLR signaling is terminated. This tolerance to a MAMP is well known from LPS; in addition, termination of MAMP-PRR induced signaling is known to be essential to a functional immune system: A continuous response to invading bacterial organisms can be dangerous because of the autotoxic effect of the overproduction of inflammatory mediators, which can lead to local or even systemic damages, i.e. septic shock⁷. Therefore, an extensive regulatory machinery controls the termination of TLR signaling and NF- κ B activation^{9,23,57}. Accordingly, constitutive NF- κ B activation absent from most normal cells (known only from mature B-cells^{12,220}, some T cells²²¹, Sertoli cells²²², and a small subset of neural cells^{223,224}) but a hallmark of many cancers⁸. Therefore, the failure of the cell to terminate the continuous NF- κ B activation induced by *L. pneumophila* indicates that this is not the usual NF- κ B activation induced by PRRs. In summary, the lack of oscillations in combination with the unnatural duration of the activation suggests that *L. pneumophila* may be actively interfering with NF- κ B signaling.

Many pathogens have evolved means to exploit the anti-apoptotic effects of NF- κ B in order to ensure the integrity of the infected cell. This particularly applies for intracellular pathogens including *L. pneumophila*^{144-148,211}. The parasite *Theileria parva*, which infects lymphocytes of cattle, sheep and goat, recruit the IKK complex to the surface of the schizont and permanently activate it, which leads to cancerogenic transformation of cells. These cells become independent of growth factors, form tumors in immunosuppressed mice and even form metastatic phenotypes²²⁵. Remarkably, if the parasite is killed, the transformation is reversed. In infections with an apicomplexa parasite related to *T. parva*, *T. gondii*, phosphorylated I κ B α can be stained around the parasitophorous vacuole membrane¹⁴⁷ and it was shown that the parasite has its own IKK kinase activity^{226,227}. In

L. pneumophila infection, two factors have been implicated in anti-apoptotic activity: SidF and SdhA (and homologs of the latter)^{210,228}. SidF directly neutralizes the activity of pro-death members of the Bcl-2-family, the mechanism by which SdhA functions is not known^{210,228}. Both SidF and SdhA do not activate NF- κ B, suggesting alternative factors that provide the stimulus¹²⁹.

Here, testing an array of bacterial factors for their importance in NF- κ B activation, it could be shown that permanent activation of NF- κ B depends on a functional Dot/Icm system and intracellular growth. *L. pneumophila* carrying mutations in genes known to be important for Dot/Icm system or intracellular growth did not cause permanent activation of NF- κ B, i.e. $\Delta dotA$, $\Delta icmB/dotO$, $\Delta enhC$ and $\Delta ptsP$. From the mutants tested lacking single effector proteins, only $\Delta sdbA$ and $\Delta lubX$ failed to elicit constitutive NF- κ B activation, and also exhibited severe growth defects. A mutant lacking *sdbA* also had a defect in intracellular growth in bone marrow-derived macrophages²¹³ and in a yeast model of infection¹²⁹. LubX is a U-box protein that has been shown to act as ubiquitin ligase (E3) and to mediate polyubiquitinylation of the host cell protein CDC-like kinase 1 (Clk1)¹³³. While deletion of *lubX* did not have an impact on intracellular growth in macrophages¹³³, it was shown here to cause severe growth defects in A549 cells.

Previous studies have shown that inhibition of the NF- κ B pathway at specific levels had different outcomes: inhibition of phosphorylation of I κ B α or of the proteasome by the chemical compounds CAPE and MG132, respectively, impaired intracellular growth in macrophages^{150,229}. In contrast, inhibition of the IKK complex using NBD peptide or by mutation of IKK α and β did not affect intracellular replication¹⁴⁴. It will be interesting in the future to elucidate whether this is an effect of different experimental settings or if indeed *L. pneumophila* replication depends on I κ B α but not on IKKs. This would indicate that *L. pneumophila* interferes with NF- κ B signaling to induce activation downstream of IKK.

Taken together, this work shows a biphasic NF- κ B activation pattern induced by *L. pneumophila* infection. The first, transient activation is mediated by flagellin, TLR5 and MyD88 and is rapidly silenced. The second activation leads to permanent nuclear translocation of p65, which is dependent on the replication of bacteria and a functional Dot/Icm system. The unusual pattern of continuous nuclear localization of p65 over hours and days with-

out oscillation hints at an active interference of the NF- κ B system by this bacterium to ensure survival of the host cell (Fig. 36).

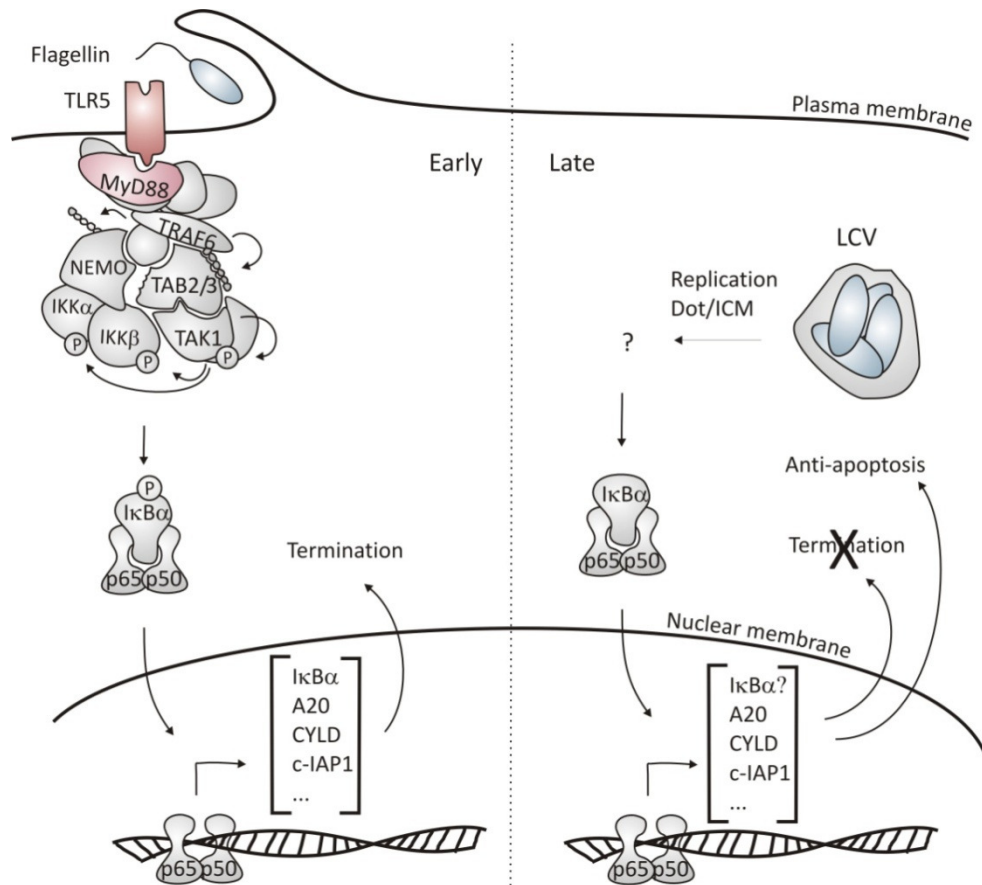


Fig. 36: Model of two tracks of NF- κ B activation by *L. pneumophila*. First, possibly during entry into the cells, bacterial flagellin activates TLR5 which signals via MyD88 (red). The signal is probably transduced via the known TLR-NF- κ B mediators (grey). This activation is transient and terminated probably due to normal negative feedback. Later during the infection, while the *Legionella* containing vacuole (LCV) is established, NF- κ B becomes permanently activated. This depends on bacterial replication and Dot/Icm secretion system. Unknown (cellular and/or bacterial) activators lead to I κ B α degradation and permanent nuclear localization of p65. Due to the anti-apoptotic effects of activated NF- κ B *L. pneumophila* ensures the survival of its host.

3 Conclusions and Outlook

In infections, the interplay between the host and the infecting agent determines the outcome of disease. NF- κ B signaling is a lynchpin in this process because once engaged by PRRs, it activates the immune response⁵ and upregulates anti-apoptotic genes⁶. This dual function is thought to promote cancerogenesis induced by *H. pylori*¹⁰ and anti-apoptosis is necessary for host cell survival in *L. pneumophila* infection¹⁴⁴. Despite this central relevance, the dynamics of NF- κ B activation and the signaling pathways leading to it are not well understood. In order to study NF- κ B, here, a new model was established enabling high-throughput as well as single cell analysis of p65-GFP nuclear translocation. Time resolved analysis of p65-GFP translocation showed temporal profiles with remarkable specificity for the cell line, the stimulus and the dose of the inducer. While activation of NF- κ B by the cytokines TNF α and IL-1 β led to single translocation peaks, the response to *H. pylori* was marked by synchronous, damped oscillations and *L. pneumophila* induced a biphasic nuclear translocation. The specific profiles are likely to fulfill a function and may have consequences for the induction of genes. This would be in accordance to previous studies showing that different temporal profiles lead to transcription of specific subsets of genes⁵⁴ and the resulting theory that dynamics confer inducer-specificity²³.

Previous studies have tested known PRRs and their signaling mediators for their influence in *H. pylori*-induced NF- κ B activation and some, such as NOD1¹²¹, MyD88, TRAF6 and TAK1¹⁰², have been shown to play a role. However, the picture is far from being complete²³⁰. Therefore, a goal of this thesis was to identify new key regulators of this signaling pathway using the unbiased, systemic approach of RNAi-based screens. Indeed, this led to the discovery of 24 factors influencing NF- κ B signaling. Further analysis of three of these factors clearly demonstrated that ALPK1 and CRKRS are necessary for NF- κ B activation by *H. pylori* whereas SKP2 is important in termination of NF- κ B signaling. Although the exact functions of these factors remain to be elucidated, their identification deepens our understanding of this important pathway and provides possible new targets for future therapeutic intervention. Further, results from the screen highlighted a link between the cell cycle network and NF- κ B via SKP2, harmonizing with the systematic view that signaling pathways do not exist in isolation but are highly interconnected^{231,232}. I expect that this has physiological consequences because the concerted action of other pathways have been shown to influence outcome of NF- κ B signaling²³².

In *L. pneumophila* infection, two opposing functions of NF- κ B activation have been shown: On one hand, signaling via TLR5 is important for the innate immune response and susceptibility to disease^{149,217,219}; on the other hand, NF- κ B signaling induced by the bacterial Dot/Icm secretion system prevents premature host cell death¹⁵⁰. It was indicated that the decision, which pathway is activated, depends on the MOI of infection, but the underlying mechanism was not clear¹⁵⁰. Here, detailed analysis of NF- κ B dynamics could clarify this effect, demonstrating biphasic nuclear translocation composed of (i) a strong but transient activation resulting from TLR5-mediated sensing of bacterial flagellin and (ii) Dot/Icm-dependent activation that included permanent nuclear localization of p65 without oscillations over days. Because permanent nuclear localization is highly unusual for NF- κ B, I speculate that *L. pneumophila* actively interferes with NF- κ B signaling. The two tracks of NF- κ B activation observed in this infection demonstrate both sides of the classical “battle” for survival between host and pathogen: While the TLR5-mediated track is a typical defense-strategy of the host, the Dot/Icm-induced manipulation of NF- κ B ensures maintenance of the niche that the pathogen needs for replication.

Insights gained from the study of host-pathogen interplay have already been highly useful in understanding cellular functions. In the future, we need to further elucidate important questions: Why is the body tolerant to some bacteria while other bacteria induce chronic inflammations that can even promote cancer? How can certain pathogens evade the immune system? How does chronic inflammation promote cancerogenesis? Why are certain individuals more prone to pathologies associated with chronic inflammations? The study of both, activation and termination of the NF- κ B pathway as well as the induction and manipulation by pathogens will contribute parts of the answers to these questions.

In respect to the here identified factors important in NF- κ B signaling, future experiments will have to examine the mechanisms of actions and the *in vivo* roles. In the case of SKP2, the phenotype of *skp2*^{-/-} knockout mice seems to largely depend on p27^{199,200}. However, functions depending on NF- κ B may not have been investigated thoroughly. I hypothesize that the connection between SKP2, the cell cycle and NF- κ B plays a role in a setting where NF- κ B signaling induced in resting cells leads to a different response than in cycling cells. A possible example for this could be AICD in T cells²⁰¹. Previous experiments have indicated an influence of NF- κ B in AICD²⁰², but the underlying mechanism remains to be elucidated. If future research could establish a role of the cell cycle and SKP2, this would be a signifi-

cant contribution to understanding AICD which has important functions in termination of immune response. Furthermore, the connection of SKP2 with NF- κ B may prove of significance for therapeutic approaches, because SKP2 and NF- κ B both play a role in development of various types of cancer¹⁸⁴. It could be valuable to consider this connection when cancer therapies target one of the two and thereby also influence the other. In the case of CRKRS and ALPK1, it should be verified in other experimental systems, whether these factors act specifically in *H. pylori* infection or in NF- κ B signaling in general. If the first holds true, this may be useful in therapeutic interventions targeting specifically the NF- κ B response to this infection. In both cases, the *in vivo* significance ought to be assessed. To my knowledge, *crkrs*^{-/-} knockout mice do not exist. *alpk1*^{-/-} knockout mice have been generated, but so far, no phenotype has been identified (Alexey Ryazanov, personal communication). It will be of key relevance to study the impact of ALPK1 on the progression of *H. pylori*-induced pathology. To assess the influence on human disease, genetic polymorphisms could be analyzed. Single nucleotide polymorphisms (SNPs) in *alpk1* or *crkrs* could be detected with genomic techniques like deep sequencing and polymorphisms from infected and uninfected individuals could be compared. This may give insights why certain individuals develop more severe disease phenotypes while others are asymptomatic.

Future research also needs to be undertaken to understand the mechanism underlying the permanent nuclear localization of p65 induced by *L. pneumophila*. This might not only deepen our knowledge about infection, but also about constitutive NF- κ B activation in general, which is a critical feature of many cancers. Studying this new model for induction of continuous active NF- κ B may lead to further insights into possible interventions that can reverse this phenotype. In addition, utilizing the association of continuous NF- κ B activation with bacterial replication, this model can be used to identify new factors that contribute to bacterial replication.

In summary, this thesis offers a new model to study NF- κ B, identified new key regulators of this important pathway in infection with *H. pylori* and demonstrated continuous NF- κ B activation induced by *L. pneumophila*. This will hopefully engage future efforts to understand NF- κ B signaling which will deepen our knowledge about host-pathogen interplay, may provide new insights into cancer development and possibly prove useful in development of therapies.

4 Material and Methods

4.1 General suppliers

If not specified otherwise, chemicals were purchased from Roth, Merck or Sigma.

4.2 DNA-constructs and molecular biology techniques

4.2.1 Construction of lentiviral vector containing p65-GFP

p65-GFP was a kind gift from Johannes A. Schmid⁷² and was cloned into pWPXL (kindly provided by Didier Trono, Ecole Polytechnique Fédérale de Lausanne, Switzerland) using the primers 5'-ATAATCGACGCGTCGATGGTGAGCAAGGGCGA-3' and 5'-ACCACCCACTAGTGTTAGGAGCTGATCTGACTCAG-3' and MluI and SpeI sites. The resulting construct pSIB02 has been verified by sequencing. The GFP is the enhanced variant EGFP (Clontech). The lentivirus contains the following elements: WPRE, a post-transcriptional regulatory element of woodchuck hepatitis virus (enhances transgene expression); cPPT (central polypurine tract), a cis-acting element that improves the efficiency of gene transfer in many targets; EF1 α , the elongation factor 1- α promoter.

4.2.2 Polymerase Chain Reaction (PCR)

Standard polymerase chain reaction was used to amplify DNA fragments for cloning. PCR reaction was mixed on ice (600 ng Template; 50 pmol forward primer; 50 pmol reverse primer; 5 μ l 10 x Pfu-buffer (Stratagene); 0.5 μ l dNTP Mix 25 mM; 1.5 U Pfu-Turbo DNA polymerase (Stratagene); ad. 50 μ l ddH₂O) and PCR was conducted using Gene Amp 2400 machine (Perkin Elmer). The following program was used: first denaturation 2 min 94°C, followed by 35 cycles of 30 sec denaturation at 94°C, 30 sec of annealing at 55°C, 3 min of polymerization at 68°C and a final polymerization step of 7 min at 68°C.

4.2.3 Enzymatic DNA digestion

Restriction enzymes SpeI and MluI were used for cloning and enzymes Sall, ApaI and XhoI were used for testing resulting clones (all NEB). Enzymes were diluted in restriction buffers (NEB) and digestion was allowed to proceed overnight at 37°C.

4.2.4 Agarose-gelectrophoration

Nucleic acids were separated by gelectrophoration using 1% (w/v) agarose (Seakem) dissolved in TBE buffer (89 mM Tris base; 89 mM Borat; 2 mM EDTA; pH 8.0) supplemented with 5 µl Ethidiumbromide 10 mg/ml (Sigma-Aldrich). Prior to loading, DNA probes were mixed with loading buffer (0.25% Bromphenol blue; 0.25% Xylencyanol; 30% Glycerine; 1 mM EDTA). To identify size of nucleic acids, standard markers (Fermentas) were used.

4.2.5 Elution of DNA from agarosegels

DNA fragments of interest were eluted from agarose gels using Qiaquick gel extraction kit (Qiagen) according to manufacturer's recommendation.

4.2.6 Ligation of DNA fragments

DNA fragments were ligated using T4 ligase (NEB) according to manufacturer's recommendation and 1:10 ratio of plasmid DNA to insert DNA.

4.2.7 Generation of competent bacteria for chemical transformation

E. coli Top10F (Invitrogen) were cultured in 5 ml Luria Bertani Medium (LB-Medium; 10 g/l Bacto tryptone (Difco), 5 g/l Bacto yeast extract (Difco), 5 g/l NaCl) overnight and subsequently grown in 400 ml LB-Medium until an OD₅₉₅ of 0.45-0.55 was reached. Cultures were cooled on ice for 15 min and all following steps were performed on ice or at 4°C. Bacteria were centrifuged for 10 min at 2000 g and the pellet resuspended in 200 ml chilled 0.1 M CaCl₂. Bacteria were incubated on ice for 30 min, again centrifuged and pellet was resuspended in 5 ml of 0.1 M CaCl₂ with 10% glycerine. Aliquots of competent cells were frozen at -80°C.

4.2.8 Transformation of bacteria

For uptake of plasmid DNA by bacteria, competent bacteria were thawed on ice and 1 µg DNA was added. After 10 min incubation, bacteria were subjected to 42°C for 90 sec. 500 µl of SOC medium (2% Bacto tryptone; 0.5% Bacto yeast extract; 10 mM NaCl, pH 7; 2.5 mM KCl, pH 7; 10 mM MgCl₂; 10 mM MgSO₄; 20 mM Glucose) was added and bacteria were grown at 37°C for 1h. Subsequently, bacteria were plated on LB-agar plates (LB-medium with 15 g/l agar) supplemented with the appropriate antibiotics.

4.2.9 Preparation of plasmid DNA

Bacteria carrying a plasmid of interest were grown in 50 ml LB medium with the appropriate antibiotics. Plasmids were isolated using the Plasmid Midi-Kit (Qiagen) according to the manufacturer's recommendation. DNA was eluted with ddH₂O and concentration was measured using NanoDrop Spectrophotometer (Thermo scientific). The concentration was adjusted to 1 µg/ml and DNA was stored at -20°C.

4.3 Eukaryotic cell culture

Cell lines AGS (ATCC CRL 1739, human gastric adenocarcinoma epithelial cell line), A549 (ATCC CCL-185, human lung carcinoma epithelial cell line), HeLa (ATCC CCL-2, human cervical adenocarcinoma) and L929 (ATCC CCL-1, mouse fibroblast cell line) and their p65-GFP expressing derivatives as well as 293T cells (Invitrogen 10938-025) were grown in RPMI (AGS, HeLa and L929) or DMEM (A549 and 293T) supplemented with 10% fetal calf serum (FCS), 2 mM L-glutamate (Invitrogen) and for DMEM additional 1 mM Na-Pyruvate. Cells were subcultured every 2-3 days.

4.4 Lentiviral transduction and generation of monoclonal cell lines

Lentiviral particles were generated by transient transfection of envelope and packaging vectors pMD2.G and psPAX2 (kindly provided by Didier Trono, Ecole Polytechnique Fédérale de Lausanne, Switzerland) together with lentiviral vector pSIB02 carrying p65-GFP. For transfection by calcium chloride complexes, 500,000 293T cells were seeded in 2 ml medium in a well of a 6-well-plate and grown overnight. Subsequently, 2 µl of chloroquine 25 mM were added and 4 µg of plasmid DNA was mixed with 250 µl of CaCl₂ 0.5 M. 250 µl of 2x HBS (27 mM HEPES, pH 7; 137 mM NaCl; 1.5 mM Na₂HPO₄) were slowly added while medium was agitated. After 30 min incubation, precipitate was slowly added to the cells. Virus particles were harvested 48 h after transfection and concentrated by ultracentrifugation at 25,000 rpm. Cell lines AGS, A549, HeLa and L929 were infected with lentiviral particles. Three days after infection, single cells were obtained by serial dilutions, separation was confirmed by eye and monoclonal cell lines AGS SIB02, A549 SIB01, HeLa SIB04 and L929 SIB01 were propagated. The number and position of lentiviral insertion was not analyzed.

4.5 Transient transfection of siRNA

To inhibit expression of genes by RNA interference in cells for subsequent protein analysis, siRNAs were transfected into eukaryotic cells in 12-well-plates. For this, 100,000 cells/well were seeded in a 12-well-plate at least 20 h prior to transfection to allow cells to grow to 70% confluency. Short interfering RNAs designed for the inhibition of the genes under investigation were transfected using the RNAiFect Transfection Kit (Qiagen). 4 μ l siRNA 20 μ M were mixed with 96 μ l serum free RPMI. After 5 min incubation, 6 μ l RNAiFect transfection reagent was added; the solution was mixed and incubated for additional 15 min. In the meantime, medium was aspirated from cells and replaced with 600 μ l RPMI with FCS. Finally, 100 μ l of transfection complex mixture was added to the cells. One day after transfection, cells were split into new wells (96-well-plate or 12-well-plate according to experimental setting). Experiments were conducted after a minimum of 60 h to allow reduction of target protein levels. Sequences of used siRNAs are listed in the appendix. Control siRNA was Allstars (Qiagen, catalog number 1027281).

4.6 Automated transient transfection of siRNA

To inhibit expression of genes by RNA interference in a high-throughput manner, siRNAs were transfected into eukaryotic cells in 96-well-plates using HiPerFect (Qiagen). One day prior to transfection 2000 AGS SIB02 cells/well were seeded. Transfection was performed on a BioRobot 8000 system (Qiagen) using a final volume of 0.5 μ l HiPerFect transfection reagent (Qiagen), a siRNA concentration of 10 nM each, in 100 μ l final volume per well. In a mixing plate, 0.5 μ l transfection reagent in 19.5 μ l RPMI were mixed with 5 μ l of 200 nM siRNA solution and incubated for 10 min. Medium was aspirated from cells and 25 μ l of fresh RPMI with 10% FCS was added. 50 μ l RPMI with FCS was added to transfection complexes and 75 μ l of the mixture were added to the cells leading to a final volume of 100 μ l. Outer wells of the 96-well-plates have been omitted from the screen because previous experiments showed unequal distribution of cells in the outer wells. In cases where two siRNAs were combined, both siRNAs were used at half concentration causing the same total siRNA concentration as with single siRNAs.

The primary screen was conducted using the library "Human Kinase siRNA Set" from Qiagen, containing 1292 siRNAs targeting 646 kinase and kinase-associated genes, two siRNAs per gene (catalog number 1027091). All other siRNAs were purchased from Qiagen.

4.7 Bacterial culture

Tab. 3: Bacterial strains used in this study. Bacteria were obtained from the departmental strain collection (*H. pylori*) or Holger Brüggeman and Antje Flieger (*L. pneumophila*). *H. pylori* gene number according to ²³³, *L. pneumophila* gene number according to ²³⁴.

Bacterium	Strain	Number in MPIIB strain collection	Mutation in gene (wild type = wt)	Resistance	Literature
<i>H. pylori</i>	P1	P1 (HP1101)	Wt		²³⁵
<i>H. pylori</i>	P1DcagA	P211	Hp0547	Cam	¹¹³
<i>H. pylori</i>	P1DvirB11	P208	Hp0525	Cam	¹¹³
<i>H. pylori</i>	P12	P12 (HP8880)	Wt		²³⁶
<i>H. pylori</i>	P12DPAI	P246	Hp0519-Hp0547	Km	¹¹³
<i>L. pneumophila</i>	Philadelphia-1	X465	Wt		²³⁷
<i>L. pneumophila</i>	Philadelphia-1 $\Delta icmB$	X483	lpg0456	Km	P. Aurass <i>et al.</i> , submitted
<i>L. pneumophila</i>	Philadelphia-1 $\Delta ptsP$	X484	lpg2871	Km	P. Aurass <i>et al.</i> , submitted
<i>L. pneumophila</i>	Philadelphia-1 $\Delta enhC$	X485	lpg2639	Km	P. Aurass <i>et al.</i> , submitted
<i>L. pneumophila</i>	Philadelphia-1 $\Delta dotA$	X499	lpg2686	Km	P. Aurass <i>et al.</i> , submitted
<i>L. pneumophila</i>	Philadelphia-1 $\Delta sdbA$	X486	lpg0275	Km	E. Siegbrecht, A. Flieger unpublished
<i>L. pneumophila</i>	Philadelphia-1 $\Delta sdhA$	X487	lpg0376	Km	E. Siegbrecht, A. Flieger unpublished
<i>L. pneumophila</i>	Philadelphia-1 $\Delta sdhB$	X488	lpg0135	Km	E. Siegbrecht, A. Flieger unpublished
<i>L. pneumophila</i>	Philadelphia-1 $\Delta sidC$	X489	lpg2511	Km	E. Siegbrecht, A. Flieger unpublished
<i>L. pneumophila</i>	JR32	X213	Wt, NaCl sensitive isolate of Philadelphia-1		²³⁸
<i>L. pneumophila</i>	JR32 $\Delta dotA$	X490	lpg2686 (Lela3118)	Km	²³⁸
<i>L. pneumophila</i>	JR32 $\Delta lubX$	X491	lpg2830	Km	P. Aurass, A. Flieger (unpublished)
<i>L. pneumophila</i>	Paris	X492	Wt		²³⁹
<i>L. pneumophila</i>	Paris $\Delta fliA$	X493	lpp1746		¹³¹
<i>L. pneumophila</i>	Paris $\Delta letA$	X494	lpp2699		Sahr, Brüggemann, Jules <i>et al</i> (unpublished).
<i>L. pneumophila</i>	Corby	X463	Wt		²⁴⁰
<i>L. pneumophila</i>	Corby $\Delta flaA$	X495		Km	²⁴¹

H. pylori clinical isolates and mutants thereof were described before (see table 3 for references) and routinely cultured on horse serum agar plates supplemented with 10 µg/ml

vancomycin, 1 µg/ml nystatin and 5 µg/ml trimethoprim at 37°C under microaerophilic conditions using campygen gas mix (Oxoid). If necessary for cultivation of mutants, 5 mg/ml chloramphenicol or 20 µg/ml kanamycin was added to agar plates. *H. pylori* were thawed from stock, replated after 3 days and used for infection after 24 h.

L. pneumophila clinical isolates and mutants thereof were described before or obtained within collaborations (see table 3 for references). Bacteria were grown on N-(2-acetamido)-2-aminoethanesulphonic acid (ACES)-buffered charcoal-yeast extract (BCYE) agar plates²⁴² (Heipha) at 37°C. *L. pneumophila* were thawed from stock and used for infection after 3 days.

4.8 Infections

For infection, bacteria were resuspended in medium (RPMI or DMEM according to the cell line) and multiplicity of infection (MOI) was calculated by optical density measured with a spectrometer (OD₅₅₀ for *H. pylori* and OD₆₆₀ for *L. pneumophila*) and a previously established standard curve. In the case of *L. pneumophila*, calculation was based on the assumption that OD₆₆₀ of 0.3 corresponds to 1x10⁸ CFU/ml. When indicated, infections were synchronized by centrifugation at 800 g for 5 min at 37°C.

4.9 Intracellular growth of *L. pneumophila*

To estimate intracellular infection, A549 were infected with bacteria at an MOI of 100 and infection was synchronized by centrifugation at 800 g for 5 min at 37°C. After 1.5 h of infection, extracellular bacteria were removed by gentle washing and remaining extracellular bacteria were killed by addition of gentamicin 100 µg/ml for 1 h. The cells were washed three times with plain medium to remove unbound bacteria and treated with 10% (w/v) saponin (Sigma) to lyse the host cells. Serial dilutions were plated on BCYE-agar and CFU were counted after 2 days. Time point 0 represents the sample taken directly after removal of gentamicin.

4.10 Automated microscopy and software-based picture analysis

Cells were transfected with siRNAs and infected or activated at least 60 h later. For other experiments, cells were seeded in 96-well-plates 1 or 2 days prior to activation. In all cases, cells at a confluency of approximately 80% were used. Before activation, medium was replaced with fresh medium (50 µl per well). For activation, another 50 µl of medium con-

taining recombinant human TNF α (BD Pharmingen, 4-12 x 10⁸ units/mg), recombinant IL-1 β (Strathmann Biotech, 1x10⁷ units/mg), LPS from *Salmonella typhosa* (Sigma), or bacteria in the appropriate concentration was added. In the case of *L. pneumophila*, 50 μ l bacterial solutions were added directly onto the cells without 50 μ l fresh medium. After the respective incubation time, cells were fixed with 100% ice-cold methanol, stained with Hoechst 33342 (2 μ g/ml) and stored in phosphate buffered saline (PBS (Gibco)) with 0.1% NaN₃. In each well, four pictures were taken by the automated microscopy system Scan^R (Olympus) using autofocus on nuclei. Pictures were subsequently analyzed by Scan^R software (Olympus) and quantification of p65-translocation was carried out using a modified existing protocol²⁴³. Here, nuclear areas were identified by Hoechst staining and around every nucleus a 1 pixel wide cytoplasmic area was set. To define compartments as accurately as possible, the nuclear area was eroded by 2 pixels and the cytoplasmic area was distanced by 1 pixel from the nucleus (see Fig. 5). In the case of L929, the nuclear region was eroded by 3 pixels and the distance from the cytosol was 2 pixels. While the setting of subcellular regions was similar to an assay described previously for cells stained with anti-p65 antibodies²⁴³, the analysis of p65-translocation was based on a different strategy. Here, the software depicts the cells in dot plots - a method well established for fluorescence activated cell sorting (FACS) analysis. Regions were set as shown in Fig. 38.

Subsequently, gates were defined: cells located in regions R01 and R02 were analyzed and were termed active, when located in region R03 and termed non-active when located in region R04. Numbers of active and non-active cells in every well were counted by the software. The percentage of activated cells per well were calculated using Microsoft Excel (percentage of active cells = active cells / sum of active and non-active cells x 100). Definition of regions and gating was optimized for every cell line and the same assay was used for every experiment. Graphs were compiled using Microsoft Excel.

Each assay was adjusted to the respective cell line. Specificities are: (i) sizes of nuclei differ (i.e. AGS SIB02 cells are quite large). (ii) Homogeneity of the GFP signal is cell line specific. While AGS SIB02 and A549 SIB01 cells export p65-GFP after activation quite evenly to the cytoplasm, L929 show slight accumulations close to the nucleus. If these accumulations are located above the nucleus, pictures acquired in epifluorescence microscopes (as used here), can lead to high mean intensities in the nuclear area. Therefore, in this cell line, nuclear regions with median fluorescence but high standard deviation of GFP signal are

excluded. (iii) Regions for nuclear translocation are either set in a direct comparison of nuclear and cytosolic mean GFP or by the ratio of the two (assay for AGS was developed first and when assays for A549 and L929 were developed, they were simplified).

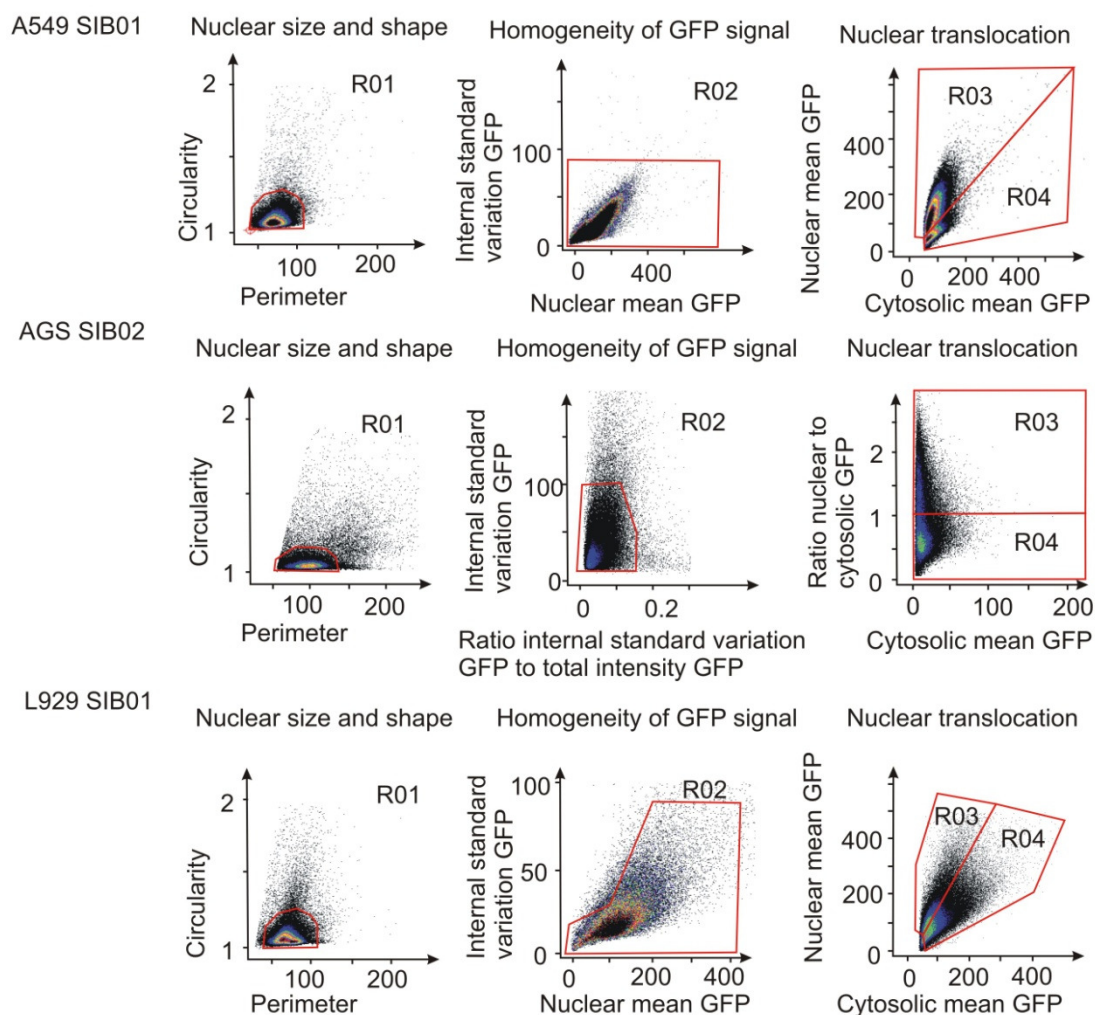


Fig. 37: Comparison of software-based picture analysis of the three p65-GFP overexpressing cell lines. Cells were seeded on 96-well-plates and partly activated with TNF α 10 ng/ml in order to have mixed populations of activated and non activated cells on the same plate. Cells were fixed, stained with Hoechst 33342 and analyzed by automated microscopy. Dot plots as depicted in analysis software are shown. Cells are gated for circularity and size (Region R01), intensity of GFP and standard variation of GFP intensity (Region R02) and the ratio of nuclear to cytoplasmic GFP intensity (Region R03 or R04).

4.11 Live cell microscopy

Cells were grown in 3.5 cm² glass bottom dishes (MatTek). Before infection, medium was changed to medium without phenolred (Invitrogen). Bacteria were harvested in the same medium, stained with Syto 61 (Molecular Probes) according to the manufacturer's recommendations and washed three times. Staining of this dye fades after a few minutes but

allows initial identification of bacteria. Images were acquired every two minutes. Microscopy was carried out in a humidified incubator (37°C, 5% CO₂) using the VT-Infinity system (Visitron Systems). The system is compiled of an Olympus IX81 (Olympus, Japan), VT-Infinity galvo scanner confocal head (Visitron Systems) and a Hamamatsu C9100-02 CCD camera (Hamamatsu Photonics K.K.). Images were acquired and processed using MetaMorph (Universal Imaging Corporation) software.

4.12 Immunofluorescence after live cell microscopy

To detect *Legionella pneumophila* after live cell microscopy, live cell microscopy was discontinued and the position of cells was documented at lower magnifications in order to find the exact cells again. Subsequently, cells were fixed in 4% paraformaldehyde for 20 min and permeabilized with 0,2% Triton X-100 in PBS for 20 min. Unspecific binding sites were blocked using blocking buffer (1% BSA; 0.05% Tween 20 in PBS) for 20 min. *Legionella pneumophila* were stained using rabbit anti-*Legionella pneumophila* primary antibodies (20943 Abcam) and Cy3-labeled, goat anti-rabbit secondary antibodies (111-165-144 Dianova). Unbound antibodies were removed by gentle washing with PBS and confocal microscopy was performed using the same system as for live cell microscopy.

4.13 SDS-PAGE

Proteins were solubilized in Laemmli buffer (125 mM Tris/HCl, pH 6.8; 200 mM SDS; 40% (v/v) glycerol; 10% (v/v) β-mercaptoethanol; bromophenolblue), denatured for 5 min at 95°C and separated by sodium dodecyl sulfate polyacrylamide gel electrophoresis (SDS-PAGE). For this, an SDS gel was prepared (10% separation gel: 3.33 ml H₂O; 2 ml separation buffer (1.5 M Tris base, pH 8.8; 0.4% SDS); 2.33 ml 30 % polyacrylamide (PAA) 8 μl tetramethylethylenediamine (TEMED); 40 μl 10% Ammonium peroxodisulfate (APS) . Stacking gel: 1.63 ml H₂O, 0.63 ml stacking buffer (0.5 M Tris base, pH 6.8; 0.4% SDS); 0.38 ml 30% PAA; 10 μl TEMED; 17.5 μl 10% APS), probes were loaded on the gel alongside with 10 μl of a prestained protein marker (NEB). The gel was placed into an electrophoresis tank (BioRad) filled with running buffer (192 mM glycine, 25 mM Tris base and 3.5 mM SDS) and proteins were electrophoretically separated.

4.14 Immunoblotting

Proteins were transferred from an SDS-PAGE to Polyvinylidene Fluoride (PVDF) (Amersham) membranes by western blotting. For this purpose, the gel was placed on PVDF,

both placed between filter paper (Whatman) and fibre layers (BioRad) and proteins were electrophoretically blotted overnight at 4°C in a tank filled with transfer buffer (20% methanol, 190 mM glycine and 25 mM Tris base). After disassembly of western blot, unspecific binding sites on the membrane were blocked by incubation in blocking buffer (3% bovine serum albumin (BSA) in TBST (14 mM NaCl; 2.5 mM Tris base, pH 7.4; 0.1% Tween 20) and PVDF was subsequently probed with primary antibodies (see list below) and HRP-conjugated secondary antibodies (Amersham). Signals were detected with enhanced chemoluminescence (ECL) reagent (ICN Biomedicals) and visualized either on film (Hyperfilm GE Healthcare) or on a phosphorimager (PhosphorImager, FLA-3000 Series; Fuji). Band intensities were quantified by 1D evaluation using AIDA software (Raytest). Overexpression of p65–GFP levels were calculated as the mean of five independent experiments visualized on phosphorimager and quantified by software. If necessary, bound antibodies were stripped from the membrane using stripping buffer (62.5 mM Tris base, pH 6.7; 100 mM β -mercaptoethanol; 2 % SDS) 20 min at 60°C and membranes were subsequently probed for another protein following the above procedure.

Tab. 4: Primary antibodies used for immunoblotting.

Antibody	Supplier	Catalog number or clonename
mouse anti-actin	Sigma	A5441
mouse anti-ERK1/2	Cell Signaling Technology	9107
mouse anti-pERK1/2	Sigma	9692
mouse anti-phospho-tyrosine	Santa Cruz	pY99
rabbit anti-CagA	Santa Cruz Biotechnology	sc-25766
rabbit anti-IKK β	Cell Signaling Technology	2370
rabbit anti-IkBa	Cell Signaling Technology	9242
rabbit anti-p38	Cell Signaling Technology	9212
rabbit anti-p65	Santa Cruz Biotechnology	sc-109
rabbit anti-p-p38	Cell Signaling Technology	9215

4.15 Kinase assay

To assay I κ B kinase activity cells were either untreated or infected with *H. pylori* at an MOI of 100 for 30 min. After PBS (Gibco) washing, cells were lysed for 20 min at 4°C with gentle agitation in lysis buffer (50 mM HEPES pH 7.5; 150 mM NaCl; 1.5 mM MgCl₂; 1 mM EDTA; 1% Triton X–100; 10% glycerol; complete protease inhibitor (Roche); 10 mM NaF; 8 mM β -glycerophosphate; 100 μ M sodium orthovanadate; 1 mM DTT). Lysates were centrifuged for 10 min at 20,000 g, protein concentration was determined using bicinchoninic

acid assay (BCA, Pierce) according to the manufacturer's recommendations and 200 µg of each extract was used for immunoprecipitation performed in 800 µl lysis buffer. Extracts were precleared with protein A agarose beads (Calbiochem) for 1 h at 4°C. Immunoprecipitation using 1 µg rabbit anti-IKK γ antibody (FL-419, Santa Cruz) was carried out overnight at 4°C. The protein A agarose was washed five times with lysis buffer and once with kinase buffer (20 mM HEPES, pH 7.5, 10 mM MgCl₂, 20 µM ATP, 20 mM β -glycerophosphate, 50 µM sodium orthovanadate, 1 mM DTT). 20 µl of kinase buffer including 1 µg purified recombinant I κ B α and 3 µCi [γ -³²P]ATP were added to the protein A agarose immune-complex and the kinase reaction was incubated for 20 min at 37°C. Reaction mixtures were then subjected to SDS-PAGE and autoradiography.

4.16 ELISA

For quantification of IL-8 in the supernatant of adherent cells, an enzyme linked immunosorbent assay (ELISA) was performed. For this purpose, the Cytoset System (BioSource International) was used according to manufacturer's recommendations. Measurements were performed in triplicates using Spectra Max 190 (Molecular Devices).

4.17 qRT-PCR

Quantification of mRNA levels was conducted by quantitative real time (qRT) PCR. RNA was isolated using RNeasy Mini Kit (Qiagen) according to manufacturer's recommendations. RT-PCR was performed using QuantiFast Sybr Green PCR Kit (Qiagen). PCR reactions (10 µl template RNA 10 ng/µl; 0.5 µl of each primer 10 µM; 10 µl Sybr Mix (Qiagen); 0.25 µl RT-Mix (Qiagen); 4.25 µl H₂O) were prepared in triplicate and PCR was performed using the Applied Biosystems 7500 fast real-time PCR system. The following program was used: an initial 30 min at 50°C allowing reverse transcription of mRNA into cDNA by reverse transcriptase, then denaturation for 15 min 95°C, followed by 40 cycles of 20 sec at 94°C, 40 sec at 60°C and 40 sec at 72°C. For comparison, house-keeping gene glyceraldehyde 3-phosphate dehydrogenase (GAPDH) was used and relative quantification was performed using a previously described model including efficiency correction for the primers²⁴⁴. Data was analyzed using software SDS 2.2.2 (Applied Biosystems) and Excel (Microsoft).

Material and Methods

Tab. 5: RT-PCR primers used. Names of genes are listed alphabetically with gene identification number (Gene ID), accession numbers (Accession #), and primer sequence 5' to 3'.

Symbol	Gene ID	Accession #	Primer	Sequence
ALPK1	80216	NM_025144	Forward	GGTATGTGGTACGAAGCAGCA
ALPK1	80216	NM_025144	Reverse	AGCAAATGGTGGTCAAACCTCC
CRKRS	51755	NM_016507	Forward	CTAACAGCAGAGAGCGTCACC
CRKRS	51755	NM_016507	Reverse	AAAGGTTTGATAACTGTGCCCA
MYD88	4615	U70451	Forward	GGCATCACCACACTTGATGAC
MYD88	4615	U70451	Reverse	ATAGACCAGACACAGGTGCCAG
NOD1	10392	AF126484	Forward	TCAGAGCAAAGTCGTGGTCAA
NOD1	10392	AF126484	Reverse	AAGCCAACCAGCTCCATGAT
SKP2	6502	NM_005983	Forward	TGCCCTGCAGACTTTGCTAAG
SKP2	6502	NM_005983	Reverse	TCTCTGACACATGCGCAACAG
TLR5	7100	AB060695.1	Forward	GTATGTGAACATGAGCTCGAG
TLR5	7100	AB060695.1	Reverse	AGAATCAAAGAGAAGGCCTGG
TNF-RI	7132	NM_001065.2	Forward	ACAGGGAGAAGAGAGATAGTG
TNF-RI	7132	NM_001065.2	Backward	AAGAAGAGATCTCCACCTGAC

5 Statistics

5.1 Statistical analysis of live cell microscopy

5.1.1 Peak alignment

Data was sampled from 9 different cells monitored in one experiment with live cell microscopy using Metamorph software (Universal Imaging Corporation). Peak alignment was performed using R statistics software. All time series signals were normalized to the unit interval as defined by their respective minimum and maximum value. A 3 step algorithm was designed to perform automatic alignment. Step 1: smoothing by applying a moving median of 9. Step 2: detection of ascending flanks by smooth step filter ($\tanh(-6:6/3)$). Step 3: identification of highest peak corresponding to the strongest ascending flank in time series. For final alignment position of ascending flank was shifted to zero. Finally, graphs were assembled in Excel (Microsoft).

5.1.2 Peak interval histogram and normal approximation

Using a data set of 33 cells, a subset of 18 curves with strong multi-modal shape was selected to determine the peak intervals. Pairs of successive maxima were identified by median smoothing and peak finding: a median of length 9 was used and a set of maximal peaks is found by iteratively first identifying the current maximal peak, then applying an exclusion region of size 30 steps around the peak. The two highest maxima were used for peak interval determination. Peak intervals were defined from pairs of successive maxima as identified by the method described above. A corresponding histogram of peak intervals was constructed. Statistics of peak intervals can be summarized by parameters mean 93.78 min, standard deviation 22.99 min. These values were employed for parameterization of a gaussian curve. All calculations were performed in R statistics software.

5.2 Statistical analysis of screen and hit validation

5.2.1 Z-Prime factor

The Z-Prime-Factor (Z') factor evaluates the robustness of an assay²⁴⁵. This factor is based on the average and standard deviations of controls on a plate. To gain data for the calculation, cells were seeded in 96-well-plates, transfected with the control siRNAs, activated and analyzed by the same conditions used for the screening format. Data shows very robust results of single wells of the control transfections (Fig. 38).

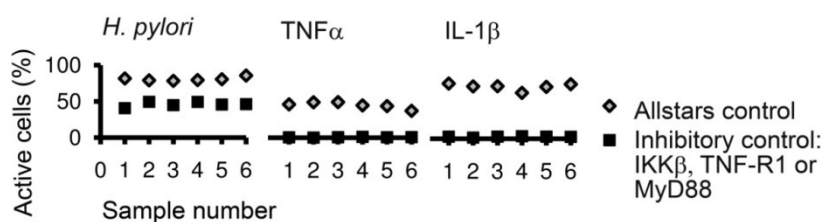


Fig. 38: Robustness of the p65 translocation assay. AGS SIB02 cells were seeded in 96-well-plates, transfected with the indicated siRNAs, activated with *H. pylori* MOI 100 for 45 min, TNF α 1 ng/ml for 30 min or IL-1 β 10 ng/ml for 45 min, fixed, stained and analyzed by automated microscopy as shown in Fig. 5. Results are presented as dot plots with each dot representing the result of a single well on the same plate. Data is representative of at least three independent experiments.

Z' is calculated using the following formula:

$$Z' \text{ Prime factor} = 1 - \frac{(3 SD_{CN} + 3 SD_{CI})}{|\bar{X}_{CN} - \bar{X}_{CI}|}$$

SD = Standard deviation
 \bar{X} = Mean
 CN = Neutral control
 CI = Inhibitory control

The results for Z' can range from negative values (unreliable assay) to 1 (very reliable assay) and recommended acceptance criterion is Z' > 0.4 (NIH website). The Z' calculated for the p65 translocation assay with the individual inducers and controls are: *H. pylori*: 0.4; TNF α : 0.6; IL-1 β : 0.7. These values are average of at least three independent experiments with each six samples of both controls.

5.2.2 Position effects

In high-throughput screens, an important quality control is the assessment of possible position effects. Previous work in the department has identified so called “edge effects” in 96-well-plates. This effect describes the phenomenon that the cells in the outer wells of a 96-well-plate will migrate towards the outer rim of the plate which leads to unequal distribution of cells in the well. Therefore, in this screen, the outer wells were not used. The remaining 60 inner wells were transfected with siRNAs according to the scheme shown in Fig. 39a. The controls (activating, neutral and inhibitory siRNA) were transfected in four replicates, of which three were activated by the inducer and one was not activated. The remaining 48 inner wells were used to test the samples each in single wells.

To examine whether a possible position effect is visible in the data of the screen, all plates of the screen were averaged regardless of inducer and time point tested (all wells B2 av-

eraged, all wells B3 averaged et cetera). For this purpose, all raw data of the screen was used which results in a total of 336 plates (14 plates x 3 inducers x 2 time points x 4 repeats). Results were displayed as a color coded plate (Fig. 39b), in which a slight left-right effect is visible. As the controls were placed on the far left and far right wells, this effect is most clear in the neutral control: neutral controls on the left of the plate have an average of 45% while the neutral control on the right of the plate has only 39% active cells.

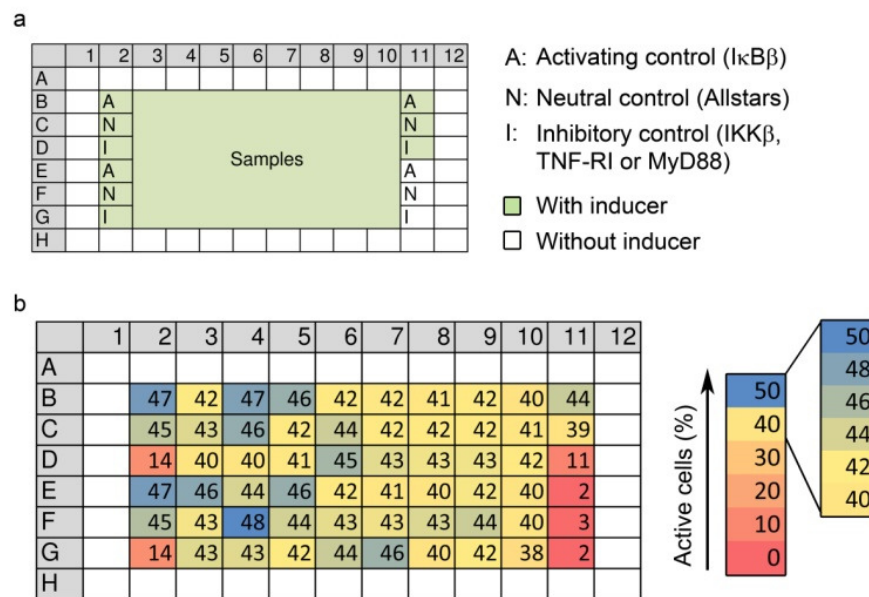


Fig. 39: Plate layout and position effect in the screen. a) siRNAs were positioned according to this scheme. Outer wells were discarded because of a previously discovered edge effect. b) Distribution of screen results on the plates. The screen was conducted as described above and the results were averaged: for each position on the plate, a mean of all plates was calculated, regardless of inducer and time tested. Results are presented as a color-coded plate displaying the mean of a total of 336 plates.

5.2.3 Normalization

In high throughput screens, data from different plates have inevitable variations. To be able to compare results from different plates and also different screens, data need to be normalized within one plate. For this normalization, there are two major possibilities: data can either be normalized to controls, or to the samples. Because in this screen a slight position effect was observed, it was decided to normalize to the samples. For this normalization, either the median or the mean can be used. The median is more robust to outliers and would therefore be the first choice. However, to normalize to the median of the samples, the data distribution on a single plate should follow a Gaussian curve. To test whether this is the case for the screen data, results of single plates of all inducers were

analyzed. The number of wells which contain a certain percentage of activated cells was determined and plotted against the percentage of active cells (Fig. 40). The resulting curves follow Gaussian curves. It was concluded that data were normally distributed and median normalization could be used.

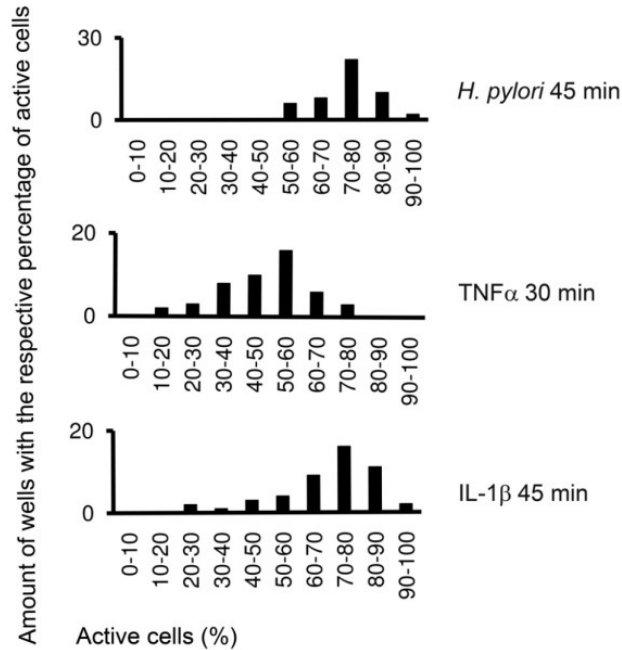


Fig. 40: Distribution of results of single plates follows Gaussian curves. The screen was conducted as described above. Briefly, AGS SIB02 cells in 96-well-plates were activated with the indicated inducer for indicated time. All wells of one plate received the same treatment. From each plate, the amount of wells with a certain percentage of activated cells was determined. Shown are results of a representative plate.

Normalization to the median was calculated using the following formula:

$$N_x = \frac{100 r_x}{r_m} - 100$$

N_x = Normalized value of x
 r_x = Raw signal value of x
 r_m = Raw signal value of median of sample wells of one plate
 r_x and r_m are percentages of activated cells in the respective well

5.2.4 Evaluation of the statistical significance

To estimate significance of changes in p65 translocation, normalized data were subjected to Welch's t-test which is an adaptation of Student's t-test. The main difference is that Welch's test takes into account the possibility of different variations of the sample groups.

Welch's t-test was calculated using the following formula:

$$t = \frac{\bar{X}_{CN} - \bar{X}_x}{\sqrt{\frac{s_{CN}^2}{n_{CN}} + \frac{s_x^2}{n_x}}}$$

\bar{X}_{CN} = Mean of neutral control
 \bar{X}_x = Mean of sample x
 s_{CN} = variance of neutral control
 s_x = variance of sample x
 n_{CN} = Sample size of neutral control
 n_x = Sample size of sample x

5.2.5 Selection of hits

An often used statistical tool for selection of hits is the z-score (also called standard score). The z-score is generated by subtracting the population mean from an individual raw score and then dividing the difference by the population standard deviation. This is a normalization which incorporates the standard deviation of the population.

Z-score was calculated using the following formula

$$z_x = \frac{r_x - \bar{X}}{SD}$$

\bar{X} = Mean of samples of the plate
 SD = Standard deviation of samples of the plate
 r_x = raw value of sample x

The most widely used criteria for selection of hits in a screen is a z-score of ≤ -2 or ≥ 2 . In other words, samples with normalized values that are 2 times the standard variation greater or smaller than the mean of all values, are understood to be statistically significant. However, the means and the standard variations of the 3 inducers used in this screen were different. Briefly, *H. pylori* and IL-1 β had high percentages of activated cells (about 70%) with low standard deviation (about 15%) and TNF α had much lower percentages of activated cells (33%) but with a similar standard deviation (16%). This difference is due to the concentration of TNF α used and for possible future screens it would be advisable to use a higher concentration of TNF α (i.e. 10 ng/ml) to yield higher percentages of activated cells per well. Nevertheless, due to this difference in levels of activation, the number of hits identified with the z-score differs between the 3 inducers (table 6).

Tab. 6: Comparison of means, standard deviations and hits selected according to z-score definition in inductions with the 3 inducers. AGS SIB02 cells were transfected with a library of siRNAs, activated with the respective stimulus and translocation of p65-GFP was analyzed by automated microscopy. Mean and standard deviation of all samples on all plates were calculated and z-scores were calculated for every sample.

Inducer and time	Mean raw data of all samples (active cells (%))	Standard deviation of all samples	Number of samples with z-score ≤ -2	Number of samples with z-score ≥ 2
<i>H. pylori</i> 45 min	69	14	24	2
<i>H. pylori</i> 90 min	29	18	2	12
TNF α 30 min	33	16	3	14
TNF α 75 min	15	11	0	12
IL-1 β 45 min	74	16	25	2
IL-1 β 90 min	35	20	0	19

In conclusion, the selection of hits based on z-score would have caused an underrepresentation of hits for TNF α . Therefore, hits were selected using a different method. For this purpose, the strength of the inhibitory or activating effect was ranked. For each inducer, approximately the best 50 targets which also had a p-value of ≤ 0.05 were selected for inhibition and approximately the best 15 genes for promoting p65 translocation. For selecting the inhibitory siRNAs, only the inhibition of p65 translocation at the early time point was taken into account. This time point was at the top of the activation curve and it was expected to find the best inhibitory effect at this time. In regards to the siRNAs that upregulated p65 translocation, both time points were taken into account. For this purpose, the difference between activation at time point 1 and activation at time point 2 was calculated, indicating the slope of the curve ($t_2 - t_1$). Again, these values were ranked, combined with a p-value of ≤ 0.05 and best hits selected. In total, 122 genes were selected for inhibition and 38 genes for promotion of p65 translocation.

5.2.6 Validation of hits

To validate the identified primary hits, four independent siRNAs were tested for each gene. The results were again subjected to z-score normalization and for comparison also normalized to the plate median. The fact that one plate harbored many siRNAs that each targeted genes selected as hit may have influenced the normalization outcome. If stringent criteria of z-score ≤ -2 or ≥ 2 were applied, many weaker effects of interesting genes were below this threshold and therefore would have been overlooked. For example, in *H. pylori* infection for 45 min, of the 4 siRNAs used for IKK α , 3 had a z-score of -1.3 to -1.5.

Therefore, it was decided to apply less stringent criteria. If the criteria of z-score ≤ -1 or ≥ 1 was applied, in total 24 out of 160 genes could be confirmed with at least two siRNAs.

5.2.7 Hit validation time courses and details of standardization

For time course experiments, cells were transfected with siRNAs in the workflow of the screen shown in Fig. 9. Cells were infected with *H. pylori* (MOI 100), activated with TNF α (1 ng/ml, 5 ng/ml or 10 ng/ml), or activated with IL-1 β 10 ng/ml. Different concentrations of TNF α were used because the activation with 1 ng/ml was unusually low at the time. However, effects of siRNAs were comparable in low or high concentrations. Cells were either fixed without activation (0 min) or after 15, 30, 45, 60, 75, 90, and 105 min of activation, Hoechst stained and analyzed by automated microscopy. To normalize experiments, first, a control curve was generated, by taking the means of percentage of activated cells of samples transfected with Allstars siRNA of at least 28 experiments for every single time point for each inducer. All time courses for the candidate genes were put in relation to this control curve in the following steps: in each experiment, the percentage of cells activated at a specific time point, inducer and siRNA were divided by the percentage of cells activated using Allstars siRNA control on the same plate with the same time point and inducer. From resulting normalization factor (i.e. TAK1-knockdown cells at time point x are 0.2 times as many activated cells as Allstars control at time point x on the same plate) a mean of at least four individual experiments was taken (in CDK2 only two experiments). This average (for time x) was then multiplied by the percentage of activated cells of Allstars standard curve (for time x).

$$F_x = \frac{R_{All}}{R_x}$$

$$N_x = \bar{X}_{Fx} \times \bar{X}_{All}$$

F_x = Factor for normalization for siRNA x at time y on one plate

R_{All} = Raw value (percentage of active cells) for allstars control at time y on one plate

R_x = Raw value (percentage of active cells) for siRNA x at time y on one plate

N_x = Normalized value for siRNA x at time y for all plates

\bar{X}_{Fx} = Mean of F_x at time y of all plates (n=4)

\bar{X}_{All} = Mean of Allstars control at time y of all plates (n = 28)

References

1. Janeway, C. A., Jr. and Medzhitov, R. Innate immune recognition. *Annu.Rev.Immunol.* 20, 197-216. 2002.
2. Delbridge, L. M. and O'Riordan, M. X. Innate recognition of intracellular bacteria. *Curr.Opin.Immunol.* 19, 10-16. 2007.
3. Medzhitov, R. and Janeway, C. A., Jr. An ancient system of host defense. *Curr.Opin.Immunol.* 10, 12-15. 1998.
4. Doyle, S. L. and O'Neill, L. A. Toll-like receptors: from the discovery of NF-kappaB to new insights into transcriptional regulations in innate immunity. *Biochem.Pharmacol.* 72, 1102-1113. 2006.
5. Kawai, T. and Akira, S. Signaling to NF-kappaB by Toll-like receptors. *Trends Mol.Med.* 13, 460-469. 2007.
6. Karin, M. and Lin, A. NF-kappaB at the crossroads of life and death. *Nat.Immunol.* 3, 221-227. 2002.
7. West, M. A. and Heagy, W. Endotoxin tolerance: A review. *Crit Care Med.* 30, S64-S73. 2002.
8. Courtois, G. and Gilmore, T. D. Mutations in the NF-kappaB signaling pathway: implications for human disease. *Oncogene* 25, 6831-6843. 2006.
9. Han, J. and Ulevitch, R. J. Limiting inflammatory responses during activation of innate immunity. *Nat.Immunol.* 6, 1198-1205. 2005.
10. Karin, M. and Greten, F. R. NF-kappaB: linking inflammation and immunity to cancer development and progression. *Nat.Rev.Immunol.* 5, 749-759. 2005.
11. Karin, M., Cao, Y., Greten, F. R., and Li, Z. W. NF-kappaB in cancer: from innocent bystander to major culprit. *Nat.Rev.Cancer* 2, 301-310. 2002.
12. Sen, R. and Baltimore, D. Multiple nuclear factors interact with the immunoglobulin enhancer sequences. *Cell* 46, 705-716. 1986.
13. Senftleben, U., Cao, Y., Xiao, G., Greten, F. R., Krahn, G., Bonizzi, G., Chen, Y., Hu, Y., Fong, A., Sun, S. C., and Karin, M. Activation by IKKalpha of a second, evolutionary conserved, NF-kappa B signaling pathway. *Science* 293, 1495-1499. 2001.
14. Scheidereit, C. IkappaB kinase complexes: gateways to NF-kappaB activation and transcription. *Oncogene* 25, 6685-6705. 2006.
15. Bonizzi, G. and Karin, M. The two NF-kappaB activation pathways and their role in innate and adaptive immunity. *Trends Immunol.* 25, 280-288. 2004.
16. Pahl, H. L. Activators and target genes of Rel/NF-kappaB transcription factors. *Oncogene* 18, 6853-6866. 1999.
17. Kunsch, C. and Rosen, C. A. NF-kappa B subunit-specific regulation of the interleukin-8 promoter. *Mol.Cell Biol.* 13, 6137-6146. 1993.
18. Collart, M. A., Baeuerle, P., and Vassalli, P. Regulation of tumor necrosis factor alpha transcription in macrophages: involvement of four kappa B-like motifs and of constitutive and inducible forms of NF-kappa B. *Mol.Cell Biol.* 10, 1498-1506. 1990.
19. Shakhov, A. N., Collart, M. A., Vassalli, P., Nedospasov, S. A., and Jongeneel, C. V. Kappa B-type enhancers are involved in lipopolysaccharide-mediated transcriptional activation of the tumor necrosis factor alpha gene in primary macrophages. *J.Exp.Med.* 171, 35-47. 1990.
20. Hiscott, J., Marois, J., Garoufalos, J., D'Addario, M., Roulston, A., Kwan, I., Pepin, N., Lacoste, J., Nguyen, H., Bensi, G., and . Characterization of a functional NF-kappa B site in the human interleukin 1 beta promoter: evidence for a positive autoregulatory loop. *Mol.Cell Biol.* 13, 6231-6240. 1993.
21. Alcamo, E., Mizgerd, J. P., Horwitz, B. H., Bronson, R., Beg, A. A., Scott, M., Doerschuk, C. M., Hynes, R. O., and Baltimore, D. Targeted mutation of TNF receptor I rescues the RelA-deficient mouse and reveals a critical role for NF-kappa B in leukocyte recruitment. *J.Immunol.* 167, 1592-1600. 2001.
22. Hinz, M., Krappmann, D., Eichten, A., Heder, A., Scheidereit, C., and Strauss, M. NF-kappaB function in growth control: regulation of cyclin D1 expression and G0/G1-to-S-phase transition. *Mol.Cell Biol.* 19, 2690-2698. 1999.

References

23. Hoffmann, A. and Baltimore, D. Circuitry of nuclear factor kappaB signaling. *Immunol.Rev.* 210, 171-186. 2006.
24. Sen, R. and Baltimore, D. Inducibility of kappa immunoglobulin enhancer-binding protein Nf-kappa B by a posttranslational mechanism. *Cell* 47, 921-928. 1986.
25. Baeuerle, P. A. and Baltimore, D. I kappa B: a specific inhibitor of the NF-kappa B transcription factor. *Science* 242, 540-546. 1988.
26. Traenckner, E. B., Wilk, S., and Baeuerle, P. A. A proteasome inhibitor prevents activation of NF-kappa B and stabilizes a newly phosphorylated form of I kappa B-alpha that is still bound to NF-kappa B. *EMBO J.* 13, 5433-5441. 1994.
27. Brown, K., Gerstberger, S., Carlson, L., Franzoso, G., and Siebenlist, U. Control of I kappa B-alpha proteolysis by site-specific, signal-induced phosphorylation. *Science* 267, 1485-1488. 1995.
28. DiDonato, J. A., Hayakawa, M., Rothwarf, D. M., Zandi, E., and Karin, M. A cytokine-responsive I kappa B kinase that activates the transcription factor NF-kappaB. *Nature* 388, 548-554. 1997.
29. Mercurio, F., Zhu, H., Murray, B. W., Shevchenko, A., Bennett, B. L., Li, J., Young, D. B., Barbosa, M., Mann, M., Manning, A., and Rao, A. IKK-1 and IKK-2: cytokine-activated I kappa B kinases essential for NF-kappaB activation. *Science* 278, 860-866. 1997.
30. Zandi, E., Rothwarf, D. M., Delhase, M., Hayakawa, M., and Karin, M. The I kappa B kinase complex (IKK) contains two kinase subunits, IKKalpha and IKKbeta, necessary for I kappa B phosphorylation and NF-kappaB activation. *Cell* 91, 243-252. 1997.
31. Regnier, C. H., Song, H. Y., Gao, X., Goeddel, D. V., Cao, Z., and Rothe, M. Identification and characterization of an I kappa B kinase. *Cell* 90, 373-383. 1997.
32. Rothwarf, D. M., Zandi, E., Natoli, G., and Karin, M. IKK-gamma is an essential regulatory subunit of the I kappa B kinase complex. *Nature* 395, 297-300. 1998.
33. Yamaoka, S., Courtois, G., Bessia, C., Whiteside, S. T., Weil, R., Agou, F., Kirk, H. E., Kay, R. J., and Israel, A. Complementation cloning of NEMO, a component of the I kappa B kinase complex essential for NF-kappaB activation. *Cell* 93, 1231-1240. 1998.
34. Hacker, H. and Karin, M. Regulation and function of IKK and IKK-related kinases. *Sci.STKE.* 2006, re13. 2006.
35. Ducut Sigala, J. L., Bottero, V., Young, D. B., Shevchenko, A., Mercurio, F., and Verma, I. M. Activation of transcription factor NF-kappaB requires ELKS, an I kappa B kinase regulatory subunit. *Science* 304, 1963-1967. 2004.
36. Hayden, M. S. and Ghosh, S. Shared principles in NF-kappaB signaling. *Cell* 132, 344-362. 2008.
37. Hinz, M., Broemer, M., Arslan, S. C., Otto, A., Mueller, E. C., Dettmer, R., and Scheidereit, C. Signal responsiveness of I kappa B kinases is determined by Cdc37-assisted transient interaction with Hsp90. *J.Biol.Chem.* 282, 32311-32319. 2007.
38. Ghosh, S. and Karin, M. Missing pieces in the NF-kappaB puzzle. *Cell* 109 Suppl, S81-S96. 2002.
39. DiDonato, J. A., Hayakawa, M., Rothwarf, D. M., Zandi, E., and Karin, M. A cytokine-responsive I kappa B kinase that activates the transcription factor NF-kappaB. *Nature* 388, 548-554. 1997.
40. Delhase, M., Hayakawa, M., Chen, Y., and Karin, M. Positive and negative regulation of I kappa B kinase activity through IKKbeta subunit phosphorylation. *Science* 284, 309-313. 1999.
41. Ben Neria, Y. Regulatory functions of ubiquitination in the immune system. *Nat.Immunol.* 3, 20-26. 2002.
42. Yaron, A., Hatzubai, A., Davis, M., Lavon, I., Amit, S., Manning, A. M., Andersen, J. S., Mann, M., Mercurio, F., and Ben Neria, Y. Identification of the receptor component of the I kappa B alpha-ubiquitin ligase. *Nature* 396, 590-594. 1998.
43. Chiao, P. J., Miyamoto, S., and Verma, I. M. Autoregulation of I kappa B alpha activity. *Proc.Natl.Acad.Sci.U.S.A* 91, 28-32. 1994.
44. Naumann, M. and Scheidereit, C. Activation of NF-kappa B in vivo is regulated by multiple phosphorylations. *EMBO J.* 13, 4597-4607. 1994.
45. Arenzana-Seisdedos, F., Thompson, J., Rodriguez, M. S., Bachelier, F., Thomas, D., and Hay, R. T. Inducible nuclear expression of newly synthesized I kappa B alpha negatively regulates DNA-binding and transcriptional activities of NF-kappa B. *Mol.Cell Biol.* 15, 2689-2696. 1995.
46. Huang, T. T., Kudo, N., Yoshida, M., and Miyamoto, S. A nuclear export signal in the N-terminal regulatory domain of I kappa B alpha controls cytoplasmic localization of inactive NF-kappaB/I kappa B alpha complexes. *Proc.Natl.Acad.Sci.U.S.A* 97, 1014-1019. 2000.

References

47. Nelson, D. E., Ihekweaba, A. E., Elliott, M., Johnson, J. R., Gibney, C. A., Foreman, B. E., Nelson, G., See, V., Horton, C. A., Spiller, D. G., Edwards, S. W., McDowell, H. P., Unitt, J. F., Sullivan, E., Grimley, R., Benson, N., Broomhead, D., Kell, D. B., and White, M. R. Oscillations in NF-kappaB signaling control the dynamics of gene expression. *Science* 306, 704-708. 2004.
48. Krappmann, D. and Scheidereit, C. A pervasive role of ubiquitin conjugation in activation and termination of IkappaB kinase pathways. *EMBO Rep.* 6, 321-326. 2005.
49. Kanayama, A., Seth, R. B., Sun, L., Ea, C. K., Hong, M., Shaito, A., Chiu, Y. H., Deng, L., and Chen, Z. J. TAB2 and TAB3 activate the NF-kappaB pathway through binding to polyubiquitin chains. *Mol. Cell* 15, 535-548. 2004.
50. Ea, C. K., Deng, L., Xia, Z. P., Pineda, G., and Chen, Z. J. Activation of IKK by TNFalpha requires site-specific ubiquitination of RIP1 and polyubiquitin binding by NEMO. *Mol. Cell* 22, 245-257. 2006.
51. Wu, C. J., Conze, D. B., Li, T., Srinivasula, S. M., and Ashwell, J. D. Sensing of Lys 63-linked polyubiquitination by NEMO is a key event in NF-kappaB activation [corrected]. *Nat. Cell Biol.* 8, 398-406. 2006.
52. Chen, Z. J., Bhoj, V., and Seth, R. B. Ubiquitin, TAK1 and IKK: is there a connection? *Cell Death Differ.* 13, 687-692. 2006.
53. Oeckinghaus, A., Wegener, E., Welteke, V., Ferch, U., Arslan, S. C., Ruland, J., Scheidereit, C., and Krappmann, D. Malt1 ubiquitination triggers NF-kappaB signaling upon T-cell activation. *EMBO J.* 26, 4634-4645. 2007.
54. Hoffmann, A., Levchenko, A., Scott, M. L., and Baltimore, D. The IkappaB-NF-kappaB signaling module: temporal control and selective gene activation. *Science* 298, 1241-1245. 2002.
55. Kearns, J. D., Basak, S., Werner, S. L., Huang, C. S., and Hoffmann, A. IkappaBepsilon provides negative feedback to control NF-kappaB oscillations, signaling dynamics, and inflammatory gene expression. *J. Cell Biol.* 173, 659-664. 2006.
56. Wertz, I. E. and Dixit, V. M. Ubiquitin-mediated regulation of TNFR1 signaling. *Cytokine Growth Factor Rev.* 19, 313-324. 2008.
57. Chuang, T. H. and Ulevitch, R. J. Triad3A, an E3 ubiquitin-protein ligase regulating Toll-like receptors. *Nat. Immunol.* 5, 495-502. 2004.
58. Wertz, I. E., O'Rourke, K. M., Zhou, H., Eby, M., Aravind, L., Seshagiri, S., Wu, P., Wiesmann, C., Baker, R., Boone, D. L., Ma, A., Koonin, E. V., and Dixit, V. M. De-ubiquitination and ubiquitin ligase domains of A20 downregulate NF-kappaB signalling. *Nature* 430, 694-699. 2004.
59. Li, X., Yang, Y., and Ashwell, J. D. TNF-RII and c-IAP1 mediate ubiquitination and degradation of TRAF2. *Nature* 416, 345-347. 2002.
60. Yamin, T. T. and Miller, D. K. The interleukin-1 receptor-associated kinase is degraded by proteasomes following its phosphorylation. *J. Biol. Chem.* 272, 21540-21547. 1997.
61. Brummelkamp, T. R., Nijman, S. M., Dirac, A. M., and Bernards, R. Loss of the cylindromatosis tumour suppressor inhibits apoptosis by activating NF-kappaB. *Nature* 424, 797-801. 2003.
62. Trompouki, E., Hatzivassiliou, E., Tschirritzis, T., Farmer, H., Ashworth, A., and Mosialos, G. CYLD is a deubiquitinating enzyme that negatively regulates NF-kappaB activation by TNFR family members. *Nature* 424, 793-796. 2003.
63. Kovalenko, A., Chable-Bessia, C., Cantarella, G., Israel, A., Wallach, D., and Courtois, G. The tumour suppressor CYLD negatively regulates NF-kappaB signalling by deubiquitination. *Nature* 424, 801-805. 2003.
64. Evans, P. C., Taylor, E. R., Coadwell, J., Heyninck, K., Beyaert, R., and Kilshaw, P. J. Isolation and characterization of two novel A20-like proteins. *Biochem. J.* 357, 617-623. 2001.
65. Saccani, S., Marazzi, I., Beg, A. A., and Natoli, G. Degradation of promoter-bound p65/RelA is essential for the prompt termination of the nuclear factor kappaB response. *J. Exp. Med.* 200, 107-113. 2004.
66. Ryo, A., Suizu, F., Yoshida, Y., Perrem, K., Liou, Y. C., Wulf, G., Rottapel, R., Yamaoka, S., and Lu, K. P. Regulation of NF-kappaB signaling by Pin1-dependent prolyl isomerization and ubiquitin-mediated proteolysis of p65/RelA. *Mol. Cell* 12, 1413-1426. 2003.
67. Werner, S. L., Barken, D., and Hoffmann, A. Stimulus specificity of gene expression programs determined by temporal control of IKK activity. *Science* 309, 1857-1861. 2005.
68. Covert, M. W., Leung, T. H., Gaston, J. E., and Baltimore, D. Achieving stability of lipopolysaccharide-induced NF-kappaB activation. *Science* 309, 1854-1857. 2005.

References

69. Nelson, G., Paraoan, L., Spiller, D. G., Wilde, G. J., Browne, M. A., Djali, P. K., Unitt, J. F., Sullivan, E., Floettmann, E., and White, M. R. Multi-parameter analysis of the kinetics of NF-kappaB signalling and transcription in single living cells. *J.Cell Sci.* 115, 1137-1148. 2002.
70. Carlotti, F., Chapman, R., Dower, S. K., and Qwarnstrom, E. E. Activation of nuclear factor kappaB in single living cells. Dependence of nuclear translocation and anti-apoptotic function on EGFPRELA concentration. *J.Biol.Chem.* 274, 37941-37949. 1999.
71. Carlotti, F., Dower, S. K., and Qwarnstrom, E. E. Dynamic shuttling of nuclear factor kappa B between the nucleus and cytoplasm as a consequence of inhibitor dissociation. *J.Biol.Chem.* 275, 41028-41034. 2000.
72. Schmid, J. A., Birbach, A., Hofer-Warbinek, R., Pengg, M., Burner, U., Furtmuller, P. G., Binder, B. R., and de Martin, R. Dynamics of NF kappa B and Ikappa Balpha studied with green fluorescent protein (GFP) fusion proteins. Investigation of GFP-p65 binding to DNA by fluorescence resonance energy transfer. *J.Biol.Chem.* 275, 17035-17042. 2000.
73. Birbach, A., Gold, P., Binder, B. R., Hofer, E., de Martin, R., and Schmid, J. A. Signaling molecules of the NF-kappa B pathway shuttle constitutively between cytoplasm and nucleus. *J.Biol.Chem.* 277, 10842-10851. 2002.
74. Barken, D., Wang, C. J., Kearns, J., Cheong, R., Hoffmann, A., and Levchenko, A. Comment on "Oscillations in NF-kappaB signaling control the dynamics of gene expression". *Science* 308, 52. 2005.
75. Krienitz, W. Ueber das Auftreten von Spirochaeten verschiedener Form im Mageninhalt bei Carcinoma ventriculi. *Dtsch.Med.Wochenschr.* 32, 872-882. 1906.
76. Marshall, B. J. and Warren, J. R. Unidentified curved bacilli in the stomach of patients with gastritis and peptic ulceration. *Lancet* 1, 1311-1315. 1984.
77. Covacci, A., Telford, J. L., Del Giudice, G., Parsonnet, J., and Rappuoli, R. Helicobacter pylori virulence and genetic geography. *Science* 284, 1328-1333. 1999.
78. Amieva, M. R. and El Omar, E. M. Host-bacterial interactions in Helicobacter pylori infection. *Gastroenterology* 134, 306-323. 2008.
79. Marshall, B. J. and Windsor, H. M. The relation of Helicobacter pylori to gastric adenocarcinoma and lymphoma: pathophysiology, epidemiology, screening, clinical presentation, treatment, and prevention. *Med.Clin.North Am.* 89, 313-44, viii. 2005.
80. Wotherspoon, A. C., Doglioni, C., Diss, T. C., Pan, L., Moschini, A., de Boni, M., and Isaacson, P. G. Regression of primary low-grade B-cell gastric lymphoma of mucosa-associated lymphoid tissue type after eradication of Helicobacter pylori. *Lancet* 342, 575-577. 1993.
81. IARC Monographs on the Evaluation of Carcinogenic Risks to Humans. 177. 1994. IARCPress, Lyon.
82. Malfertheiner, P., Sipponen, P., Naumann, M., Moayyedi, P., Megraud, F., Xiao, S. D., Sugano, K., and Nyren, O. Helicobacter pylori eradication has the potential to prevent gastric cancer: a state-of-the-art critique. *Am.J.Gastroenterol.* 100, 2100-2115. 2005.
83. Lochhead, P. and El Omar, E. M. Gastric cancer. *Br.Med.Bull.* 85, 87-100. 2008.
84. Hohenberger, P. and Gretschel, S. Gastric cancer. *Lancet* 362, 305-315. 2003.
85. Blaser, M. J. and Atherton, J. C. Helicobacter pylori persistence: biology and disease. *J.Clin.Invest.* 113, 321-333. 2004.
86. Bauerfeind, P., Garner, R., Dunn, B. E., and Mobley, H. L. Synthesis and activity of Helicobacter pylori urease and catalase at low pH. *Gut* 40, 25-30. 1997.
87. Schreiber, S., Konradt, M., Groll, C., Scheid, P., Hanauer, G., Werling, H. O., Josenhans, C., and Suerbaum, S. The spatial orientation of Helicobacter pylori in the gastric mucus. *Proc.Natl.Acad.Sci.U.S.A* 101, 5024-5029. 2004.
88. Ilver, D., Arnqvist, A., Ogren, J., Frick, I. M., Kersulyte, D., Incecik, E. T., Berg, D. E., Covacci, A., Engstrand, L., and Boren, T. Helicobacter pylori adhesin binding fucosylated histo-blood group antigens revealed by retagging. *Science* 279, 373-377. 1998.
89. Montecucco, C. and Rappuoli, R. Living dangerously: how Helicobacter pylori survives in the human stomach. *Nat.Rev.Mol.Cell Biol.* 2, 457-466. 2001.
90. Segal, E. D., Cha, J., Lo, J., Falkow, S., and Tompkins, L. S. Altered states: involvement of phosphorylated CagA in the induction of host cellular growth changes by Helicobacter pylori. *Proc.Natl.Acad.Sci.U.S.A* 96, 14559-14564. 1999.
91. Backert, S. and Meyer, T. F. Type IV secretion systems and their effectors in bacterial pathogenesis. *Curr.Opin.Microbiol.* 9, 207-217. 2006.

References

92. Hatakeyama, M. SagA of CagA in *Helicobacter pylori* pathogenesis. *Curr.Opin.Microbiol.* 11, 30-37. 2008.
93. El Omar, E. M., Carrington, M., Chow, W. H., McColl, K. E., Bream, J. H., Young, H. A., Herrera, J., Lissowska, J., Yuan, C. C., Rothman, N., Lanyon, G., Martin, M., Fraumeni, J. F., Jr., and Rabkin, C. S. Interleukin-1 polymorphisms associated with increased risk of gastric cancer. *Nature* 404, 398-402. 2000.
94. El Omar, E. M., Rabkin, C. S., Gammon, M. D., Vaughan, T. L., Risch, H. A., Schoenberg, J. B., Stanford, J. L., Mayne, S. T., Goedert, J., Blot, W. J., Fraumeni, J. F., Jr., and Chow, W. H. Increased risk of noncardia gastric cancer associated with proinflammatory cytokine gene polymorphisms. *Gastroenterology* 124, 1193-1201. 2003.
95. Smith, M. G., Hold, G. L., and Rabkin, C. S. The IL-8-251 promoter polymorphism is associated with high IL-8 production, severe inflammation and increased risk of pre-malignant changes in *H. pylori* positive subjects. *Gastroenterology* 124, A23. 2004.
96. Azuma, T., Ito, S., Sato, F., Yamazaki, Y., Miyaji, H., Ito, Y., Suto, H., Kuriyama, M., Kato, T., and Kohli, Y. The role of the HLA-DQA1 gene in resistance to atrophic gastritis and gastric adenocarcinoma induced by *Helicobacter pylori* infection. *Cancer* 82, 1013-1018. 1998.
97. Cohen, S. M., Purtilo, D. T., and Ellwein, L. B. Ideas in pathology. Pivotal role of increased cell proliferation in human carcinogenesis. *Mod.Pathol.* 4, 371-382. 1991.
98. Peek, R. M., Jr. and Blaser, M. J. *Helicobacter pylori* and gastrointestinal tract adenocarcinomas. *Nat.Rev.Cancer* 2, 28-37. 2002.
99. Crabtree, J. E., Wyatt, J. I., Trejdosiewicz, L. K., Peichl, P., Nichols, P. H., Ramsay, N., Primrose, J. N., and Lindley, I. J. Interleukin-8 expression in *Helicobacter pylori* infected, normal, and neoplastic gastroduodenal mucosa. *J.Clin.Pathol.* 47, 61-66. 1994.
100. Li, Q., Withoff, S., and Verma, I. M. Inflammation-associated cancer: NF-kappaB is the lynchpin. *Trends Immunol.* 26, 318-325. 2005.
101. Ferrero, R. L., Ave, P., Ndiaye, D., Bambou, J. C., Huerre, M. R., Philpott, D. J., and Memet, S. NF-kappaB activation during acute *Helicobacter pylori* infection in mice. *Infect.Immun.* 76, 551-561. 2008.
102. Hirata, Y., Ohmae, T., Shibata, W., Maeda, S., Ogura, K., Yoshida, H., Kawabe, T., and Omata, M. MyD88 and TNF receptor-associated factor 6 are critical signal transducers in *Helicobacter pylori*-infected human epithelial cells. *J.Immunol.* 176, 3796-3803. 2006.
103. Mai, U. E., Perez-Perez, G. I., Wahl, L. M., Wahl, S. M., Blaser, M. J., and Smith, P. D. Soluble surface proteins from *Helicobacter pylori* activate monocytes/macrophages by lipopolysaccharide-independent mechanism. *J.Clin.Invest* 87, 894-900. 1991.
104. Harris, P. R., Ernst, P. B., Kawabata, S., Kiyono, H., Graham, M. F., and Smith, P. D. Recombinant *Helicobacter pylori* urease activates primary mucosal macrophages. *J.Infect.Dis.* 178, 1516-1520. 1998.
105. Lin, S. N., Ayada, K., Zhao, Y., Yokota, K., Takenaka, R., Okada, H., Kan, R., Hayashi, S., Mizuno, M., Hirai, Y., Fujinami, Y., and Oguma, K. *Helicobacter pylori* heat-shock protein 60 induces production of the pro-inflammatory cytokine IL8 in monocytic cells. *J.Med.Microbiol.* 54, 225-233. 2005.
106. Muotiala, A., Helander, I. M., Pyhala, L., Kosunen, T. U., and Moran, A. P. Low biological activity of *Helicobacter pylori* lipopolysaccharide. *Infect.Immun.* 60, 1714-1716. 1992.
107. Bliss, C. M., Jr., Golenbock, D. T., Keates, S., Linevsky, J. K., and Kelly, C. P. *Helicobacter pylori* lipopolysaccharide binds to CD14 and stimulates release of interleukin-8, epithelial neutrophil-activating peptide 78, and monocyte chemotactic protein 1 by human monocytes. *Infect.Immun.* 66, 5357-5363. 1998.
108. Censini, S., Lange, C., Xiang, Z., Crabtree, J. E., Ghiara, P., Borodovsky, M., Rappuoli, R., and Covacci, A. *cag*, a pathogenicity island of *Helicobacter pylori*, encodes type I-specific and disease-associated virulence factors. *Proc.Natl.Acad.Sci.U.S.A* 93, 14648-14653. 1996.
109. Sharma, S. A., Tummuru, M. K., Blaser, M. J., and Kerr, L. D. Activation of IL-8 gene expression by *Helicobacter pylori* is regulated by transcription factor nuclear factor-kappa B in gastric epithelial cells. *J.Immunol.* 160, 2401-2407. 1998.
110. Nilsson, C., Sillen, A., Eriksson, L., Strand, M. L., Enroth, H., Normark, S., Falk, P., and Engstrand, L. Correlation between *cag* pathogenicity island composition and *Helicobacter pylori*-associated gastroduodenal disease. *Infect.Immun.* 71, 6573-6581. 2003.

References

111. Glocker, E., Lange, C., Covacci, A., Bereswill, S., Kist, M., and Pahl, H. L. Proteins encoded by the *cag* pathogenicity island of *Helicobacter pylori* are required for NF-kappaB activation. *Infect.Immun.* 66, 2346-2348. 1998.
 112. Fischer, W., Puls, J., Buhrdorf, R., Gebert, B., Odenbreit, S., and Haas, R. Systematic mutagenesis of the *Helicobacter pylori* *cag* pathogenicity island: essential genes for CagA translocation in host cells and induction of interleukin-8. *Mol.Microbiol.* 42, 1337-1348. 2001.
 113. Selbach, M., Moese, S., Meyer, T. F., and Backert, S. Functional analysis of the *Helicobacter pylori* *cag* pathogenicity island reveals both VirD4-CagA-dependent and VirD4-CagA-independent mechanisms. *Infect.Immun.* 70, 665-671. 2002.
 114. Brandt, S., Kwok, T., Hartig, R., Konig, W., and Backert, S. NF-kappaB activation and potentiation of proinflammatory responses by the *Helicobacter pylori* CagA protein. *Proc.Natl.Acad.Sci.U.S.A* 102, 9300-9305. 2005.
 115. Backhed, F., Rokbi, B., Torstensson, E., Zhao, Y., Nilsson, C., Seguin, D., Normark, S., Buchan, A. M., and Richter-Dahlfors, A. Gastric mucosal recognition of *Helicobacter pylori* is independent of Toll-like receptor 4. *J.Infect.Dis.* 187, 829-836. 2003.
 116. Lee, S. K. and Josenhans, C. *Helicobacter pylori* and the innate immune system. *Int.J.Med.Microbiol.* 295, 325-334. 2005.
 117. Smith, M. F., Jr., Mitchell, A., Li, G., Ding, S., Fitzmaurice, A. M., Ryan, K., Crowe, S., and Goldberg, J. B. Toll-like receptor (TLR) 2 and TLR5, but not TLR4, are required for *Helicobacter pylori*-induced NF-kappa B activation and chemokine expression by epithelial cells. *J.Biol.Chem.* 278, 32552-32560. 2003.
 118. Lee, S. K., Stack, A., Katzowitsch, E., Aizawa, S. I., Suerbaum, S., and Josenhans, C. *Helicobacter pylori* flagellins have very low intrinsic activity to stimulate human gastric epithelial cells via TLR5. *Microbes.Infect.* 5, 1345-1356. 2003.
 119. Andersen-Nissen, E., Smith, K. D., Strobe, K. L., Barrett, S. L., Cookson, B. T., Logan, S. M., and Adrem, A. Evasion of Toll-like receptor 5 by flagellated bacteria. *Proc.Natl.Acad.Sci.U.S.A* 102, 9247-9252. 2005.
 120. Maeda, S., Akanuma, M., Mitsuno, Y., Hirata, Y., Ogura, K., Yoshida, H., Shiratori, Y., and Omata, M. Distinct mechanism of *Helicobacter pylori*-mediated NF-kappa B activation between gastric cancer cells and monocytic cells. *J.Biol.Chem.* 276, 44856-44864. 2001.
 121. Viala, J., Chaput, C., Boneca, I. G., Cardona, A., Girardin, S. E., Moran, A. P., Athman, R., Memet, S., Huerre, M. R., Coyle, A. J., DiStefano, P. S., Sansonetti, P. J., Labigne, A., Bertin, J., Philpott, D. J., and Ferrero, R. L. Nod1 responds to peptidoglycan delivered by the *Helicobacter pylori* *cag* pathogenicity island. *Nat.Immunol.* 5, 1166-1174. 2004.
 122. Hirata, Y., Maeda, S., Ohmae, T., Shibata, W., Yanai, A., Ogura, K., Yoshida, H., Kawabe, T., and Omata, M. *Helicobacter pylori* induces IkappaB kinase alpha nuclear translocation and chemokine production in gastric epithelial cells. *Infect.Immun.* 74, 1452-1461. 2006.
 123. Maeda, S., Yoshida, H., Ogura, K., Mitsuno, Y., Hirata, Y., Yamaji, Y., Akanuma, M., Shiratori, Y., and Omata, M. H. *pylori* activates NF-kappaB through a signaling pathway involving IkappaB kinases, NF-kappaB-inducing kinase, TRAF2, and TRAF6 in gastric cancer cells. *Gastroenterology* 119, 97-108. 2000.
 124. Foryst-Ludwig, A. and Naumann, M. p21-activated kinase 1 activates the nuclear factor kappa B (NF-kappa B)-inducing kinase-Ikappa B kinases NF-kappa B pathway and proinflammatory cytokines in *Helicobacter pylori* infection. *J.Biol.Chem.* 275, 39779-39785. 2000.
 125. Neumann, M., Foryst-Ludwig, A., Klar, S., Schweitzer, K., and Naumann, M. The PAK1 autoregulatory domain is required for interaction with NIK in *Helicobacter pylori*-induced NF-kappaB activation. *Biol.Chem.* 387, 79-86. 2006.
 126. Ohmae, T., Hirata, Y., Maeda, S., Shibata, W., Yanai, A., Ogura, K., Yoshida, H., Kawabe, T., and Omata, M. *Helicobacter pylori* activates NF-kappaB via the alternative pathway in B lymphocytes. *J.Immunol.* 175, 7162-7169. 2005.
 127. Kunsch, C., Ruben, S. M., and Rosen, C. A. Selection of optimal kappa B/Rel DNA-binding motifs: interaction of both subunits of NF-kappa B with DNA is required for transcriptional activation. *Mol.Cell Biol.* 12, 4412-4421. 1992.
 128. Muder, R. R., Yu, V. L., and Woo, A. H. Mode of transmission of *Legionella pneumophila*. A critical review. *Arch.Intern.Med.* 146, 1607-1612. 1986.
-

References

129. Isberg, R. R., O'Connor, T. J., and Heidtman, M. The Legionella pneumophila replication vacuole: making a cosy niche inside host cells. *Nat.Rev.Microbiol.* 7, 13-24. 2009.
130. Molofsky, A. B. and Swanson, M. S. Differentiate to thrive: lessons from the Legionella pneumophila life cycle. *Mol.Microbiol.* 53, 29-40. 2004.
131. Bruggemann, H., Hagman, A., Jules, M., Sismeiro, O., Dillies, M. A., Gouyette, C., Kunst, F., Steinert, M., Heuner, K., Coppee, J. Y., and Buchrieser, C. Virulence strategies for infecting phagocytes deduced from the in vivo transcriptional program of Legionella pneumophila. *Cell Microbiol.* 8, 1228-1240. 2006.
132. Bitar, D. M., Molmeret, M., and Abu, K. Y. Molecular and cell biology of Legionella pneumophila. *Int.J.Med.Microbiol.* 293, 519-527. 2004.
133. Kubori, T., Hyakutake, A., and Nagai, H. Legionella translocates an E3 ubiquitin ligase that has multiple U-boxes with distinct functions. *Mol.Microbiol.* 67, 1307-1319. 2008.
134. Ninio, S. and Roy, C. R. Effector proteins translocated by Legionella pneumophila: strength in numbers. *Trends Microbiol.* 15, 372-380. 2007.
135. Nash, T. W., Libby, D. M., and Horwitz, M. A. Interaction between the legionnaires' disease bacterium (Legionella pneumophila) and human alveolar macrophages. Influence of antibody, lymphokines, and hydrocortisone. *J.Clin.Invest* 74, 771-782. 1984.
136. Hippenstiel, S., Opitz, B., Schmeck, B., and Suttorp, N. Lung epithelium as a sentinel and effector system in pneumonia--molecular mechanisms of pathogen recognition and signal transduction. *Respir.Res.* 7, 97. 2006.
137. Schmeck, B., N'Guessan, P. D., Ollomang, M., Lorenz, J., Zahlten, J., Opitz, B., Flieger, A., Suttorp, N., and Hippenstiel, S. Legionella pneumophila-induced NF-kappaB- and MAPK-dependent cytokine release by lung epithelial cells. *Eur.Respir.J.* 29, 25-33. 2007.
138. Mody, C. H., Paine, R., III, Shahrabadi, M. S., Simon, R. H., Pearlman, E., Eisenstein, B. I., and Toews, G. B. Legionella pneumophila replicates within rat alveolar epithelial cells. *J.Infect.Dis.* 167, 1138-1145. 1993.
139. Gao, L. Y., Stone, B. J., Brieland, J. K., and Abu, K. Y. Different fates of Legionella pneumophila pm1 and mil mutants within macrophages and alveolar epithelial cells. *Microb.Pathog.* 25, 291-306. 1998.
140. Cianciotto, N. P., Stamos, J. K., and Kamp, D. W. Infectivity of Legionella pneumophila mip mutant for alveolar epithelial cells. *Curr.Microbiol.* 30, 247-250. 1995.
141. Maruta, K., Miyamoto, H., Hamada, T., Ogawa, M., Taniguchi, H., and Yoshida, S. Entry and intracellular growth of Legionella dumoffii in alveolar epithelial cells. *Am.J.Respir.Crit Care Med.* 157, 1967-1974. 1998.
142. Chang, B., Amemura-Maekawa, J., Kura, F., Kawamura, I., and Watanabe, H. Expression of IL-6 and TNF-alpha in human alveolar epithelial cells is induced by invading, but not by adhering, Legionella pneumophila. *Microb.Pathog.* 37, 295-302. 2004.
143. Teruya, H., Higa, F., Akamine, M., Ishikawa, C., Okudaira, T., Tomimori, K., Mukaida, N., Tateyama, M., Heuner, K., Fujita, J., and Mori, N. Mechanisms of Legionella pneumophila-induced interleukin-8 expression in human lung epithelial cells. *BMC.Microbiol.* 7, 102. 2007.
144. Abu-Zant, A., Jones, S., Asare, R., Suttles, J., Price, C., Graham, J., and Kwaik, Y. A. Anti-apoptotic signalling by the Dot/Icm secretion system of L. pneumophila. *Cell Microbiol.* 9, 246-264. 2007.
145. Clifton, D. R., Goss, R. A., Sahni, S. K., van Antwerp, D., Baggs, R. B., Marder, V. J., Silverman, D. J., and Sporn, L. A. NF-kappa B-dependent inhibition of apoptosis is essential for host cell survival during Rickettsia rickettsii infection. *Proc.Natl.Acad.Sci.U.S.A* 95, 4646-4651. 1998.
146. Molestina, R. E., Payne, T. M., Coppens, I., and Sinai, A. P. Activation of NF-kappaB by Toxoplasma gondii correlates with increased expression of antiapoptotic genes and localization of phosphorylated I kappa B to the parasitophorous vacuole membrane. *J.Cell Sci.* 116, 4359-4371. 2003.
147. Payne, T. M., Molestina, R. E., and Sinai, A. P. Inhibition of caspase activation and a requirement for NF-kappaB function in the Toxoplasma gondii-mediated blockade of host apoptosis. *J.Cell Sci.* 116, 4345-4358. 2003.
148. Heussler, V. T., Machado, J., Jr., Fernandez, P. C., Botteron, C., Chen, C. G., Pearse, M. J., and Dobbelaere, D. A. The intracellular parasite Theileria parva protects infected T cells from apoptosis. *Proc.Natl.Acad.Sci.U.S.A* 96, 7312-7317. 1999.

References

149. Hawn, T. R., Verbon, A., Lettinga, K. D., Zhao, L. P., Li, S. S., Laws, R. J., Skerrett, S. J., Beutler, B., Schroeder, L., Nachman, A., Ozinsky, A., Smith, K. D., and Aderem, A. A common dominant TLR5 stop codon polymorphism abolishes flagellin signaling and is associated with susceptibility to legionnaires' disease. *J.Exp.Med.* 198, 1563-1572. 2003.
150. Losick, V. P. and Isberg, R. R. NF-kappaB translocation prevents host cell death after low-dose challenge by *Legionella pneumophila*. *J.Exp.Med.* 203, 2177-2189. 2006.
151. Meister, G. and Tuschl, T. Mechanisms of gene silencing by double-stranded RNA. *Nature* 431, 343-349. 2004.
152. Fire, A., Xu, S., Montgomery, M. K., Kostas, S. A., Driver, S. E., and Mello, C. C. Potent and specific genetic interference by double-stranded RNA in *Caenorhabditis elegans*. *Nature* 391, 806-811. 1998.
153. Elbashir, S. M., Harborth, J., Lendeckel, W., Yalcin, A., Weber, K., and Tuschl, T. Duplexes of 21-nucleotide RNAs mediate RNA interference in cultured mammalian cells. *Nature* 411, 494-498. 2001.
154. Nguyen, D. G., Wolff, K. C., Yin, H., Caldwell, J. S., and Kuhlen, K. L. "UnPAKing" human immunodeficiency virus (HIV) replication: using small interfering RNA screening to identify novel cofactors and elucidate the role of group I PAKs in HIV infection. *J.Virol.* 80, 130-137. 2006.
155. Brass, A. L., Dykxhoorn, D. M., Benita, Y., Yan, N., Engelman, A., Xavier, R. J., Lieberman, J., and Elledge, S. J. Identification of host proteins required for HIV infection through a functional genomic screen. *Science* 319, 921-926. 2008.
156. Zhou, H., Xu, M., Huang, Q., Gates, A. T., Zhang, X. D., Castle, J. C., Stec, E., Ferrer, M., Strulovici, B., Hazuda, D. J., and Espeseth, A. S. Genome-scale RNAi screen for host factors required for HIV replication. *Cell Host.Microbe* 4, 495-504. 2008.
157. Kuijl, C., Savage, N. D., Marsman, M., Tuin, A. W., Janssen, L., Egan, D. A., Ketema, M., van den, N. R., van den Eeden, S. J., Geluk, A., Poot, A., van der, M. G., Beijersbergen, R. L., Overkleeft, H., Otenhoff, T. H., and Neefjes, J. Intracellular bacterial growth is controlled by a kinase network around PKB/AKT1. *Nature* 450, 725-730. 2007.
158. Krishnan, M. N., Ng, A., Sukumaran, B., Gilfoy, F. D., Uchil, P. D., Sultana, H., Brass, A. L., Adametz, R., Tsui, M., Qian, F., Montgomery, R. R., Lev, S., Mason, P. W., Koski, R. A., Elledge, S. J., Xavier, R. J., Agaisse, H., and Fikrig, E. RNA interference screen for human genes associated with West Nile virus infection. *Nature* 455, 242-245. 2008.
159. Tsai, T. Y., Choi, Y. S., Ma, W., Pomerening, J. R., Tang, C., and Ferrell, J. E., Jr. Robust, tunable biological oscillations from interlinked positive and negative feedback loops. *Science* 321, 126-129. 2008.
160. Becskei, A., Boselli, M. G., and van Oudenaarden, A. Amplitude control of cell-cycle waves by nuclear import. *Nat Cell Biol.* 6, 451-457. 2004.
161. Htun, H., Barsony, J., Renyi, I., Gould, D. L., and Hager, G. L. Visualization of glucocorticoid receptor translocation and intranuclear organization in living cells with a green fluorescent protein chimera. *Proc.Natl.Acad.Sci.U.S.A* 93, 4845-4850. 1996.
162. Jacquet, M., Renault, G., Lallet, S., De Mey, J., and Goldbeter, A. Oscillatory nucleocytoplasmic shuttling of the general stress response transcriptional activators Msn2 and Msn4 in *Saccharomyces cerevisiae*. *J.Cell Biol.* 161, 497-505. 2003.
163. Lahav, G., Rosenfeld, N., Sigal, A., Geva-Zatorsky, N., Levine, A. J., Elowitz, M. B., and Alon, U. Dynamics of the p53-Mdm2 feedback loop in individual cells. *Nat Genet.* 36, 147-150. 2004.
164. Shibasaki, F., Price, E. R., Milan, D., and McKeon, F. Role of kinases and the phosphatase calcineurin in the nuclear shuttling of transcription factor NF-AT4. *Nature* 382, 370-373. 1996.
165. Cheong, R., Bergmann, A., Werner, S. L., Regal, J., Hoffmann, A., and Levchenko, A. Transient I-kappaB kinase activity mediates temporal NF-kappaB dynamics in response to a wide range of tumor necrosis factor-alpha doses. *J.Biol.Chem.* 281, 2945-2950. 2006.
166. Sillitoe, K., Horton, C., Spiller, D. G., and White, M. R. Single-cell time-lapse imaging of the dynamic control of NF-kappaB signalling. *Biochem.Soc.Trans.* 35, 263-266. 2007.
167. Karin, M., Yamamoto, Y., and Wang, Q. M. The IKK NF-kappa B system: a treasure trove for drug development. *Nat Rev Drug Discov.* 3, 17-26. 2004.
168. Jackson, A. L., Bartz, S. R., Schelter, J., Kobayashi, S. V., Burchard, J., Mao, M., Li, B., Cavet, G., and Linsley, P. S. Expression profiling reveals off-target gene regulation by RNAi. *Nat.Biotechnol.* 21, 635-637. 2003.

References

169. Jackson, A. L. and Linsley, P. S. Noise amidst the silence: off-target effects of siRNAs? *Trends Genet.* 20, 521-524. 2004.
170. Kulkarni, M. M., Booker, M., Silver, S. J., Friedman, A., Hong, P., Perrimon, N., and Mathey-Prevot, B. Evidence of off-target effects associated with long dsRNAs in *Drosophila melanogaster* cell-based assays. *Nat.Methods* 3, 833-838. 2006.
171. Bridge, A. J., Pebernard, S., Ducraux, A., Nicoulaz, A. L., and Iggo, R. Induction of an interferon response by RNAi vectors in mammalian cells. *Nat.Genet.* 34, 263-264. 2003.
172. Sledz, C. A., Holko, M., de Veer, M. J., Silverman, R. H., and Williams, B. R. Activation of the interferon system by short-interfering RNAs. *Nat.Cell Biol.* 5, 834-839. 2003.
173. Chen, K. and Rajewsky, N. The evolution of gene regulation by transcription factors and microRNAs. *Nat.Rev.Genet.* 8, 93-103. 2007.
174. Birmingham, A., Anderson, E. M., Reynolds, A., Ilesley-Tyree, D., Leake, D., Fedorov, Y., Baskerville, S., Maksimova, E., Robinson, K., Karpilow, J., Marshall, W. S., and Khvorova, A. 3' UTR seed matches, but not overall identity, are associated with RNAi off-targets. *Nat.Methods* 3, 199-204. 2006.
175. Jackson, A. L., Burchard, J., Schelter, J., Chau, B. N., Cleary, M., Lim, L., and Linsley, P. S. Widespread siRNA "off-target" transcript silencing mediated by seed region sequence complementarity. *RNA.* 12, 1179-1187. 2006.
176. Cullen, B. R. Enhancing and confirming the specificity of RNAi experiments. *Nat.Methods* 3, 677-681. 2006.
177. Echeverri, C. J., Beachy, P. A., Baum, B., Boutros, M., Buchholz, F., Chanda, S. K., Downward, J., Ellenberg, J., Fraser, A. G., Hacohen, N., Hahn, W. C., Jackson, A. L., Kiger, A., Linsley, P. S., Lum, L., Ma, Y., Mathey-Prevot, B., Root, D. E., Sabatini, D. M., Taipale, J., Perrimon, N., and Bernards, R. Minimizing the risk of reporting false positives in large-scale RNAi screens. *Nat.Methods* 3, 777-779. 2006.
178. von Mering, C., Jensen, L. J., Kuhn, M., Chaffron, S., Doerks, T., Kruger, B., Snel, B., and Bork, P. STRING 7--recent developments in the integration and prediction of protein interactions. *Nucleic Acids Res.* 35, D358-D362. 2007.
179. Drees, B. L., Thorsson, V., Carter, G. W., Rives, A. W., Raymond, M. Z., Avila-Campillo, I., Shannon, P., and Galitski, T. Derivation of genetic interaction networks from quantitative phenotype data. *Genome Biol.* 6, R38. 2005.
180. Hartman, J. L., Garvik, B., and Hartwell, L. Principles for the buffering of genetic variation. *Science* 291, 1001-1004. 2001.
181. Heine, M., Cramm-Behrens, C. I., Ansari, A., Chu, H. P., Ryazanov, A. G., Naim, H. Y., and Jacob, R. Alpha-kinase 1, a new component in apical protein transport. *J.Biol.Chem.* 280, 25637-25643. 2005.
182. Chen, H. H., Wang, Y. C., and Fann, M. J. Identification and characterization of the CDK12/cyclin L1 complex involved in alternative splicing regulation. *Mol.Cell Biol.* 26, 2736-2745. 2006.
183. Barre, B. and Perkins, N. D. A cell cycle regulatory network controlling NF-kappaB subunit activity and function. *EMBO J.* 26, 4841-4855. 2007.
184. Frescas, D. and Pagano, M. Deregulated proteolysis by the F-box proteins SKP2 and beta-TrCP: tipping the scales of cancer. *Nat.Rev.Cancer* 8, 438-449. 2008.
185. Fedorov, Y., Anderson, E. M., Birmingham, A., Reynolds, A., Karpilow, J., Robinson, K., Leake, D., Marshall, W. S., and Khvorova, A. Off-target effects by siRNA can induce toxic phenotype. *RNA.* 12, 1188-1196. 2006.
186. Ma, Y., Creanga, A., Lum, L., and Beachy, P. A. Prevalence of off-target effects in *Drosophila* RNA interference screens. *Nature* 443, 359-363. 2006.
187. Tischler, J., Lehner, B., Chen, N., and Fraser, A. G. Combinatorial RNA interference in *Caenorhabditis elegans* reveals that redundancy between gene duplicates can be maintained for more than 80 million years of evolution. *Genome Biol.* 7, R69. 2006.
188. Lehner, B., Crombie, C., Tischler, J., Fortunato, A., and Fraser, A. G. Systematic mapping of genetic interactions in *Caenorhabditis elegans* identifies common modifiers of diverse signaling pathways. *Nat.Genet.* 38, 896-903. 2006.
189. Bargou, R. C., Emmerich, F., Krappmann, D., Bommert, K., Mapara, M. Y., Arnold, W., Royer, H. D., Grinstein, E., Greiner, A., Scheiderei, C., and Dorken, B. Constitutive nuclear factor-kappaB-RelA activation is required for proliferation and survival of Hodgkin's disease tumor cells. *J.Clin.Invest* 100, 2961-2969. 1997.

References

190. Guttridge, D. C., Albanese, C., Reuther, J. Y., Pestell, R. G., and Baldwin, A. S., Jr. NF-kappaB controls cell growth and differentiation through transcriptional regulation of cyclin D1. *Mol.Cell Biol.* 19, 5785-5799. 1999.
191. Schneider, G., Saur, D., Siveke, J. T., Fritsch, R., Greten, F. R., and Schmid, R. M. IKKalpha controls p52/RelB at the *skp2* gene promoter to regulate G1- to S-phase progression. *EMBO J.* 25, 3801-3812. 2006.
192. Duckett, C. S., Perkins, N. D., Leung, K., Agranoff, A. B., and Nabel, G. J. Cytokine induction of nuclear factor kappa B in cycling and growth-arrested cells. Evidence for cell cycle-independent activation. *J.Biol.Chem.* 270, 18836-18840. 1995.
193. Habraken, Y., Piret, B., and Piette, J. S phase dependence and involvement of NF-kappaB activating kinase to NF-kappaB activation by camptothecin. *Biochem.Pharmacol.* 62, 603-616. 2001.
194. Nigg, E. A. Mitotic kinases as regulators of cell division and its checkpoints. *Nat.Rev.Mol.Cell Biol.* 2, 21-32. 2001.
195. Kittler, R., Surendranath, V., Heninger, A. K., Slabicki, M., Theis, M., Putz, G., Franke, K., Caldarelli, A., Grabner, H., Kozak, K., Wagner, J., Rees, E., Korn, B., Frenzel, C., Sachse, C., Sonnichsen, B., Guo, J., Schelter, J., Burchard, J., Linsley, P. S., Jackson, A. L., Habermann, B., and Buchholz, F. Genome-wide resources of endoribonuclease-prepared short interfering RNAs for specific loss-of-function studies. *Nat.Methods* 4, 337-344. 2007.
196. Nakayama, K. I. and Nakayama, K. Regulation of the cell cycle by SCF-type ubiquitin ligases. *Semin.Cell Dev.Biol.* 16, 323-333. 2005.
197. Bai, C., Sen, P., Hofmann, K., Ma, L., Goebel, M., Harper, J. W., and Elledge, S. J. SKP1 connects cell cycle regulators to the ubiquitin proteolysis machinery through a novel motif, the F-box. *Cell* 86, 263-274. 1996.
198. Nakayama, K., Nagahama, H., Minamishima, Y. A., Matsumoto, M., Nakamichi, I., Kitagawa, K., Shirane, M., Tsunematsu, R., Tsukiyama, T., Ishida, N., Kitagawa, M., Nakayama, K., and Hatakeyama, S. Targeted disruption of *Skp2* results in accumulation of cyclin E and p27(Kip1), polyploidy and centrosome overduplication. *EMBO J.* 19, 2069-2081. 2000.
199. Kossatz, U., Dietrich, N., Zender, L., Buer, J., Manns, M. P., and Malek, N. P. Skp2-dependent degradation of p27kip1 is essential for cell cycle progression. *Genes Dev.* 18, 2602-2607. 2004.
200. Nakayama, K., Nagahama, H., Minamishima, Y. A., Miyake, S., Ishida, N., Hatakeyama, S., Kitagawa, M., Iemura, S., Natsume, T., and Nakayama, K. I. Skp2-mediated degradation of p27 regulates progression into mitosis. *Dev.Cell* 6, 661-672. 2004.
201. Brenner, D., Krammer, P. H., and Arnold, R. Concepts of activated T cell death. *Crit Rev.Oncol.Hematol.* 66, 52-64. 2008.
202. Mittal, A., Papa, S., Franzoso, G., and Sen, R. NF-kappaB-dependent regulation of the timing of activation-induced cell death of T lymphocytes. *J.Immunol.* 176, 2183-2189. 2006.
203. Drennan, D. and Ryazanov, A. G. Alpha-kinases: analysis of the family and comparison with conventional protein kinases. *Prog.Biophys.Mol.Biol.* 85, 1-32. 2004.
204. Pinna, L. A. and Ruzzene, M. How do protein kinases recognize their substrates? *Biochim.Biophys.Acta* 1314, 191-225. 1996.
205. Ryazanov, A. G., Pavur, K. S., and Dorovkov, M. V. Alpha-kinases: a new class of protein kinases with a novel catalytic domain. *Curr.Biol.* 9, R43-R45. 1999.
206. Ko, T. K., Kelly, E., and Pines, J. CrkRS: a novel conserved Cdc2-related protein kinase that colocalises with SC35 speckles. *J.Cell Sci.* 114, 2591-2603. 2001.
207. Lapidot-Lifson, Y., Patinkin, D., Prody, C. A., Ehrlich, G., Seidman, S., Ben Aziz, R., Benseler, F., Eckstein, F., Zakut, H., and Soreq, H. Cloning and antisense oligodeoxynucleotide inhibition of a human homolog of *cdc2* required in hematopoiesis. *Proc.Natl.Acad.Sci.U.S.A* 89, 579-583. 1992.
208. Chiou, J. Y., Huang, S. J., Huang, S. T., and Cho, W. L. Identification of immune-related protein kinases from mosquitoes (*Aedes aegypti*). *J.Biomed.Sci.* 5, 120-126. 1998.
209. Hammer, B. K., Tateda, E. S., and Swanson, M. S. A two-component regulator induces the transmission phenotype of stationary-phase *Legionella pneumophila*. *Mol.Microbiol.* 44, 107-118. 2002.
210. Laguna, R. K., Creasey, E. A., Li, Z., Valtz, N., and Isberg, R. R. A *Legionella pneumophila*-translocated substrate that is required for growth within macrophages and protection from host cell death. *Proc.Natl.Acad.Sci.U.S.A* 103, 18745-18750. 2006.

References

211. Weber, S. S., Ragaz, C., Reus, K., Nyfeler, Y., and Hilbi, H. Legionella pneumophila exploits PI(4)P to anchor secreted effector proteins to the replicative vacuole. *PLoS.Pathog.* 2, e46. 2006.
212. Molmeret, M., Alli, O. A., Zink, S., Fliieger, A., Cianciotto, N. P., and Kwaik, Y. A. icmT is essential for pore formation-mediated egress of Legionella pneumophila from mammalian and protozoan cells. *Infect.Immun.* 70, 69-78. 2002.
213. Luo, Z. Q. and Isberg, R. R. Multiple substrates of the Legionella pneumophila Dot/Icm system identified by interbacterial protein transfer. *Proc.Natl.Acad.Sci.U.S.A* 101, 841-846. 2004.
214. Cirillo, S. L., Lum, J., and Cirillo, J. D. Identification of novel loci involved in entry by Legionella pneumophila. *Microbiology* 146 (Pt 6), 1345-1359. 2000.
215. Liu, M., Conover, G. M., and Isberg, R. R. Legionella pneumophila EnhC is required for efficient replication in tumour necrosis factor alpha-stimulated macrophages. *Cell Microbiol.* 10, 1906-1923. 2008.
216. Higa, F. and Edelstein, P. H. Potential virulence role of the Legionella pneumophila ptsP ortholog. *Infect.Immun.* 69, 4782-4789. 2001.
217. Hawn, T. R., Berrington, W. R., Smith, I. A., Uematsu, S., Akira, S., Aderem, A., Smith, K. D., and Skerrett, S. J. Altered inflammatory responses in TLR5-deficient mice infected with Legionella pneumophila. *J.Immunol.* 179, 6981-6987. 2007.
218. Sansonetti, P. J. The innate signaling of dangers and the dangers of innate signaling. *Nat.Immunol.* 7, 1237-1242. 2006.
219. Hawn, T. R., Smith, K. D., Aderem, A., and Skerrett, S. J. Myeloid differentiation primary response gene (88)- and toll-like receptor 2-deficient mice are susceptible to infection with aerosolized Legionella pneumophila. *J.Infect.Dis.* 193, 1693-1702. 2006.
220. Miyamoto, S., Chiao, P. J., and Verma, I. M. Enhanced I kappa B alpha degradation is responsible for constitutive NF-kappa B activity in mature murine B-cell lines. *Mol.Cell Biol.* 14, 3276-3282. 1994.
221. Korner, M., Tarantino, N., and Debre, P. Constitutive activation of NF-kB in human thymocytes. *Biochem.Biophys.Res.Comm.* 181, 80-86. 1991.
222. Delfino, F. and Walker, W. H. Stage-specific nuclear expression of NF-kappaB in mammalian testis. *Mol.Endocrinol.* 12, 1696-1707. 1998.
223. Corboy, J. R., Buzy, J. M., Zink, M. C., and Clements, J. E. Expression directed from HIV long terminal repeats in the central nervous system of transgenic mice. *Science* 258, 1804-1808. 1992.
224. Kaltschmidt, C., Kaltschmidt, B., Neumann, H., Wekerle, H., and Baeuerle, P. A. Constitutive NF-kappa B activity in neurons. *Mol.Cell Biol.* 14, 3981-3992. 1994.
225. Dobbelaere, D. A. and Kuenzi, P. The strategies of the Theileria parasite: a new twist in host-pathogen interactions. *Curr.Opin.Immunol.* 16, 524-530. 2004.
226. Molestina, R. E. and Sinai, A. P. Detection of a novel parasite kinase activity at the Toxoplasma gondii parasitophorous vacuole membrane capable of phosphorylating host I kappa B alpha. *Cell Microbiol.* 7, 351-362. 2005.
227. Molestina, R. E. and Sinai, A. P. Host and parasite-derived IKK activities direct distinct temporal phases of NF-kappaB activation and target gene expression following Toxoplasma gondii infection. *J.Cell Sci.* 118, 5785-5796. 2005.
228. Banga, S., Gao, P., Shen, X., Fiscus, V., Zong, W. X., Chen, L., and Luo, Z. Q. Legionella pneumophila inhibits macrophage apoptosis by targeting pro-death members of the Bcl2 protein family. *Proc.Natl.Acad.Sci.U.S.A* 104, 5121-5126. 2007.
229. Dorer, M. S., Kirton, D., Bader, J. S., and Isberg, R. R. RNA interference analysis of Legionella in Drosophila cells: exploitation of early secretory apparatus dynamics. *PLoS.Pathog.* 2, e34. 2006.
230. Ferrero, R. L. Innate immune recognition of the extracellular mucosal pathogen, Helicobacter pylori. *Mol.Immunol.* 42, 879-885. 2005.
231. Friedman, A. and Perrimon, N. Genetic screening for signal transduction in the era of network biology. *Cell* 128, 225-231. 2007.
232. Perkins, N. D. Integrating cell-signalling pathways with NF-kappaB and IKK function. *Nat.Rev.Mol.Cell Biol.* 8, 49-62. 2007.
233. Tomb, J. F., White, O., Kerlavage, A. R., Clayton, R. A., Sutton, G. G., Fleischmann, R. D., Ketchum, K. A., Klenk, H. P., Gill, S., Dougherty, B. A., Nelson, K., Quackenbush, J., Zhou, L., Kirkness, E. F., Peterson, S., Loftus, B., Richardson, D., Dodson, R., Khalak, H. G., Glodek, A., McKenney, K., Fitzgerald, L. M., Lee, N., Adams, M. D., Hickey, E. K., Berg, D. E., Gocayne, J. D., Utterback, T. R., Peterson, J. D.,

References

- Kelley, J. M., Cotton, M. D., Weidman, J. M., Fujii, C., Bowman, C., Watthey, L., Wallin, E., Hayes, W. S., Borodovsky, M., Karp, P. D., Smith, H. O., Fraser, C. M., and Venter, J. C. The complete genome sequence of the gastric pathogen *Helicobacter pylori*. *Nature* 388, 539-547. 1997.
234. Cazalet, C., Rusniok, C., Bruggemann, H., Zidane, N., Magnier, A., Ma, L., Tichit, M., Jarraud, S., Bouchier, C., Vandenesch, F., Kunst, F., Etienne, J., Glaser, P., and Buchrieser, C. Evidence in the *Legionella pneumophila* genome for exploitation of host cell functions and high genome plasticity. *Nat.Genet.* 36, 1165-1173. 2004.
235. Corthesy-Theulaz, I., Porta, N., Pringault, E., Racine, L., Bogdanova, A., Kraehenbuhl, J. P., Blum, A. L., and Michetti, P. Adhesion of *Helicobacter pylori* to polarized T84 human intestinal cell monolayers is pH dependent. *Infect.Immun.* 64, 3827-3832. 1996.
236. Schmitt, W. and Haas, R. Genetic analysis of the *Helicobacter pylori* vacuolating cytotoxin: structural similarities with the IgA protease type of exported protein. *Mol.Microbiol.* 12, 307-319. 1994.
237. Brenner, D. J., Steigerwalt, A. G., and McDade, J. E. Classification of the Legionnaires' disease bacterium: *Legionella pneumophila*, genus novum, species nova, of the family Legionellaceae, familia nova. *Ann.Intern.Med.* 90, 656-658. 1979.
238. Sadosky, A. B., Wiater, L. A., and Shuman, H. A. Identification of *Legionella pneumophila* genes required for growth within and killing of human macrophages. *Infect.Immun.* 61, 5361-5373. 1993.
239. Lawrence, C., Reyrolle, M., Dubrou, S., Forey, F., Decludt, B., Goulvestre, C., Matsiota-Bernard, P., Etienne, J., and Nauciel, C. Single clonal origin of a high proportion of *Legionella pneumophila* serogroup 1 isolates from patients and the environment in the area of Paris, France, over a 10-year period. *J.Clin.Microbiol.* 37, 2652-2655. 1999.
240. Jepras, R. I., Fitzgeorge, R. B., and Baskerville, A. A comparison of virulence of two strains of *Legionella pneumophila* based on experimental aerosol infection of guinea-pigs. *J.Hyg.(Lond)* 95, 29-38. 1985.
241. Dietrich, C., Heuner, K., Brand, B. C., Hacker, J., and Steinert, M. Flagellum of *Legionella pneumophila* positively affects the early phase of infection of eukaryotic host cells. *Infect.Immun.* 69, 2116-2122. 2001.
242. Feeley, J. C., Gibson, R. J., Gorman, G. W., Langford, N. C., Rasheed, J. K., Mackel, D. C., and Baine, W. B. Charcoal-yeast extract agar: primary isolation medium for *Legionella pneumophila*. *J.Clin.Microbiol.* 10, 437-441. 1979.
243. Ding, G. J., Fischer, P. A., Boltz, R. C., Schmidt, J. A., Colaianne, J. J., Gough, A., Rubin, R. A., and Miller, D. K. Characterization and quantitation of NF-kappaB nuclear translocation induced by interleukin-1 and tumor necrosis factor-alpha. Development and use of a high capacity fluorescence cytometric system. *J.Biol.Chem.* 273, 28897-28905. 1998.
244. Pfaffl, M. W. A new mathematical model for relative quantification in real-time RT-PCR. *Nucleic Acids Res.* 29, e45. 2001.
245. Zhang, J. H., Chung, T. D., and Oldenburg, K. R. A Simple Statistical Parameter for Use in Evaluation and Validation of High Throughput Screening Assays. *J.Biomol.Screen.* 4, 67-73. 1999.

Publications

Bartfeld, S., Hess, S., Bauer, B., Machuy, N., Schuchhardt, J., Meyer, T.F. High-throughput and single-cell imaging of NF- κ B oscillations using monoclonal cell lines. Submitted

Bartfeld, S., Engels, C., Bauer, B., Aurass, P., Flieger, A., Brüggemann, H., Meyer, T.F. Temporal resolution of two tracked NF- κ B activation by *Legionella pneumophila*. *Cell. Microbiol.* 2009. In Press

Bauer, B., Bartfeld, S., Meyer, T.F. *H. pylori* selectively blocks EGFR endocytosis via the non-receptor kinase c-Abl and CagA. *Cell Microbiol.* 11(1):156-69. 2009.

Niesner, U., Albrecht, I., Janke, M., Doebis, C., Loddenkemper, C., Lexberg, M.H., Eulenburg, K., Kreher, S., Koeck, J., Baumgrass, R., Bonhagen, K., Kamradt, T., Enghard, P., Humrich, J.Y., Rutz, S., Schulze-Topphoff, U., Aktas, O., Bartfeld, S., Radbruch, H., Baumgart, D.C., Duchmann, R., Rudwaleit, M., Haeupl, T., Gitelman, I., Krenn, V., Gruen, J., Sieper, J., Zeitz, M., Wiedenmann, B., Zipp, F., Hamann, A., Janitz, M., Scheffold, A., Burmester, G.R., Chang, H.D., Radbruch, A. Autoregulation of Th1-mediated inflammation by twist1. *J. Ex. Med.* 205(8):1889-901. 2008.

Bauer, B., Moese, S., Bartfeld, S., Meyer, T.F., Selbach, M. Analysis of cell type-specific responses mediated by the type IV secretion system of *Helicobacter pylori*. *Infect Immun.* 73(8):4643-52. 2005.

Manuscripts in preparation:

Bartfeld, S., Rechner, C., Bauer, B., Karlas, A., Maeurer, A.P., Machuy, N., Meyer, T.F. RNAi-based screen identifies new factors in NF- κ B signalling

Liu, J., Machuy, N., Maeurer, A.P., Bartfeld, S., Rechner, C., Meyer, T.F. Genome-wide RNAi based screen identified new factors in *Helicobacter pylori*-induced NF- κ B signalling

Bauer, B., Asakura, H., Machuy, N., Bartfeld, S., Meyer, T.F. A genome-wide screen for NF- κ B effectors, T4SS components and bacterial adhesins of *Helicobacter pylori*

Bauer, B., Bartfeld, S., Holland, C., Maeurer, A.P., Meyer, T.F. Prolonged infections with *Helicobacter pylori* impair epithelial wound healing by interfering EGFR signalling

Brüggemann, H., Rechner, C., Holland, C., Bartfeld, S., Fassi-Fehri, L. Epigenetic changes induced by *Helicobacter pylori*

Asakura, H., Jungblut, P., Bauer, B., Bartfeld, S., Churin, Y., Meyer, T.F. Disruption of the *Helicobacter pylori* hp0158 gene increases flagellin glycosylation and bacterial motility

Selbstständigkeitserklärung

Hiermit erkläre ich, dass ich die vorliegende Arbeit selbstständig und nur mit den angegebenen Hilfsmitteln erstellt habe.

Berlin, den

Acknowledgements

I owe deepest thank to so many people who supported this work. I thank Prof. Thomas Meyer for supervision, scientific discussions and support in every way. I thank Prof. Wolfgang Uckert not only for supervision during this thesis, but for ten years of much more than guidance. I thank Prof. Claus Scheidereit for helpful discussions and the opportunity to do experiments in his lab. For collaborations in experiments shown in this thesis I thank Dr. Michael Hinz, Dr. Johannes Schuchhardt and Bianca Bauer. For further guidance or helpful discussions I thank Dr. Nikolaus Machuy, Dr. Simone Hess, Dr. André Mäurer, Dr. Holger Brüggemann and Dr. Antje Flieger. Especially Nik I want to thank for a lot more: ideas, set-up of the RNAi screening facility, help with statistics, critically reading this thesis and always being of great help. Similarly, Simone I want to also thank for setting up automated microscopy and the initial assay, many ideas and for critically reading the first manuscript. Also, to André I owe further thank for help with automated microscopy, statistics and improving this thesis. To Bianca also thanks for fruitful collaborations, ideas and the good times in the lab. I further thank Dr. Lesley Ogilvie, Dr. Holger Brüggemann, Dr. Kirsten Keyser and Michael Stiller for critically reading and improving manuscripts or this thesis. I am deeply grateful to Dominique Khalil, Jörg Angermann and Chris Dimmler for outstanding technical assistance, you were a fantastic help. I thank Dr. Alexander Karlas and Hajar Habibi for support with lentiviral work. For help with technical systems such as robots and microscopes, I further thank David Manntz, Hans Thorn, Anette Rejman-Lipinski and Volker Brinkmann. For providing material I thank Dr. Antje Flieger, Phillipp Aurass, Enrico Siegbrecht, Prof. Johannes Schmid and Prof. Didier Trono. For help with statistical analysis I also thank Dr. Hans-Peter Pleissner, Dr. Oliver Duerr and Dr. Carolin Andreas. For discussions and practical help in the lab I thank Dr. Stefan Moese, Dr. Matthias Selbach, Dr. Juri Churin, Dr. Cindy Rechner, Malvika Pompaiah, Christian Sommer, Cecilia Engels, Daniel de Graaf, Katharina Ross, Dr. Peter Braun and Oliver Riede. Thanks to my friends – in the lab or somewhere else – for just being them. Special thanks to the coffee crew for constant mental support. Thanks to my family, especially Roselis-Christine Bartfeld and Sven Bartfeld, for all the support and encouraging me to do what I really like. Finally, Bas Kast, I do not know how to thank you. If all that a scientist can wish to find is cause and meaning, you are my cause, and all the meaning I need.